

**UNCLASSIFIED**

---

---

**AD 274 114**

*Reproduced  
by the*

**ARMED SERVICES TECHNICAL INFORMATION AGENCY  
ARLINGTON HALL STATION  
ARLINGTON 12, VIRGINIA**



---

---

**UNCLASSIFIED**

NOTICE: When government or other drawings, specifications or other data are used for any purpose other than in connection with a definitely related government procurement operation, the U. S. Government thereby incurs no responsibility, nor any obligation whatsoever; and the fact that the Government may have formulated, furnished, or in any way supplied the said drawings, specifications, or other data is not to be regarded by implication or otherwise as in any manner licensing the holder or any other person or corporation, or conveying any rights or permission to manufacture, use or sell any patented invention that may in any way be related thereto.

AFCRL-62-37

274114

ASTIA

CATALOGED BY

AS 60160

FINAL REPORT

ON

**A LOW-NOISE, X-BAND  
PARAMETRIC AMPLIFIER**

CONTRACT NO. AF 19(604)-4088

DATE OF REPORT

5 January 1962

Project 4610

Task 46108

Prepared for  
**ELECTRONICS RESEARCH DIRECTORATE  
AIR FORCE CAMBRIDGE RESEARCH LABORATORY  
OFFICE OF AEROSPACE RESEARCH  
UNITED STATES AIR FORCE  
BEDFORD, MASSACHUSETTS**



**MOTOROLA INC.**

**Solid State Systems Division**

3102 N. 56th Street Phoenix, Arizona • Phone 945 6311

FINAL REPORT  
ON  
A LOW-NOISE, X-BAND  
PARAMETRIC AMPLIFIER

12 May 1958 to 30 November 1961

DATE OF REPORT  
5 January 1962

CONTRACT NO. AF 19(604)-4088

Project 4610  
Task 46108

Prepared for  
ELECTRONICS RESEARCH DIRECTORATE  
AIR FORCE CAMBRIDGE RESEARCH LABORATORY  
OFFICE OF AEROSPACE RESEARCH  
UNITED STATES AIR FORCE  
BEDFORD, MASSACHUSETTS



**MOTOROLA INC.**

**Solid State Systems Division**

3102 N 56th Street Phoenix, Arizona • Phone 945 6311

**NOTICES**

**Requests for additional copies by Agencies of the Department of Defense, their contractors, and other Government agencies should be directed to the:**

**ARMED SERVICES TECHNICAL INFORMATION AGENCY  
ARLINGTON HALL STATION  
ARLINGTON 12, VIRGINIA**

**Department of Defense contractors must be established for ASTIA services or have their 'need to know' certified by the cognizant military agency of their project or contract.**

**All other persons and organizations should apply to the:**

**U. S. DEPARTMENT OF COMMERCE  
OFFICE OF TECHNICAL SERVICES  
WASHINGTON 25, D. C.**

**PROPRIETARY NOTICE**

**This document contains information proprietary to Motorola and is submitted solely for your evaluation. The information herein shall not be duplicated, used, or disclosed for design, procurement, manufacturing, or any other purpose, in whole or in part, without Motorola's consent.**

## ABSTRACT

This report describes the investigative development of parametric amplifiers and related devices from vhf to X-band. The investigative development was made by Motorola Inc., for the United States Air Force under Contract AF19(604)-4088.

The basic theory of parametric amplifiers is given for the negative resistance amplifier, upper and lower sideband converters, and the traveling-wave parametric amplifier.

The diode development effort and the techniques employed to evaluate varactor diodes are described. Development of both silicon junction and gallium arsenide point contact diodes was undertaken, the gallium arsenide effort being somewhat more successful. Houlding's method of measuring diode quality proved to be the most satisfactory.

The development of a vhf parametric amplifier is described. This amplifier needed only 1 mw pump power at 1500 mc for amplification from 180 to 270 mc. Further, the noise figure is less than 1.5 db with 16 db gain and 1 mc bandwidth.

An S-band amplifier also developed during this program is described. The amplifier utilizing filters and an idler termination achieves 70 mc bandwidth with 17 db gain and a 2 db noise figure.

Two X-band amplifiers are described, one operating in a degenerate mode and the other in a nondegenerate mode. The degenerate-mode amplifier gives 16 db gain with a 5.3 db single-channel noise figure. The nondegenerate amplifier gives 15 db gain, 12 mc bandwidth, and a 3.5 db single-channel noise figure. The nondegenerate amplifier is tunable from 8250 to 8650 mc using an OKI 24V10 klystron. Pump power required is 200 mw.

A design of a broadband X-band amplifier is presented which theoretically yields 600 mc bandwidth. However, it is shown that with the diodes available, a practical realization of this design cannot be realized.

Diodes' requirements for achieving  $K_u$ , K and V-band parametric amplifiers are given. It is believed that diodes meeting these requirements will soon be available.

A resumé is given of a feasibility study on a thin-film amplifier and oscillator. However, such a device is probably not feasible.

A stabilizing technique for parametric amplifiers is presented that improves parametric amplifier stability 6 to 1 for pump-power changes, and 8 to 1 for antenna-impedance changes.

A brief discussion of cooling parametric amplifiers is given as well as anticipated results.

Finally, the description of a corporate research study on tunnel-diode amplifiers is given. An amplifier for 450 mc has been achieved with a 5 db noise figure, 15 mc bandwidth, and 15 db gain.

## TABLE OF CONTENTS

<u>Section</u>		<u>Page</u>
	ABSTRACT . . . . .	
1	OBJECTIVES . . . . .	1-1
	1.1 Program Objectives . . . . .	1-1
	1.2 Resume' of Program Status . . . . .	1-4
	1.3 Scientific Reports and Papers . . . . .	1-4
	1.4 Visitors During the Program . . . . .	1-5
	1.5 Travel on Contract . . . . .	1-5
	1.6 Personnel and Administration . . . . .	1-5
	1.7 Fiscal Information . . . . .	1-5
2	SUMMARY OF SCIENTIFIC PROGRESS . . . . .	2-1
	2.1 Theory of Parametric Amplifier Operation . . . . .	2-1
	2.2 Development and Measurement of Varactor Diodes . . . . .	2-7
	2.3 The VHF Amplifier . . . . .	2-18
	2.4 The S-Band Amplifier . . . . .	2-19
	2.5 The X-Band Amplifier . . . . .	2-36
	2.6 Study of the K- and V-Band Amplifiers . . . . .	2-60
	2.7 The Thin-Film Amplifier and Oscillator . . . . .	2-62
	2.8 Stability of Parametric Amplifiers. . . . .	2-66
	2.9 Effect of Cooling a Parametric Amplifier . . . . .	2-72
	2.10 Study of Other Variable-Reactance and Negative-Resistance Devices . . . . .	2-72
3	SUMMARY AND CONCLUSIONS . . . . .	3-1
	3.1 The VHF Parametric Amplifier . . . . .	3-1
	3.2 The S-Band Parametric Amplifier. . . . .	3-1
	3.3 The X-Band Parametric Amplifier. . . . .	3-1
	3.4 Broadband X-Band Amplifier. . . . .	3-2
	3.5 Study of K- and V-Band Amplifiers . . . . .	3-2
	3.6 Measurement of Varactor Quality . . . . .	3-2
	3.7 Stabilizing Parametric Amplifiers. . . . .	3-2
	3.8 Thin-Film Amplifier . . . . .	3-2
	3.9 The Tunnel-Diode Amplifier . . . . .	3-2
	BIBLIOGRAPHY	

LIST OF ILLUSTRATIONS

<u>Figure</u>		<u>Page</u>
2-1	Schematic Representation of a Parametric Amplifier . . . . .	2-2
2-2	Schematic Representation of a Parametric Amplifier Using a Circulator . . . . .	2-5
2-3	Equivalent Circuit of the Traveling-Wave Parametric Amplifier . . . . .	2-5
2-4	Block Diagram Representation of an Up-Converter Amplifier . . . .	2-7
2-5	Varactor Equivalent Circuit . . . . .	2-10
2-6	Simplified Varactor Representation . . . . .	2-10
2-7	Block Diagram - Test Equipment for Measuring $f_c$ - Harrison's and Houlding's Method . . . . .	2-12
2-8	Schematic Representation of Tuner and Diode Under Matched Conditions. . . . .	2-12
2-9	Typical Plot for Measurement of $f_c$ by Harrison's Technique . . . .	2-14
2-10	Cross-Sectional View of Parametric Amplifier for 170 to 250 MC. . . . .	2-20
2-11	Noise Figure vs Signal Frequency for Parametric Amplifier (Model LPA01) . . . . .	2-21
2-12	Bandwidth vs Signal Frequency for Parametric Amplifier (Model LPA01) . . . . .	2-22
2-13	Output Power vs Input Power for Parametric Amplifier (Model LPA01) with 170-MC Signal Frequency . . . . .	2-23
2-14	Output Power vs Input Power for Parametric Amplifier (Model LPA01) with 210-MC Signal Frequency . . . . .	2-24
2-15	Output Power vs Input Power for Parametric Amplifier (Model LPA01) with 190-MC Signal Frequency . . . . .	2-25
2-16	Output Power vs Input Power for Parametric Amplifier (Model LPA01) with 230-MC Signal Frequency . . . . .	2-26
2-17	Output Power vs Input Power for Parametric Amplifier (Model LPA01) with 250-MC Signal Frequency . . . . .	2-27
2-18	Pump Power vs Signal Frequency for Parametric Amplifier (Model LPA01) with Gain Constant at 16 DB. . . . .	2-28
2-19	Pump Frequency vs Signal Frequency for Parametric Amplifier (Model LPA01) . . . . .	2-29
2-20	Stability to Pump Power for Parametric Amplifier (Model LPA01) with Gain Constant at 16 DB . . . . .	2-30
2-21	Stability to Pump Power for Parametric Amplifier (Model LPA01) with Gain Constant at 13 DB . . . . .	2-31
2-22	Stability to Pump Power for Parametric Amplifier (Model LPA01) with Gain Constant at 10 DB . . . . .	2-32

LIST OF ILLUSTRATIONS (Continued)

<u>Figure</u>		<u>Page</u>
2-23	Pump Bandwidth vs Signal Frequency for Parametric Amplifier (Model LPA01) . . . . .	2-33
2-24	S-Band Parametric Amplifier . . . . .	2-35
2-25	Block Diagram of S-Band Parametric Amplifier (Model SPA01) . . . . .	2-36
2-26	Experimental X-Band Degenerate Mode Amplifier . . . . .	2-37
2-27	Arrangement for Bench Testing of X-Band Parametric Amplifier, Block Diagram . . . . .	2-38
2-28	OKI 24V10 Klystron S/N 131 Output Power versus Frequency . . . . .	2-42
2-29	Photograph of the 8.3 gc Parametric Amplifier . . . . .	2-43
2-30	Block Diagram of X-Band Test Setup . . . . .	2-44
2-31	Gain versus Pump Frequency for Two Modes of Operation. . . . .	2-48
2-32	Typical Gain versus Pump Power for the X-Band Parametric Amplifier . . . . .	2-49
2-33	Noise Figure versus Signal Frequency for X-Band Amplifier . . . . .	2-50
2-34	Temperature Characteristics of the X-Band Amplifier . . . . .	2-51
2-35	Model of Varactor Diodes Used in the Analysis . . . . .	2-52
2-36	Nondegenerate Parametric Amplifier Representation. . . . .	2-53
2-37	Relations for Design of Lumped Element Bandpass Filters Low-Pass Prototypes . . . . .	2-55
2-38	Charts for Determining the Bandwidth of Nondegenerate Parametric Amplifiers . . . . .	2-59
2-39	Noise Figures vs Varactor Characteristics . . . . .	2-61
2-40	Theoretical X-Band Cavity System for Thin-Film Amplifier-Oscillator . . . . .	2-62
2-41	Test Arrangement for Measuring Q's of Inactive Cavity . . . . .	2-64
2-42	Schematic of Test Arrangement for Thin-Film Amplifier-Oscillator . . . . .	2-65
2-43	Schematic of Test Arrangement for Second Series of Amplifier-Oscillator Tests . . . . .	2-65
2-44	Block Diagram of Gain Control System Using Noise Level to Control Paramp Gain. . . . .	2-67
2-45	Insertion Loss versus Bias for X-Band Diode Attenuator . . . . .	2-68
2-46	Pump Power Feedback Amplifier . . . . .	2-70
2-47	Effect of I-F Noise Control of Parametric Pump Level to Stabilize Parametric Amplifier to Pump Changes. . . . .	2-71

**LIST OF ILLUSTRATIONS (Continued)**

<u>Figure</u>		<u>Page</u>
2-48	Effect of Antenna Mismatch with and without Feedback, Nominal Gain 15 db . . . . .	2-73
2-49	Typical I-V Characteristic of a Tunnel Diode . . . . .	2-74
2-50	450-MC Tunnel Diode Amplifier . . . . .	2-75
2-51	Schematic of 450-MC Tunnel Diode Amplifier . . . . .	2-76
2-52	Circuits Used to Determine Tunnel Diode Characteristics . . . . .	2-77
2-53	Gain versus Frequency of Wideband Tunnel Diode Amplifier, GE IN 2939 Diode . . . . .	2-78
2-54	Gain versus Frequency of Narrowband Tunnel Diode Amplifier, GE IN 2939 Diode . . . . .	2-79

## SECTION 1

### 1. OBJECTIVES

This final report describes the work performed by Motorola Inc. in studying low-noise parametric amplifiers and related devices under Contract AF19 (604)-4088.

#### 1.1 PROGRAM OBJECTIVES

The objectives of this program were to investigate techniques for achieving optimum design of parametric amplifiers, to develop a low-noise X-band parametric amplifier suitable for airborne operation, to study techniques for stabilizing parametric amplifiers, to evolve high frequency varactors, and investigate devices related to the parametric amplifier. This program had the following phases:

##### 1.1.1 Item 1 - Feasibility Investigation and Study of Building a Low-Noise Parametric Amplifier

The first phase of the program is an investigation and study of the feasibility of building a low-noise microwave parametric amplifier using a specially prepared semiconductor diode as the active element. This study entails:

- (1) Theoretical and experimental investigation of diode parameters necessary to permit low-noise amplification.
- (2) Construction and measurement of several diodes guided by the results of (1) above.
- (3) Theoretical and experimental study of microwave designs that produce optimum operation of the amplifier.
- (4) Construction of an optimum amplifier guided by the results of this study, the goal being to produce an amplifier operating at frequencies between 1 and 1000 mc with a noise figure less than 2 db.
- (5) Investigation of factors that limit stability in the regenerative mode of operation and determination of methods to stabilize the gain.
- (6) Construction of an optimum amplifier guided by results of work performed under paragraphs (1) through (4) with the goal of producing a stable amplifier to operate at S-band frequencies with the lowest possible effective noise temperature.

##### 1.1.2 Item 2 - Theoretical and Experimental Investigation of a Thin-Film Amplifier and Oscillator

This phase is a theoretical and experimental investigation to develop a device that amplifies microwave frequencies by varying the conductance of a thin monocrystalline film of semiconductor that couples to resonant cavities. The electric field in one cavity, which is transverse to the thin semiconductor crystal, causes a conductivity change in the crystal

resulting in a current modulation through the semiconductor. The radial field variation in the semiconductor that results from this modulation permits coupling to the second cavity. This investigation includes:

- (1) Development of techniques for preparation of the monocrystalline film of semi-conducting material by epitaxial growth or other crystal-growing techniques.
- (2) Using techniques developed in paragraph (1), preparation of crystals of different materials and selection of the crystal that is optimum with respect to mechanical and electrical properties.
- (3) Design and construction of an oscillator comprising a Rhumbatron-type microwave cavity and associated feedback cavity.

**1.1.3 Item 3 - Theoretical and Experimental Investigation to Extend the Frequency Range of Parametric Amplifiers**

This phase is a theoretical and experimental investigation of techniques and configurations necessary to extend the useful range of parametric amplifiers to the highest frequencies possible. This will involve:

- (1) Theoretical and experimental study of microwave structures and operating modes that will permit operation at the highest frequency.
- (2) Utilization of mesa transistor construction techniques to provide diodes with sufficiently high Q for high-frequency operation.
- (3) Construction of laboratory models to test theoretical designs and diodes.

**1.1.4 Item 4 - Study of Ways to Obtain Low-Noise-Figure, X-Band Parametric Amplifiers**

- (1) Investigate circuit modifications of the degenerate-mode amplifier to determine how the noise figure can be improved.
- (2) Construct amplifiers operating in the nondegenerate mode.
- (3) Investigate the effect on noise figure by cooling either part or all of the parametric amplifier.

**1.1.5 Item 5 - Configuration and Circuit Improvement of the X-Band Parametric Amplifier with the Goal of Producing an Amplifier Suitable for Airborne Application**

- (1) Determine those mechanical improvements necessary for airborne operation.
- (2) Investigate temperature effects.
- (3) Measure stability with respect to variation in antenna impedance and pump frequency to determine necessary isolation and frequency stability.
- (4) If necessary, develop circuits using diode limiters or other devices to maintain constant pump power.
- (5) Perform vibration and shock tests to insure suitable ruggedness.

- (6) Construct and deliver an 8.3-gc parametric amplifier with a noise figure as low as the state of the art permits; gain greater than 20 db; bandwidth to 10 mc; and demonstrated reliable operation in an airborne environment.

**1.1.6 Item 6 - Study of Other Variable Reactance and Negative Resistance Devices**

- (1) Evaluate low-noise amplifiers using other variable reactance and negative resistance devices.
- (2) Investigate feasibility of using other variable reactance and negative resistance devices as pump oscillators for the parametric amplifier.

**1.1.7 Item 7 - Investigation of Means of Stabilizing Parametric and Tunnel Diode Amplifiers Beyond the Present State of the Art to Eliminate the Need of Isolating Devices and Elaborate Regulating Circuits. The Studies will be Done in the Band from 200 to 10,000 MC**

- (1) Inject and detect a test signal to control tunnel diode bias or parametric amplifier pump level.
- (2) Detect noise output from an i-f amplifier to control tunnel diode bias or parametric amplifier pump level.
- (3) Apply negative feedback to a cascaded pair of amplifiers. At lower frequencies, the second amplifier would utilize a transistor, and at higher frequencies it would use a circulator-coupled tunnel diode or parametric amplifier.

**1.1.8 Item 8 - Application of the Broadbanding Techniques Developed at S-Band to X-Band**

- (1) Study degenerate-mode amplifier using multiple-filter theory.
- (2) Study nondegenerate-mode amplifier utilizing multiple filter theory as used on the S-band amplifier.
- (3) Evaluate and determine diode parameters for varactors capable of achieving wideband operation.

**1.1.9 Item 9 - Investigation of Parametric Amplifiers at K and V-Band**

- (1) Determine diode parameters for narrow and wideband amplifier at K and V-band.
- (2) Develop gallium arsenide diodes with high cutoff and self-resonant frequencies, and evaluate at X-band. Interpolate diode tests to K-band operation.

In Section 2, results of the program in light of the above objectives are discussed. Rather than following an outline exactly parallel to the program objectives, a combining of objectives is employed to provide more continuity in the discussion. The paragraph headings for the technical discussion are "Theory of Parametric Amplifier Operation," "Development and Measurement of Varactor Diodes," "The VHF Amplifier," "The S-Band Amplifier," "The X-Band Amplifier," "Study of the K and V-Band Amplifiers," "The Thin-Film Amplifier and Oscillator," "Stability of Parametric Amplifiers," "Effort of Cooling

a Parametric Amplifier," and "Study of Other Variable Reactance and Negative Resistance Devices."

## 1.2 RESUME' OF PROGRAM STATUS

Successful parametric amplifier developments were undertaken from 220 mc to 8.3 gc. The 220-mc amplifier operated with less than 1 mw pump power while achieving less than 2 db noise figure. A wideband amplifier for 2.5 gc was developed which achieved 70 mc bandwidth with a 2 db noise figure. At the time of its development, that amplifier had the highest gain-bandwidth product for any nondegenerate amplifier reported. Finally, a nondegenerate X-band amplifier was developed which achieved less than 4 db single-channel noise figure.

In addition to the specific amplifier developments, an effective stabilizing technique for parametric amplifiers was developed. This technique consists of feeding back a rectified i-f noise signal to control pump power. A 6 to 1 improvement of gain stability with respect to pump power changes and an 8 to 1 improvement of gain stability with respect to antenna impedance changes was obtained.

The feasibility of achieving a broadband X-band amplifier was studied. It was shown that a 600-mc bandwidth with a nondegenerate configuration is theoretically possible, but part of the geometry needed to achieve this bandwidth would be difficult to fabricate. However, as improved diodes having higher self-resonant frequencies are made available, X-band amplifiers with extremely large bandwidths should be achievable using the design techniques outlined.

Other facets of the subject program are the investigation of feasibility of a thin-film amplifier, monitoring a corporate study on tunnel diode amplifiers, a diode development program, and a study of diode requirements for K and V-band amplifiers. The results of these phases showed:

- (a) The thin-film amplifier is not feasible.
- (b) Tunnel-diode amplifiers with 5 db noise figure at 450 mc are possible.
- (c) Gallium arsenide point contact diodes are excellent for X-band and above amplifiers but have some serious life problems.
- (d) For K and V-band amplifiers, diodes having cutoffs in excess of 200 gc are needed for 4 db or lower amplifier noise figure.

## 1.3 SCIENTIFIC REPORTS AND PAPERS

1. Schaffner, Gerald, "A 220-mc Parametric Amplifier Requiring Low Pump Power" 1959 Electron Devices Conference.
2. G. Schaffner and F. Voorhaar, "A Nondegenerate S-Band Parametric Amplifier with Wide Bandwidth" Proceedings of the IRE, April 1961.

**1.4 VISITORS DURING THE PROGRAM**

Gerald Fabringer    AFCRL  
Richard Waetjen     AFCRL

**1.5 TRAVEL ON CONTRACT**

G. Schaffner

1. To AFCRL
2. To Washington D. C. for Electron Devices Conference
3. To New York City to attend a meeting of the Advisory Committee on Electron Devices

**1.6 PERSONNEL AND ADMINISTRATION**

No personnel changes were made.

**1.7 FISCAL INFORMATION**

Approximately zero dollars remain on the project.

## SECTION 2

### 2. SUMMARY OF SCIENTIFIC PROGRESS

#### 2.1 THEORY OF PARAMETRIC AMPLIFIER OPERATION

##### 2.1.1 Introduction to Theory of the Parametric Amplifier

New and promising techniques utilizing phenomena occurring in the solid state have recently been developed for obtaining amplification at microwave frequencies. These solid-state amplifiers are characterized by an extremely low noise figure and excellent reliability. At present, most interest is concentrated on the parametric amplifier type. Basically, the parametric amplifier utilizes a reactance, either capacitive or inductive, which varies with application of a high-frequency pump signal. When a pump signal and a lower frequency signal are applied to this device, energy flows from the pump signal to the lower frequency signal and to the sidebands resulting from the mixing action. Thus, power amplification is possible. Since the parametric amplifier is not a resistance device and does not utilize an electron beam, the noise generated is very low. Noise figures on the order of 1 or 2 db are possible. The most promising type of parametric amplifier developed utilizes a P-N semiconductor junction and is called a diode-type parametric amplifier.

##### 2.1.2 The Diode-Type Parametric Amplifier

Rather than representing one particular type of amplifier, the diode parametric amplifier refers to a whole class of amplifiers. In the following sections, various types of parametric amplifiers will be discussed.

Basically, the parametric amplifier utilizes a P-N junction (varactor) biased in the reverse direction to form a fairly high-Q capacitance. This capacitance can be varied with the application of either a different bias voltage, or a high-frequency pump signal. With the parametric amplifier there are always two signal inputs: (1) the incoming signal, and (2) a pump signal at a higher frequency. Because of nonlinearities present in the P-N junction, new frequencies are generated. These frequencies are the sum, the difference, and harmonics of the sum, difference, incoming frequency, and the pump frequency. It is usually desirable to short circuit all but one of these new frequencies. The mixing product for which a real termination is provided is usually either the sum, or the difference, of the pump and the incoming signal frequencies. If the difference frequency is so terminated, the circuitry resulting is known as a negative-resistance amplifier. The power relationships existing in the negative-resistance amplifier are:<sup>1</sup>

$$P_d = -P_p \frac{f_d}{f_p} \tag{1}$$
$$P_s = P_d \frac{f_s}{f_d}$$

<sup>1</sup> Superscripts refer to similar numbered entries in the List of References.

where

$P_d$  is power flowing out at the difference frequency

$P_p$  is power flowing out at the pump frequency

$P_s$  is power flowing out at the signal frequency

$f_d$  is the difference frequency

$f_s$  is the signal frequency.

The above equation shows that power flows out of the varactor at both the difference frequency and the signal frequency. This latter phenomenon means that a negative resistance is presented to the incoming signal, which can result in gain or oscillation. There is more energy coming from the varactor at the difference frequency than at the signal frequency.

Schematically, it is possible to represent the parametric amplifier as shown in Figure 2-1. Associated with  $f_1$ , the incoming signal frequency, is a circuit consisting of  $L_1$ ,  $C_1$ , and  $G_{t1}$ . The conductance  $G_{t1}$  represents the loading due to the source resistance, the load resistance, and the internal losses in the resonant circuit. Similarly, the sideband frequency  $f_2$  has an associated resonant circuit represented by  $L_2$ ,  $C_2$ , and  $G_{t2}$ . The capacitance  $C_3$  represents the variable nonlinear element (varactor), the value of which changes with the incoming pump frequency. If  $C_3$  is proportional to pump amplitude, the upper and lower sideband are the only mixing products obtained.

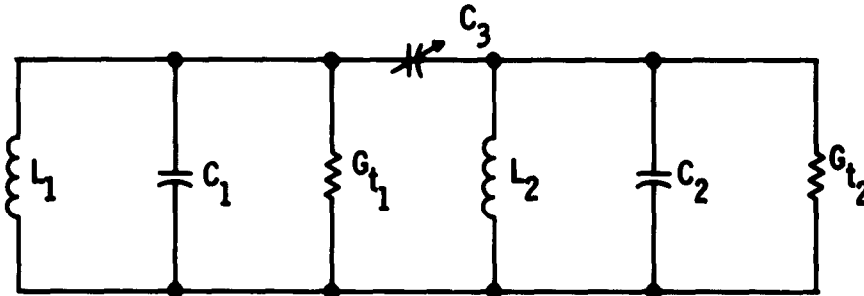


Figure 2-1. Schematic Representation of a Parametric Amplifier

Nomenclature for various types of parametric amplifiers has not been clearly defined throughout the industry. To prevent confusion, the following nomenclature is established and will be used in this report.

- (1) Negative Resistance Amplifier - If the output frequency is the signal frequency, the device is called a negative resistance amplifier.
- (2) Regenerative Up-Converter Amplifier - If the output frequency is the difference frequency, the device is called a regenerative up-converter amplifier.
- (3) Up-Converter Amplifier - If the output frequency is the sum frequency, the device is called an up-converter amplifier.

Each of these three amplifier types will be discussed separately in the following paragraphs.

### 2.1.3 Negative Resistance Amplifier

If the upper sideband is suppressed, and the output taken at the signal frequency, then a negative resistance amplifier results. A negative resistance is presented to the signal frequency as given by the following equation.<sup>2</sup>

$$G = \frac{\omega_1 \omega_2 C_3^2}{4G_{t2}} \quad (2)$$

where

$G$  is the negative conductance presented to the signal frequency circuit in mhos.

$\omega_1$  is the signal frequency in radians per second

$\omega_2$  is the difference frequency in radians per second

$C_3$  is the varactor capacitance

$G_{t2}$  is the difference frequency resonant circuit loading in mhos.

Using the negative conductance calculated in equation (2), the gain at resonance can be given by

$$\text{Gain} = \frac{4G_g G_L}{(G_{t1} - G)^2} \quad (3)$$

where

$G_g$  is the loading of the signal frequency circuit due to source

$G_L$  is the loading of the signal frequency circuit due to load.

It is clear that if  $G = G_{t1}$ , oscillation occurs because gain is infinity.

One type of figure-of-merit for this amplifier is the product of gain to the one-half power and bandwidth. The square root of gain times bandwidth is given by

$$(\text{Power gain})^{1/2} (\text{bandwidth}) = \frac{2\omega_2 (G_g G_L)^{1/2}}{2\omega_2 Q_1 G_{t1} + \omega_1 Q_2 G} \quad (4)$$

where  $Q_1$  and  $Q_2$  are gains ( $Q$ ) for the signal and difference frequency circuits, respectively.

It is clear from the examination of equation (4) that for a large gain bandwidth product, the ratio of  $\omega_2$  to  $\omega_1$  should be large; that is, the highest difference frequency possible should be used.

Another important figure-of-merit for this amplifier is the noise figure. The noise figure is given by

$$F = 1 + \frac{G_1}{G_g} + \frac{G \omega_1}{G_g \omega_2} + (\text{shot noise}) + (\text{gain fluctuation}) \quad (5)$$

where  $F$  is the noise figure, and  $G_1$  is the conductance loading the signal circuit due to internal losses. The shot noise comes from the inverse current, and gain fluctuations come from pump power variation. If the shot noise terms and the gain fluctuation terms are small, the noise figure can be expressed as

$$F = 1 + \frac{G_1}{G_g} + \frac{G}{G_g} \frac{\omega_1}{\omega_2} \quad (6)$$

Replacing  $G$  by  $G_{t1}$ , which for high gains is approximately equal to  $G$ , the following is obtained:

$$F = 1 + \frac{G_1}{G_g} + \frac{G_{t1}}{G_g} \frac{\omega_1}{\omega_2} . \quad (7)$$

It can be seen from equation (7) that the lowest possible noise figure obtainable is equal to  $1 + \omega_1/\omega_2$ . For low-noise operation therefore, the use of the highest difference frequency possible is indicated. The equation also indicates that proper adjustment of coupling is important in obtaining low noise figures.

Stability appears to be the most formidable deterrent to practical operation of parametric amplifiers of the type outlined above. Because of the regeneration, the gain as given by equation (3) is a sensitive function of source and load conductances. Since source conductance usually represents antenna conductance, a factor which varies with position or environment of the antenna, stable operation of an amplifier without some isolation does not appear possible.

Fortunately recent developments of ferrite isolators and circulators have permitted utilization of low-loss isolating devices at all but the lowest vhf frequencies. By using these ferrite devices quite stable amplifiers have been achieved.

In addition to stabilizing the parametric amplifier, the circulator improves noise figure of parametric amplifiers. This fact can be demonstrated by analysis of the equivalent circuit shown in Figure 2-2. The gain of a parametric amplifier using a circulator is given by equation (8).

$$\text{Gain} = \left| \frac{G_{t1} + G}{G_{t1} - G} \right|^2 \quad (8)$$

where  $G_{t1} = G_g + \text{cavity losses}$ .

Minimum noise figure is given by

$$F = 1 + \frac{G_1}{G_g} + \frac{(G_1 + G_g) \omega_1}{G_g \omega_2} . \quad (9)$$

If the diode is perfect and internal losses are zero,  $G_1 = 0$ ; then

$$F_{\min} = 1 + \frac{\omega_1}{\omega_2} . \quad (10)$$

There are several configurations that can be used for the negative resistance amplifier. For instance, a single diode can be used either in cavities or in broadband structures; pairs of diodes can be used either in cavities or in broadband structures, or a traveling-wave structure can be used. The cavity structure with the single diode is simplest, as it leads to the most compact package, giving low noise figure and requiring very little pump power. However, it has a narrow bandwidth.

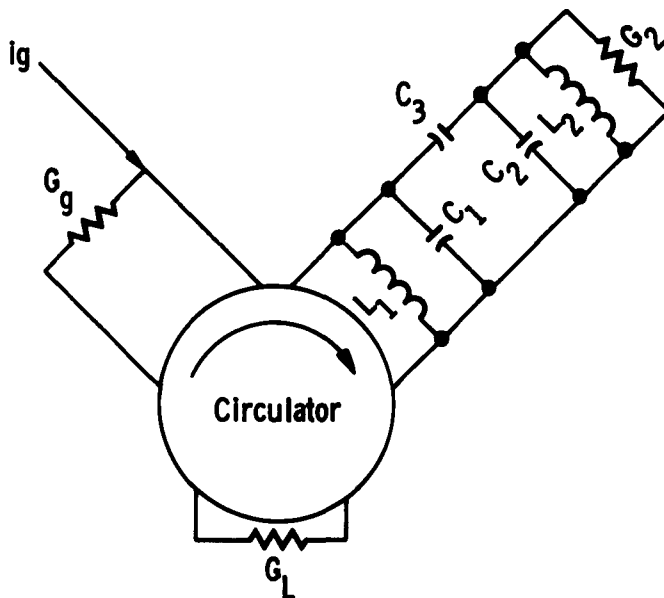


Figure 2-2. Schematic Representation of a Parametric Amplifier and a Circulator

A theoretically attractive configuration of the negative resistance amplifier utilizes a traveling-wave structure. In this structure, several diodes are used, each diode giving a small amount of gain. Amplification of the signal power in the traveling-wave amplifier is obtained in the form of a growing wave propagating in a structure consisting of shunt varactor diodes separated by series inductances. The structure possesses two propagating modes. One mode is excited by the signal at the input end and the other is used as an idling circuit. The structure also supports the traveling-wave supplied by a pump which provides, by modulation of the varactor diodes, a time varying coupling between the two propagating modes. An equivalent circuit of the traveling-wave amplifier is shown in Figure 2-3.

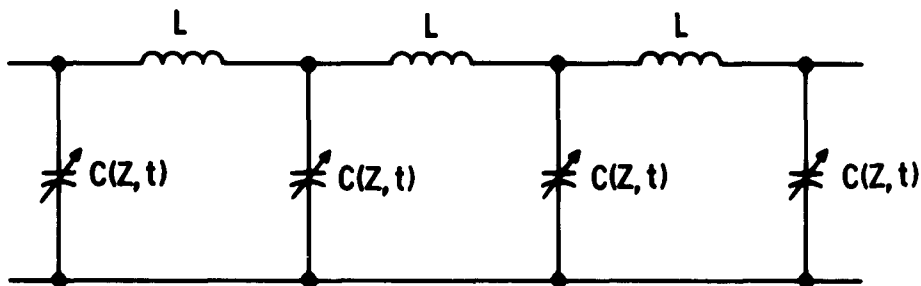


Figure 2-3. Equivalent Circuit of the Traveling-Wave Parametric Amplifier

The capacitances  $C(Z, t)$  are the varactor diodes whose capacitance is a function of time and position. The capacitance is a function of position because the amplifier acts as a terminated transmission line several wavelengths long to the pump signal.

Theoretically, the traveling-wave parametric amplifier has potential for extremely wide bandwidth. Full realization of the theoretical possibilities have not occurred primarily because of the difficulty in maintaining proper phase relationships. Amplifiers built to date have had low gain, poor stability, and poor noise figures; further, there is no immediate prospect for improvement.

#### 2.1.4 Up-Converter Amplifier

Another kind of parametric amplifier is the up-converter amplifier. The up-converter amplifier is characterized by wide bandwidth, low noise figure, generally low gain, and unconditionally stable operation. Like the negative resistance amplifier, the up-converter amplifier has two incoming frequencies. One frequency is the pump and the other frequency is the signal. With the up-converter amplifier, the lower sideband is suppressed and a termination is provided for the upper sideband. The output is taken from the circuit resonant to the upper sideband. Equation (11) gives the power relations existing in the up-converter.

$$P_h = -P_s \frac{f_h}{f_s} \quad (11)$$

where  $P_h$  is power flowing out of the varactor at the sum frequency  $f_h$ .

Examination of equation (11) shows that the power output at the upper sideband frequency is higher than the power input at the signal frequency. For example, a 400-mc amplifier has been constructed using a 9000-mc pump. This amplifier has 10 db of gain, a 100-mc bandwidth, and a noise figure of 1.75 db. The required pump power is about 40 milliwatts. It is interesting to note that the gain is about 3 db less than theoretical. The 3-db difference from the theoretical gain is explained by circuit losses. A block diagram of a typical up-converter amplifier is shown in Figure 2-4. The EH tuner and filter suppress the lower sideband and eliminate the pump signal from the output. If the lower sideband is not completely short circuited, some instability results. Therefore, for completely stable operation, the lower sideband should be completely eliminated. At the present, the up-converter amplifier does not have much application above 500-mc input. Unfortunately, above 500 mc, the resultant gain is low and noise figures tend to increase.

#### 2.1.5 Regenerative Up-Converter Amplifier

The regenerative up-converter amplifier has the same configurations as the up-converter amplifier but with the upper sideband suppressed. The regenerative up-converter amplifier is characterized by high gain, low noise figure, narrow bandwidth, and potentially unstable operation. However, the regenerative up-converter amplifier provides more gain with less regeneration than is the case with the negative resistance amplifier. The fact that the output frequency of the regenerative up-converter amplifier depends on the pump frequency can in some cases be a disadvantage.

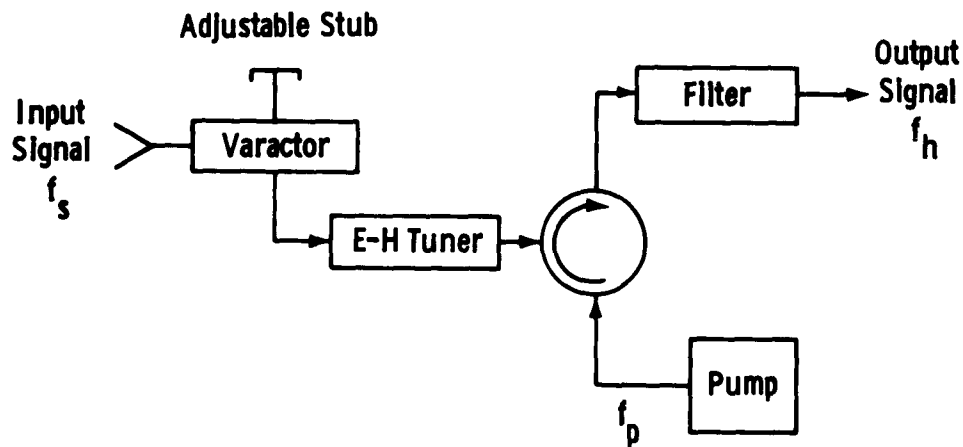


Figure 2-4. Block Diagram Representation of an Up-Converter Amplifier

## 2.2 DEVELOPMENT AND MEASUREMENT OF VARACTOR DIODES

During this program, a two-phase investigation was made to develop high-frequency varactor diodes. One phase was concerned with development of silicon junction diodes while the other phase was concerned with development of gallium arsenide diodes. The most promising result was the attainment of a point-contact gallium arsenide diode which operated an X-band amplifier. However, a deterioration of that diode occurred over a six-month interval which precluded its use in any finalized amplifier.

### 2.2.1 Silicon Diode Development

The objective of this phase of the program was to design and fabricate variable-capacitance silicon diodes for use in parametric amplifiers. The specific goals were the attainment of diodes with cutoff frequencies equal to and higher than the present state of the art, and attainment of a package suitable for operation at X-band and higher frequencies. This work was done by the Motorola Semiconductor Division.

P-type silicon with resistivity on the order of 0.005 to 0.01 ohm cm was used because low resistivities minimize spreading resistance. Some N-type silicon was used in this phase, but because of the lower capacitances obtained, and because of etching difficulties not encountered with P-type materials, these materials were not utilized in optimum devices. A description of the diffusion, mesa formation, and packaging follows.

The diffusion process employed techniques of painting opposite faces of the wafer with solutions of phosphorus pentoxide and boron trioxide, respectively. Prior to mesa formation, wafers were nickel-and gold-plated using electroless plating.\* Fabrication of the wafers employed the painting technique of diffusion followed by the lapping of one wafer face. Diffusion into polished surfaces to provide more uniform junctions resulted in poor plating adherence and subsequent difficulty in mesa etching.

Sand-blast honing of mesas was abandoned in favor of cavitroning and wax evaporating techniques. The latter method was used currently since it resulted in more economical and facile operation. Wax evaporation minimized mechanical damage but required a delicate waxing and etching operation. A Buckbee-Mears mask was obtained for evaporating 2- to 5-mil wax dots for this purpose.

Attempts at lowering package capacitance were made by:

- (1) Using a C-bend in place of the present S-bend lead
- (2) Reducing die base area
- (3) Designing a new package utilizing a dimpled diaphragm for die contact.

The packages incorporating the C-bend were found to have approximately  $0.3 \mu\mu f$  capacitance, similar to the  $0.3-0.4 \mu\mu f$  value of commercial diodes. Packages also were constructed with the dimpled diaphragm die contact. Although the reading for this package was approximately  $0.8 \mu\mu f$ , this does not indicate a limit, since the package was relatively crude. Glass diode packages were also fabricated. Capacitances of  $0.27$  and  $0.28 \mu\mu f$  were measured for C- and S-bend leads, respectively.

Further tests on the silicon diodes showed the series resistance to be excessive. Work on the silicon diode was then terminated in favor of the more promising gallium arsenide diode.

### 2.2.2 Gallium Arsenide Diode

The purpose of this phase of the program was to develop a microwave diode for use in the Motorola X-band parametric amplifier. This was accomplished in two phases: Phase 1 consisted of an experiment designed to provide information on the optimum process steps in the assembly of a finished diode, and Phase 2, where the information obtained in Phase 1 was used to assemble units for evaluation at X-band frequencies.

Phase 1 was accomplished by forming point contacts on three different gallium arsenide wafers. The point pressure, forming conditions, and crystal size were varied in a known manner. Measurements of the d-c characteristics were taken and the data were statistically analyzed. The most promising process conditions were incorporated in the assembly of finished diodes.

Phase 2 was accomplished by assembling a number of packaged diodes, in which the crystal thickness, point structure, forming conditions, and package design were varied.

A description of the diode that evolved follows.

---

\* Defined in Cooke and Markus' Electronics and Nucleonics Dictionary as: Chemical deposition of a metal on a material, without electrolytic or electroplating action.

N-type gallium arsenide, which has a resistivity on the order of 0.003 ohm/cm, was used in the making of the point-contact microwave diodes. The process consisted of cutting the gallium-arsenide ingot into 0.010-inch thick wafers and lapping the wafers to an 0.008-inch thickness. Gold was vacuum-deposited and alloyed into one side of the wafer. The wafer was then electrolessly plated with nickel and gold, after which the unplated side of the wafer was polished and again lapped. The wafer thickness at this point was 0.004 inch. The wafers were scribed and broken into parts that were approximately 0.018-inch square. A 0.025-inch diameter gold-plated nickel stud was soldered to each part using 60/40 solder. Before assembly, each part was etched in NaOH-H<sub>2</sub>O<sub>2</sub> etch for 30 seconds.

The package consisted of two gold-plated nickel headers and a 1-mm bore quartz tube. The three parts were assembled using a thermal setting resin which was cured at 120 C for 1 hour. A bond of this type permitted the use of quartz instead of glass. Quartz is desirable because it is less lossy than glass at microwave frequencies.

The whisker was a 0.002-inch phosphor bronze wire that was welded to the gold-plated nickel stud. The whisker was bent into a "C" shape and electrolytically pointed. By controlling the voltage across the system, the points obtained by electrolytic etching were readily reproducible. The whisker was rinsed in deionized water and dried in a nitrogen atmosphere before assembly.

The three processed parts were assembled in the following manner.

The stud with the whisker attached was inserted through one header and soldered using pure indium. The wire was then inspected to ensure that the whisker was not disturbed during insertion, and corrections, if necessary, were made. The stud, with the crystal mounted, was inserted from the opposite end and advanced until contact was made. After contact, the stud was advanced a distance determined by the pressure desired on the point. The stud was then soldered in place, using indium as the solder.

Typical values obtained using the procedures outlined above are shown in Table 2-1.

TABLE 2-1. GALLIUM-ARSENIDE POINT-CONTACT MICROWAVE DIODE CHARACTERISTICS

<u>Measurement</u>	<u>Typical Value</u>
Reverse Current at 0.5 V	0.010 $\mu$ a
Spreading Resistance	20 ohms
Voltage Breakdown	4 volts
Capacitance at 0 bias	0.12 $\mu\mu$ f
Package Capacitance	0.08 $\mu\mu$ f

As stated previously, one of the gallium arsenide diodes operated the degenerate mode X-band amplifier giving a 6.5 db single channel noise figure. However, this diode deteriorated in approximately three months indicating that a poisoning of the gallium arsenide occurred.

### 2.2.3 Measurement of Varactor Diode Quality

Generally, varactor diode losses account for almost all of the internal loading,  $G_1$ , discussed in Section 2.1.1. Therefore, to predict amplifier noise figure, the designer should know the quality of the varactor used. During this program, three techniques were investigated to measure diode quality; these are Harrison's, Houlding's and modified Houlding's. A discussion of each method follows.

The varactor diode can be represented schematically by the circuit shown in Figure 2-5.

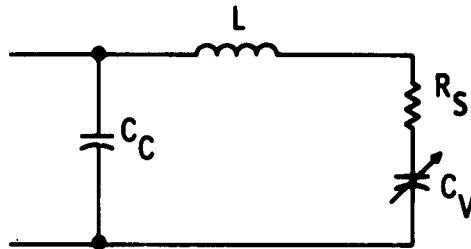


Figure 2-5. Varactor Equivalent Circuit

The case capacity,  $C_C$ , and the inductance,  $L$ , are functions of the case configuration only, and have no effect upon the  $F_c$  of the diode. The factors  $C_C$  and  $L$  do, however, affect the operating frequency and bandwidth of a parametric amplifier, and must be considered in the amplifier design. For calculation of  $F_c$ , the varactor equivalent circuit (Figure 2-5) can be simplified to that shown in Figure 2-6.



Figure 2-6. Simplified Varactor Representation

In a varactor, the capacity,  $C_V$ , is a function (equation (12)) of the applied voltage and type of junction.

$$C_V = \frac{C_0}{\left(1 - \frac{V}{\mu}\right)^{1/2}} \quad (12)$$

where

$C_0$  = crystal capacity at zero volts

$V$  = applied voltage - this must include polarity sign as noted in Figure 2-6

$\theta$  = a constant dependent upon semiconductor material

$N$  = a constant dependent upon the type of junction

$N = 2$  for an abrupt junction

$N = 3$  for a diffused junction .

The cutoff frequency of a varactor diode is defined as the frequency where the capacitive reactance  $X_{C_V}$  is equal to  $R_S$  .

$$\frac{1}{2\pi f_c C_V} = R_S \quad (13)$$

$$f_c = \frac{1}{2\pi R_S C_V}$$

The  $Q$  of a diode at any frequency is given by equation (14).

$$Q_f = \frac{1}{2\pi f C_V R_S} \quad (14)$$

And  $Q_f$  is related to the  $f_c$  of a varactor as follows:

$$f_{Q_f} = \frac{1}{2\pi R_S C_V} = f_c \quad (15)$$

The following conditions and assumptions from equation (15) can be noted:

1. It is assumed that  $R_S$  is constant with frequency and applied voltage. This assumption has been verified by experimental results.
2. It is assumed that  $C_V$  varies with voltage only, and is independent of the applied frequency. This also has been verified by experimental investigation<sup>3</sup>.
3. It should be noted that  $f_c$  is a function of the bias voltage  $V$ . This is of extreme importance in calculating  $f_c$  and its relationship to the noise figure.

Following is a summary of the procedures and techniques for three methods of measuring the  $f_c$  of varactors.

#### Harrison's Method<sup>4</sup>

In this method, the impedance of the diode is measured at a high r-f frequency (usually 10,000 mc) as the bias voltage is varied. A block diagram of the test equipment for making the impedance measurement is shown in Figure 2-7.

Extreme care must be taken to maintain a low r-f signal voltage across the diode. To reduce the r-f voltage to a minimum, it is customary to interchange the signal generator and the standing-wave detector from the conventional connection shown in Figure 2-7. It can be shown that this interchange will effectively reduce the incident r-f level by 20 db, while maintaining good measuring accuracy and sensitivity.

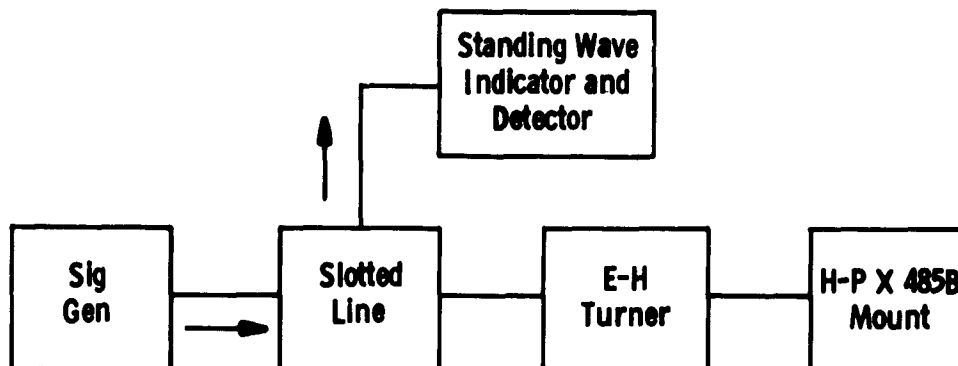


Figure 2-7. Block Diagram - Test Equipment for Measuring  $f_c$  - Harrison's and Houlding's Method

The procedure for measuring the varactor is as follows:

1. Insert diode under test into the X485B mount, with 0 volts bias; adjust E. H. tuner until the diode is matched. The tuner-diode combination can then be represented as shown in Figure 2-8.

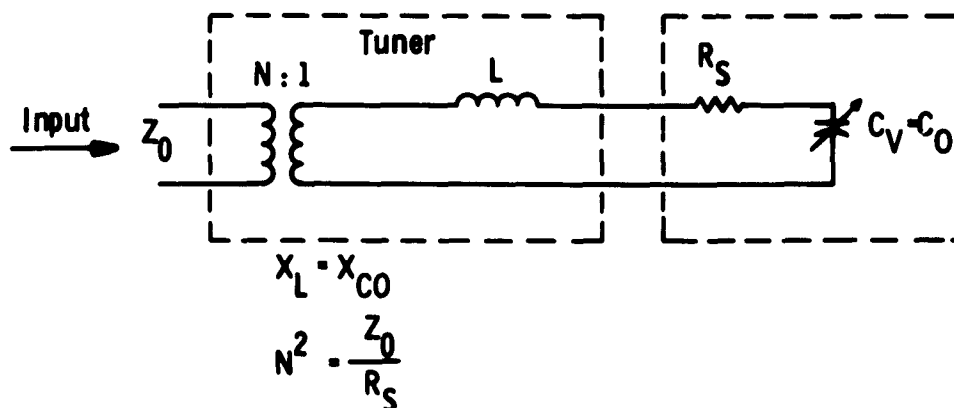


Figure 2-8. Schematic Representation of Tuner and Diode Under Matched Conditions

2. The diode is then replaced by a short circuit and the input impedance is measured. The choice of reference point for measurement of the impedance will have no effect upon the final result and, therefore, can arbitrarily be chosen for convenience. To achieve an effective short without removing the diode, high forward bias current (1 to 2 ma) can be applied to the diode. With 1 ma forward current, the diode has sufficiently low impedance to approximate a short circuit.
3. The diode impedance is then measured for various applied biases. These points are plotted on Figure 2-9. The impedance vs bias curve should approximate a circle of radius  $R_0 = 1$ . A circle of radius  $R_0 = 1$ , is fitted to impedance plot and rotated on angle  $\theta$  (in the example case 129 degrees) until the fitted circle coincides with the  $R_0 = 1$  circle.
4. The impedance plot of the short is rotated on angle  $\theta$  in the same direction as the fitted circle was rotated.
5. It can be shown that when the points on the fitted circle are extrapolated to a point on the outer edge, this point represents an open circuit. Using the short and open circuit points, it can be shown that the impedance of the shorted point is equal to

$$\frac{X_L}{R_s} \text{ or } \frac{X_{Co}}{R_s} \text{ because } X_L = X_{Co} .$$

6. The ratio  $\frac{X_{Co}}{R_s} = \frac{1}{2\pi f C_0 R_s} = Q_f .$

Therefore, the cutoff frequency at zero volts can be calculated as

$$f_c = Q_f f .$$

7. To calculate the  $f_c$  at a bias point other than zero volts, the reactive component ( $\frac{X'_c}{R_s}$ ) of the diode impedance is determined from the graph at the voltage level in question. The reactive impedance ( $\frac{X'_c}{R_s}$ ) is then added to the zero volt capacity ( $\frac{X_{Co}}{R_s}$ ). The sum of these two terms is the  $Q$  of the diode at the bias level corresponding to the  $\frac{X'_c}{R_s}$  value used.

8. The results of the demonstration plot shown in Figure 2-9 are given in Table 2-2.

The Harrison method calculates the  $f_c$  of the varactor without requiring the measurement of the diode capacity. It is straightforward in technique, but complex and difficult in operation. The accuracies and complexities required in measuring the diode impedance at various levels makes this system inconvenient. It is felt that either of the next two measurement techniques described is better.

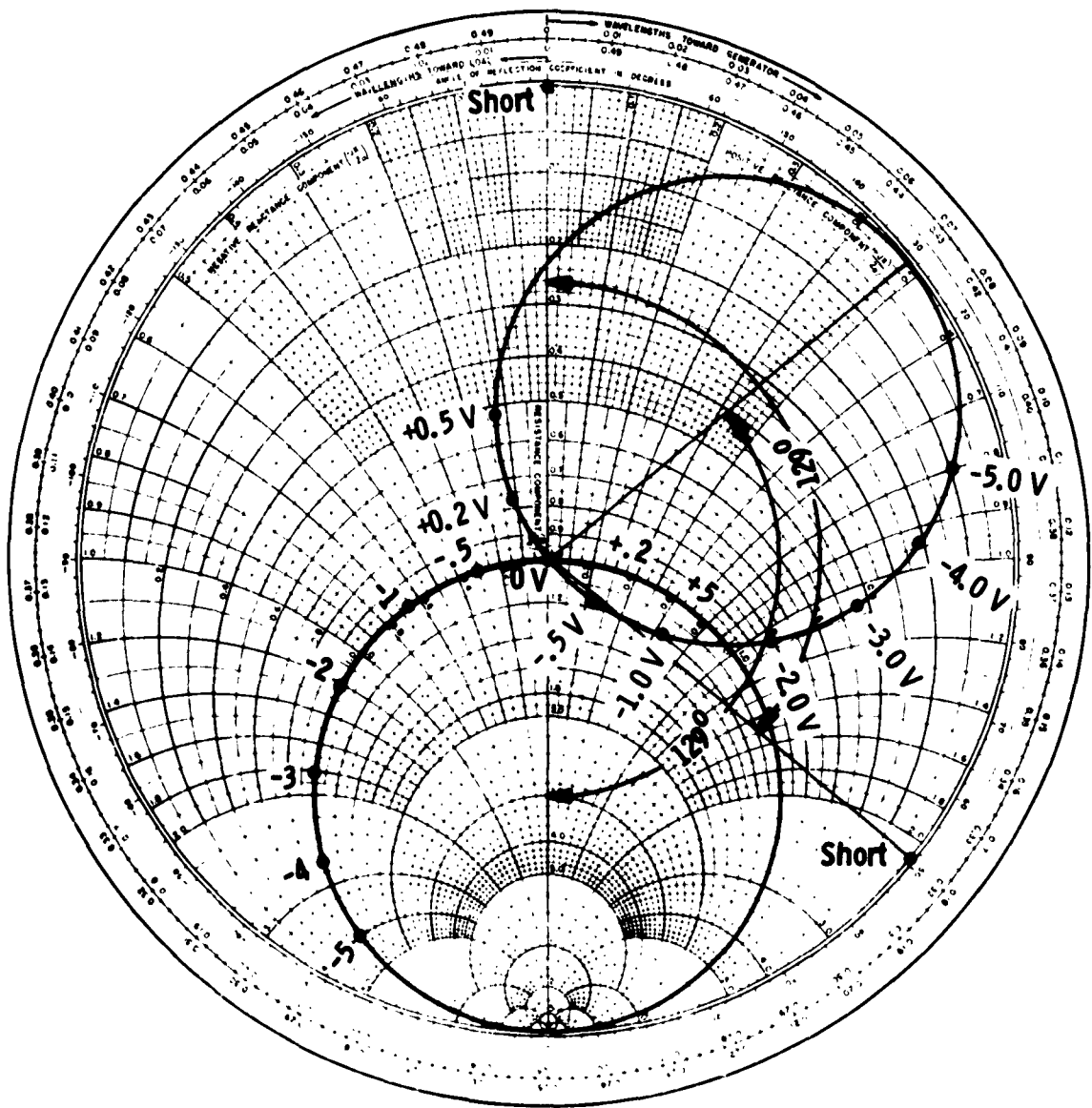


Figure 2-9. Typical Plot for Measurement of  $f_c$  by Harrison's Technique

TABLE 2-2

Bias	$\frac{X_{Co}}{R_s}$	$\frac{X_{C'}}{R_s}$	$Q'_f$	$F_C$
0	2.11	0	2.11	21.1
- .5	2.11	0.28	2.39	23.9
-1	2.11	0.69	2.80	28.0
-2	2.11	1.25	3.36	33.6
-3	2.11	1.88	3.99	39.9
-4	2.11	2.8	4.91	49.1
-5	2.11	4.3	6.41	64.1

### Houlding's Method<sup>5</sup>

In Houlding's method as compared to Harrison's, the capacity vs voltage characteristic of the diode is measured. Because of the independency of capacity with frequency, these measurements are made at 100 kc because accurate capacity bridges are available at this frequency. If the capacity-voltage characteristic is known, only the  $R_s$  of the diode is required and  $f_c$  of the diode at any voltage level can be calculated. It should be noted at this time that the capacity to be used in calculating  $f_c$  is the crystal capacity  $C_V$  only, and does not include the cartridge capacity  $C_C$ . It is, therefore, required that the case capacity  $C_C$  be subtracted from the over-all capacity measured.

A block diagram of test equipment for measuring  $R_s$  is shown in Figure 2-7. The procedure for  $R_s$  measurement is as follows:

1. The diode is inserted in the X485B mount and matched at zero volts bias.
2. The bias is increased to any voltage,  $V_1$ , for which the capacity was measured in Step 1.
3. With the voltage  $V_1$  applied to the diode, the VSWR is measured. It is noted that in this method (Houlding's), only the magnitude of the VSWR is required, and not both the magnitude and phase, as was required in Harrison's method.
4. With the VSWR known for a voltage change from 0 to  $V_1$  and the corresponding change in capacity, the  $R_s$  of the diode can be calculated by the following equations:

$$\text{VSWR} = \frac{1 + \left( \frac{\Delta X^2}{4R_s^2 + \Delta X^2} \right)^{1/2}}{1 - \left( \frac{\Delta X^2}{4R_s^2 + \Delta X^2} \right)^{1/2}} \quad (16)$$

Where

$$\begin{aligned} \Delta X &= X C_1 - X C_0 \\ &= \frac{1}{2 \pi f C_1} - \frac{1}{2 \pi f C_0} = \frac{1}{2 \pi f} \left( \frac{C_0 - C_1}{C_0 C_1} \right) \end{aligned} \quad (17)$$

for high-Q diodes  $\frac{\Delta X^2}{R_s^2} \gg 2$  equation (16) reduces to

$$VSWR \approx 1 + \frac{\Delta X^2}{R_s^2} \quad (18)$$

by algebraic manipulation, equation (18) can be rewritten

$$R_s = \frac{\frac{C_0 - C_1}{C_0 C_1}}{2 \pi f (VSWR - 1)^{1/2}}$$

5. After  $R_s$  is calculated, the  $f_c$  at various bias levels can be calculated by the equation

$$f_c = \frac{1}{2 \pi R_s C_v} \quad (19)$$

where  $C$  is the value of crystal capacity.

The Houlding technique is advantageous in requiring only the magnitude of one VSWR measurement at X-band as compared to the many VSWR measurements required of Harrison's method. The Houlding method appears to be the most popular throughout the industry and is the method Motorola is presently using. The only disadvantage of this method is that the capacity  $C_v$  must be independent of frequency. This is believed to be a logical assumption and, as was mentioned in the introduction, has been verified theoretically and experimentally.

#### Modified Houlding's Method<sup>5</sup>

To overcome the possibility of error in assuming that the capacity is independent of frequency, a modified measurement procedure has been derived.

In this technique, the voltage change,  $\Delta V$ , between the matched and unmatched condition is specifically chosen such that the VSWR measured is directly proportional to the  $Q$  of the diode. As was shown in equation (18),

$$VSWR \approx 1 + \frac{\Delta X^2}{R_s^2} \quad (20)$$

$$\frac{\Delta X}{R_s} = \sqrt{\text{VSWR} - 1}$$

where

$$\Delta X = X_2 - X_1$$

$X_1$  is reactance at  $V_1$  (where  $f_c$  is to be determined) and  $X_2$  is reactions at  $V_2$ .

$$X_1 = \frac{N\sqrt{\theta - V_1}}{2\pi f C_0 N\sqrt{\theta}} \quad (22)$$

$$X_2 = \frac{N\sqrt{\theta - V_2}}{2\pi f C_0 N\sqrt{\theta}} \quad (23)$$

$$\frac{X_1}{X_2} = \sqrt{\frac{\theta - V_1}{\theta - V_2}} \quad (24)$$

where  $\theta$  is a function of the diode material, and  $N$  depends upon the type of junction.

The voltage  $V_2$  is chosen such that

$$\frac{X_1}{X_2} = \frac{5}{4} \quad (|V_1| > |V_2|) \quad (25)$$

and

$$\frac{5}{4} = \sqrt{\frac{\theta - V_1}{\theta - V_2}} \quad (26)$$

or

$$-V_2 = \frac{\theta - V_1}{(5/4)^N} \pm \theta \quad (27)$$

The diode is matched as in Houlding's method with  $V_1$  applied, and the VSWR is measured when  $V_2$  is applied. Therefore, as in Houlding's method,

$$\begin{aligned} \text{VSWR} &= 1 + \frac{\Delta X^2}{R_s^2} & \Delta X &= X_1 - X_2 & (28) \\ & & X_2 &= \frac{4}{5} X_1 \\ & & \Delta X &= \frac{X_1}{5} \end{aligned}$$

Therefore,

$$\frac{\Delta X}{R_s} = \sqrt{\text{VSWR} - 1}$$

$$\frac{X_1}{5R_s} = \sqrt{\text{VSWR} - 1}$$

$$\frac{X_1}{R_s} = Q_f = 5 \sqrt{VSWR - 1} \quad (29)$$

This method of measuring  $f_c$  does not depend upon the assumption that capacity is independent of frequency. It does depend, though, upon the assumption that the capacity obeys a given law with respect to the applied voltage.

In summary, Table 2-3 lists the three methods, and compares the ease and accuracies of the measurements.

TABLE 2-3

Method	Complexity	Assumptions and Conditions	Remarks
Harrison	High - requires many measurements with high accuracies.	None	Needs no assumption, but requires many tedious measurements. Good for checking accuracies of other methods.
Houilding	Simple - one measurement at r-f, and low frequency measurement of capacity.	Capacity independent of frequency, and must know cartridge capacity.	Most widely used method. Easiest and fastest, actually measures $R_s$ of diode.
Modified Houilding	Simple.	Assumes that $C_v = \frac{C_0}{(1 - \frac{V}{\theta})} N$ where $N = 1/3$ for diffused and equals 1/2 for abrupt.	Extremely easy. Initial test shows good accuracy; does not give information regarding capacity or $R_s$ .

### 2.3 THE VHF AMPLIFIER

During this program, Motorola developed a low-noise 220-mc parametric amplifier as requested by AFCRL and to fulfill the objective (4) of paragraph 1.1.1.

Basically, this parametric amplifier consists of two capacitively-foreshortened, quarter-wave cavities coupled by the varactor diode at the high impedance points. The input cavity is tuned in the quarter wavelength mode to the signal frequency. A higher order mode is utilized for the pump injection. The signal input and output are coupled via loops while the pump is injected via a capacitive hat. Tuning is accomplished by a coaxial capacitor. The varactor couples the signal and idler cavities. A means is provided for biasing the varactor diode either by a self-bias resistor which is included in the cavity or by external bias. The idler is also a tuned coaxial tank.

The signal and the pump, both of which are injected into the input cavity, mix in the varactor diode to excite the idler tank. The idler then mixes with the pump again in the varactor diode to produce the signal frequency in a positive feedback phase.

A sketch of the Motorola Model LPA01 parametric amplifier for 180 to 270 mc is shown in Figure 2-10. The pump and signal tank circuits are combined into one coaxial line, being resonant to the signal in the quarter wavelength mode, and to the pump in a higher order mode. The varactor couples the signal tank to the idler, which is in the form of a coaxial line with an adjustable short circuit. The signal is coupled in and taken out via loops. It is important to note that the input coupling is greater than the output coupling. This provision minimizes the effect of noise coming from the remainder of the receiver and being amplified in the parametric amplifier and then returned to the receiver. A lower over-all noise figure is thereby obtained.

The pump is coupled by an adjustable capacitive hat. The signal tuning is provided by a coaxial capacitance in the form of a screw and the idler is tuned by adjusting the shorted line.

The Motorola Model LPA01 parametric amplifier is tunable from 180 to 270 mc. It is capable of producing 16 db of gain with greater than 1.0 mc bandwidth over the tuning range. The noise figure is less than 1.5 db over the tuning range, 1.4 db being measured at most frequencies with a system measurement accuracy of  $\pm 1$  db. The pump power required is about 1 mw for all frequencies. The pump frequency varies from about 1200 mc to 1700 mc, depending on signal frequency. The amplifier is stable with relatively constant pump conditions and constant input and output loading.

The Model LPA01 parametric amplifier has been designed to give the lowest possible over-all noise figure for a given system and yet require the minimum of pump power. The coupling is adjusted to minimize the effect of mixer noise entering the parametric amplifier, being amplified, and then sent back to the mixer. This is accomplished without the use of a circulator. The low pump power requirement is obtained by use of a built-in matching system, the signal cavity resonance at the pump frequency. The low pump power makes possible an all-transistorized pump source, leading to an all-solid-state receiver with a parametric amplifier.

Included in this section are performance curves for an early prototype of LPA01. Figures 2-11 through 2-23 are curves of frequency versus noise figure, bandwidth, dynamic range, pump power, pump frequency, stability, and pump bandwidth.

When amplifier LPA01 was designed, no circulator was available. As a result, relatively poor stability with respect to antenna impedance changes had to be tolerated. Now, however, circulators at 220 mc are feasible. The use of these circulators is strongly recommended when stability is a problem.

#### 2.4 THE S-BAND AMPLIFIER

As stated in item 6 of paragraph 1.1.1, the construction of an optimum amplifier to operate at S-band is an objective of this program. Such an amplifier was developed and

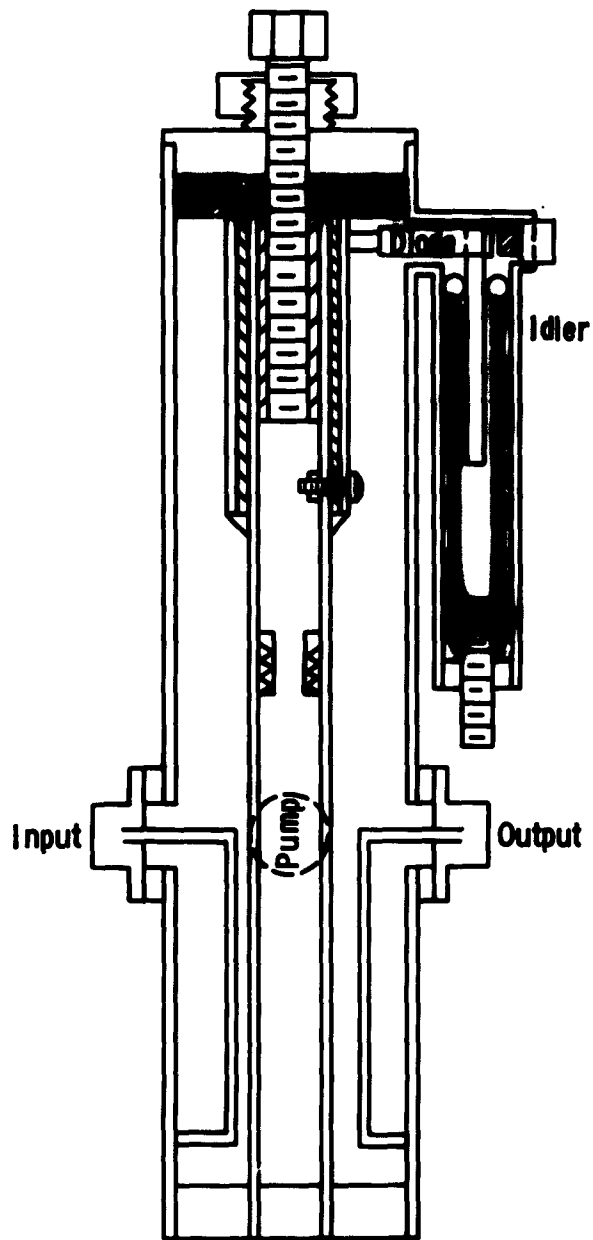


Figure 2-10. Cross-Sectional View of Parametric Amplifier for 170 to 250 MC

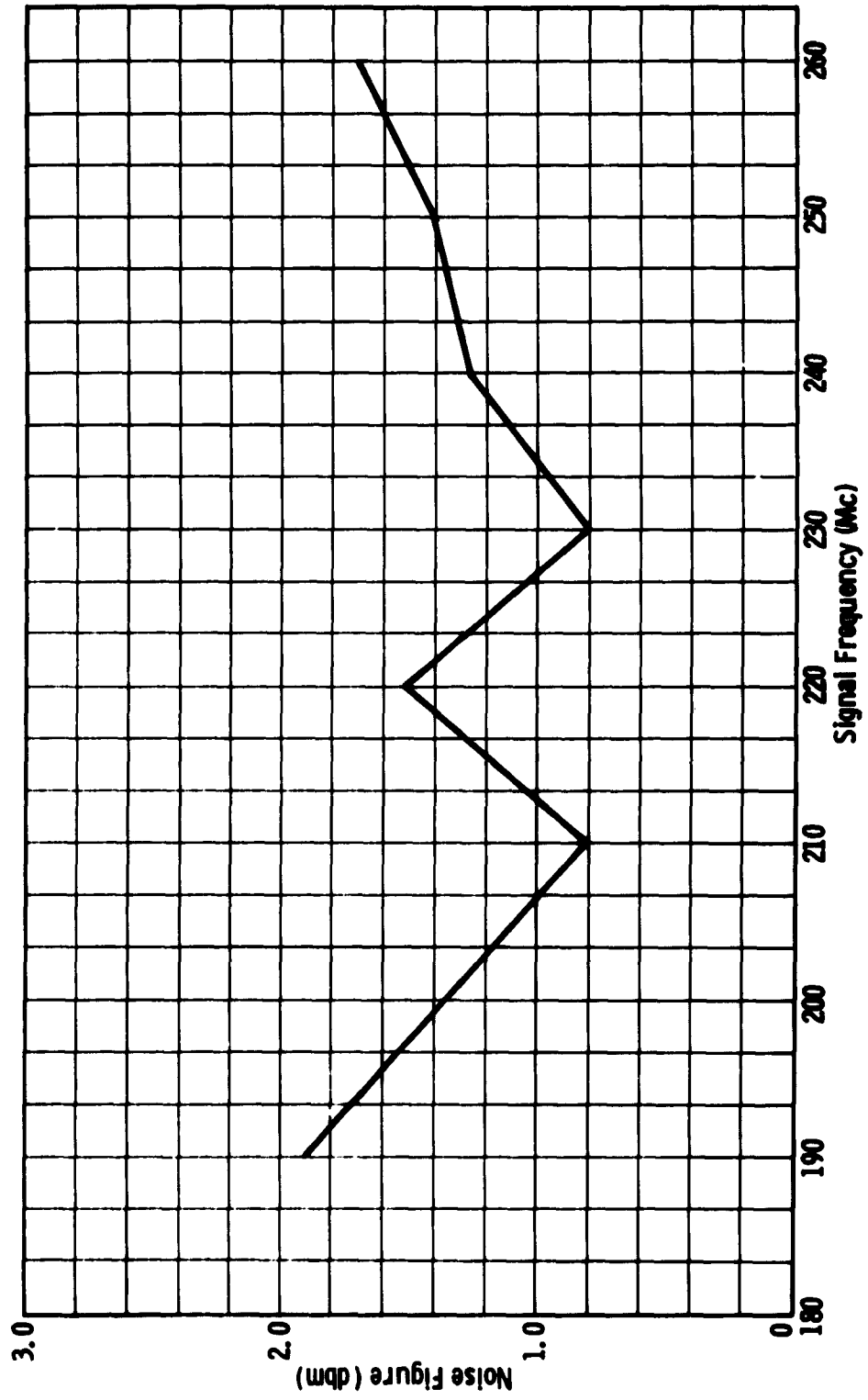


Figure 2-11. Noise Figure vs Signal Frequency for Parametric Amplifier (Model LPA01)

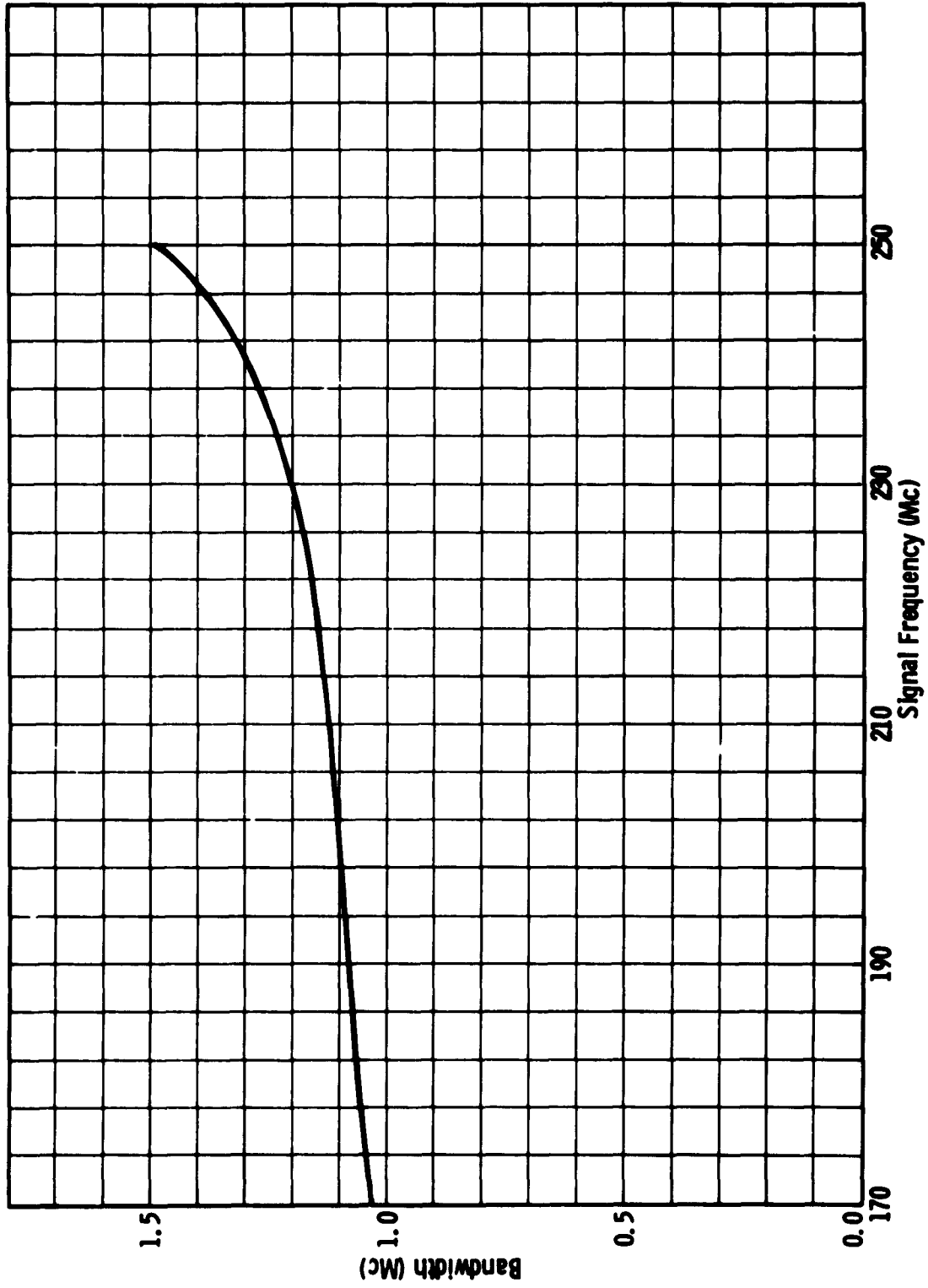


Figure 2-12. Bandwidth vs Signal Frequency for Parametric Amplifier (Model LPA01)

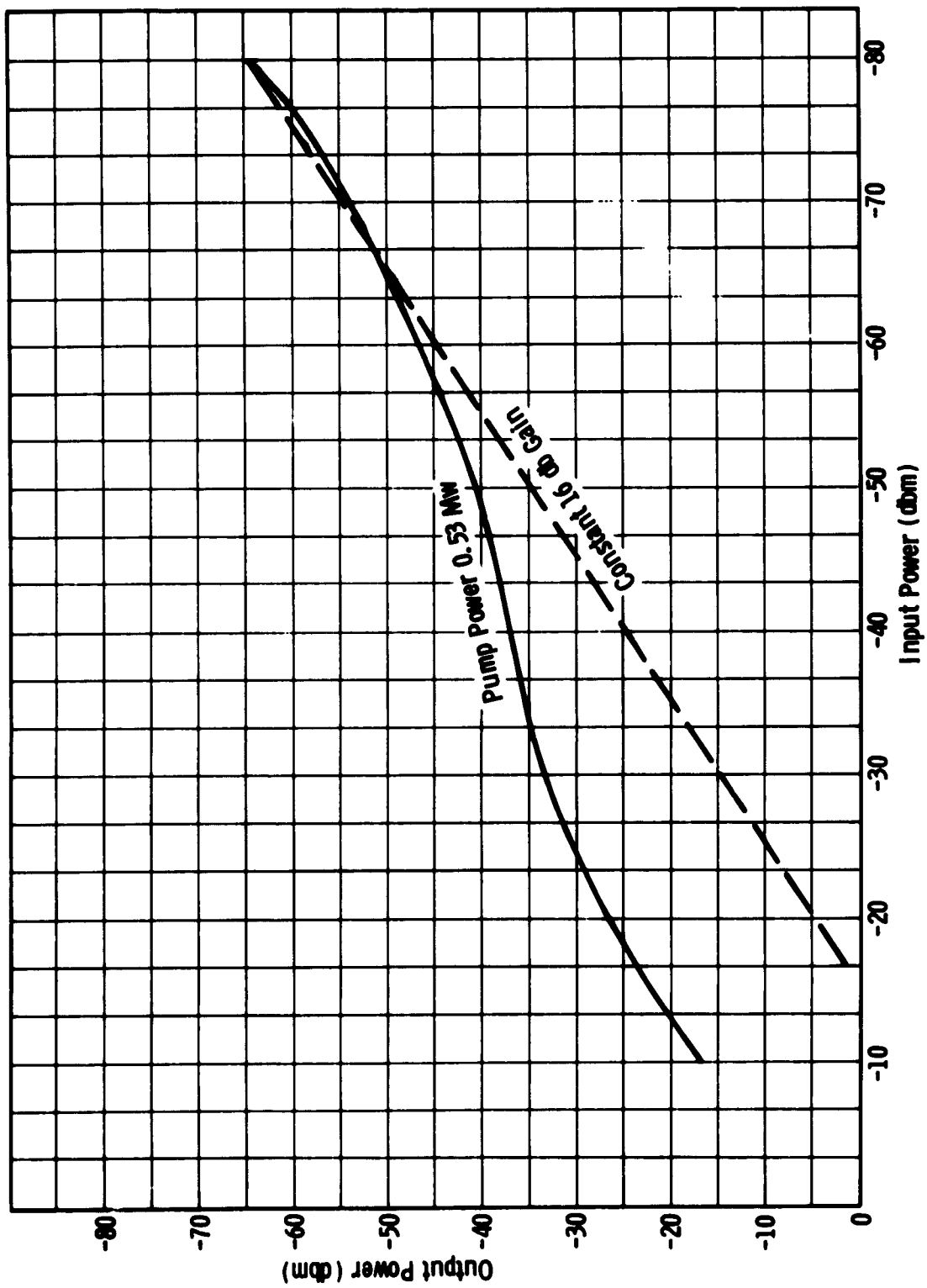


Figure 2-13. Output Power vs Input Power for Parametric Amplifier (Model LPA01) with 170 MC Signal Frequency

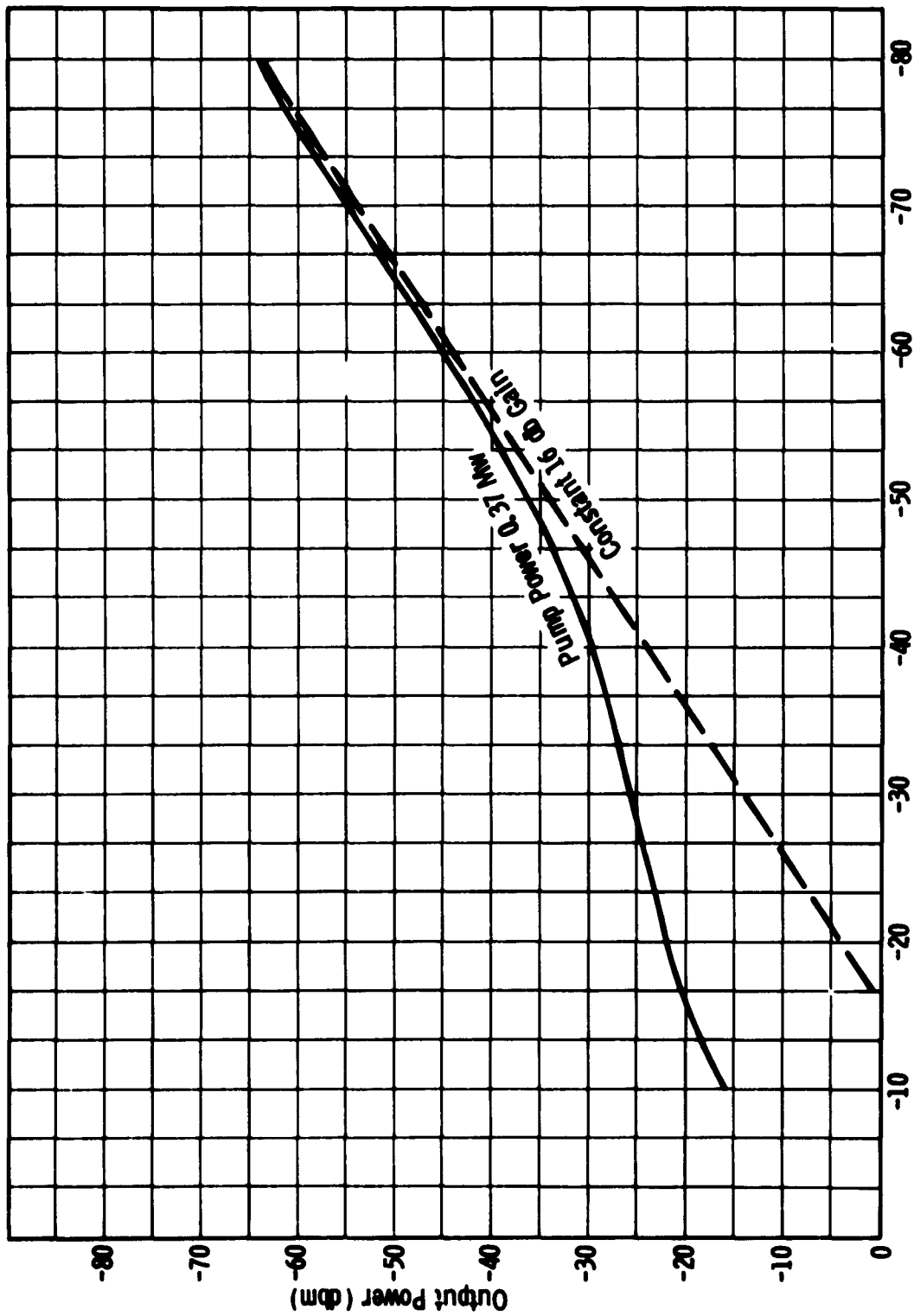


Figure 2-14. Output Power vs Input Power for Parametric Amplifier (Model LPA01) with 210-MC Signal Frequency

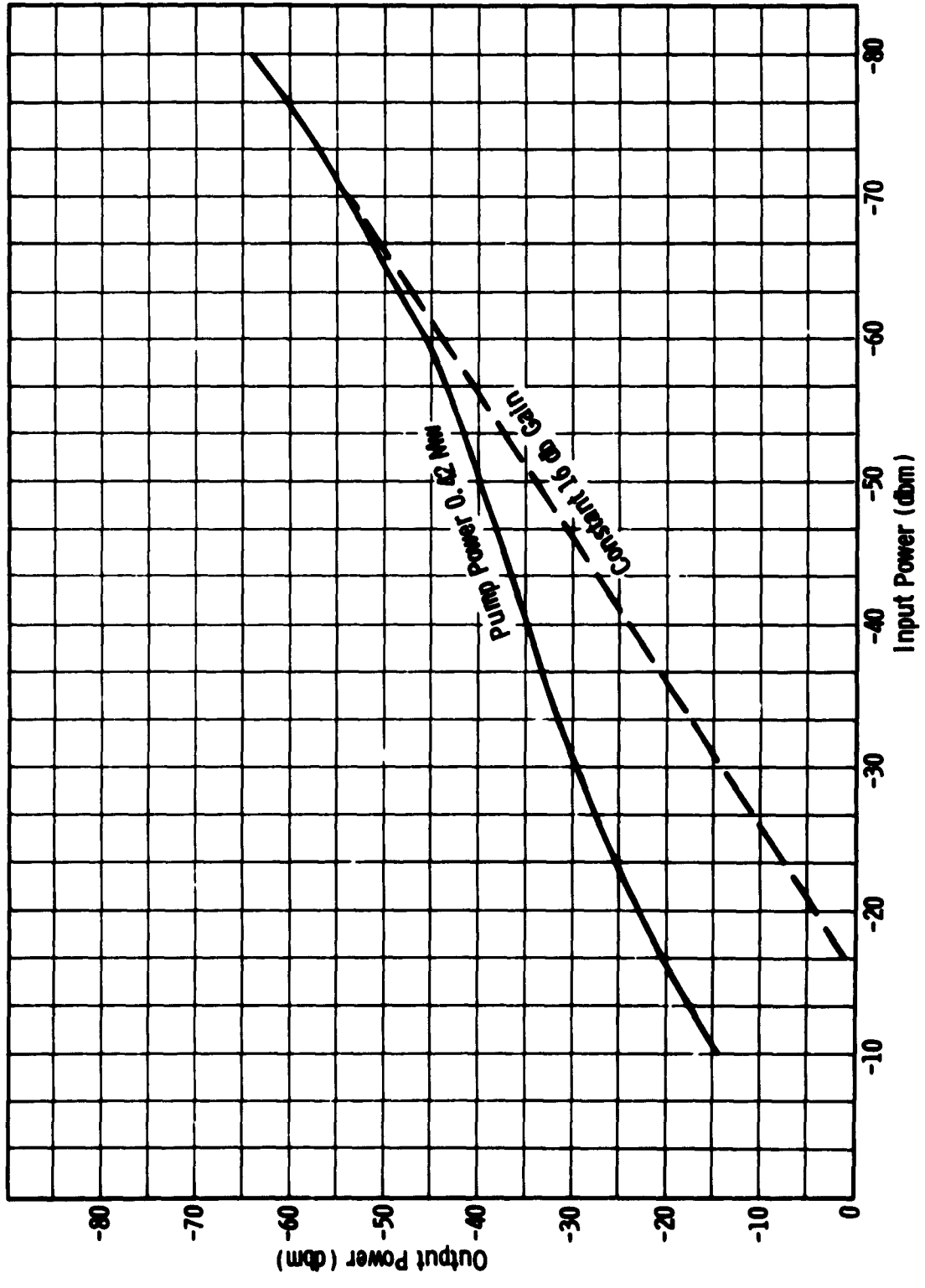


Figure 2-15. Output Power vs Input Power for Parametric Amplifier (Model LPA01) with 190-MC Signal Frequency

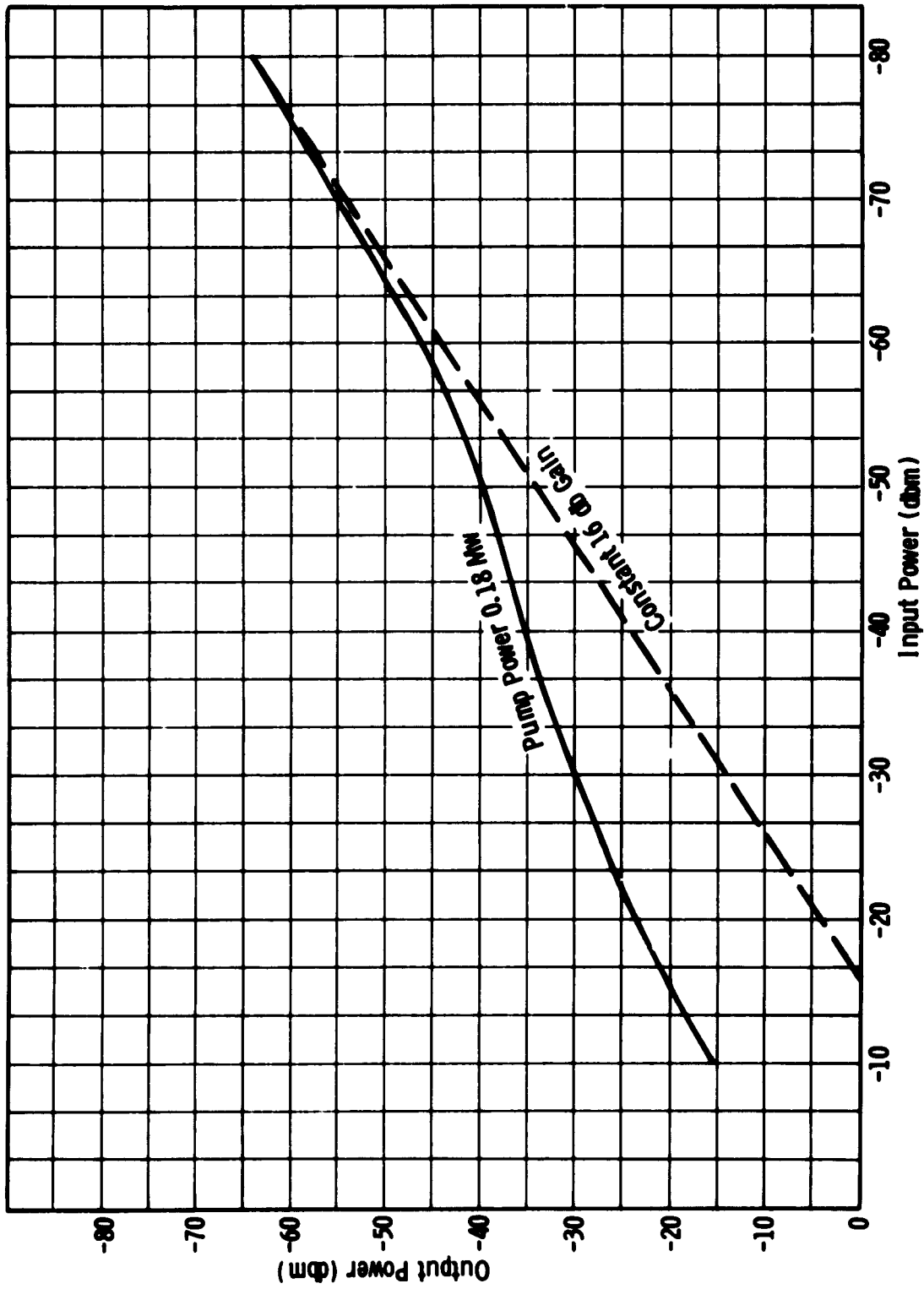


Figure 2-16. Output Power vs Input Power for Parametric Amplifier Model LPA01) with 230-MC Signal Frequency

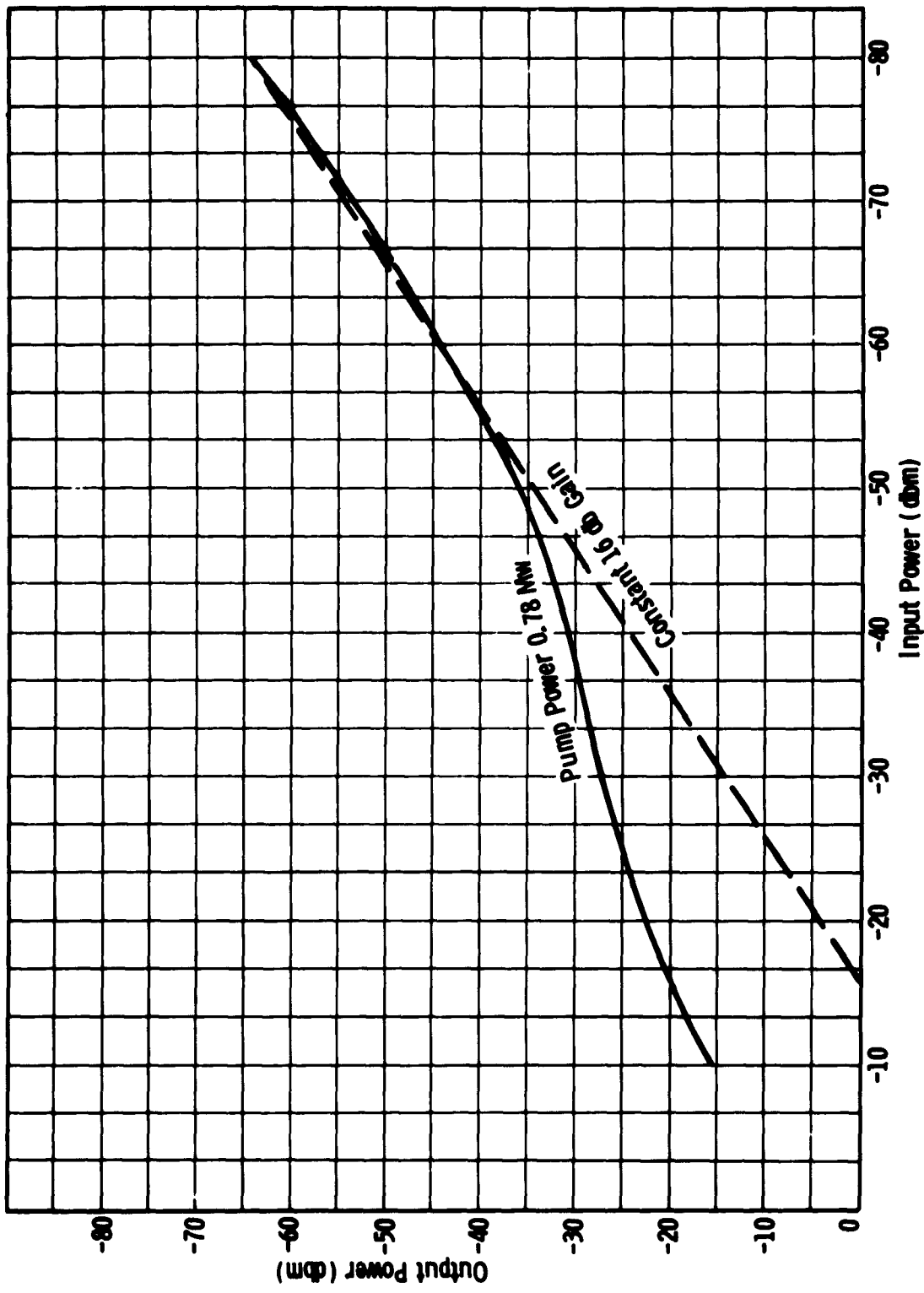


Figure 2-17. Output Power vs Input Power for Parametric Amplifier (Model LPA01) with 250-MC Signal Frequency

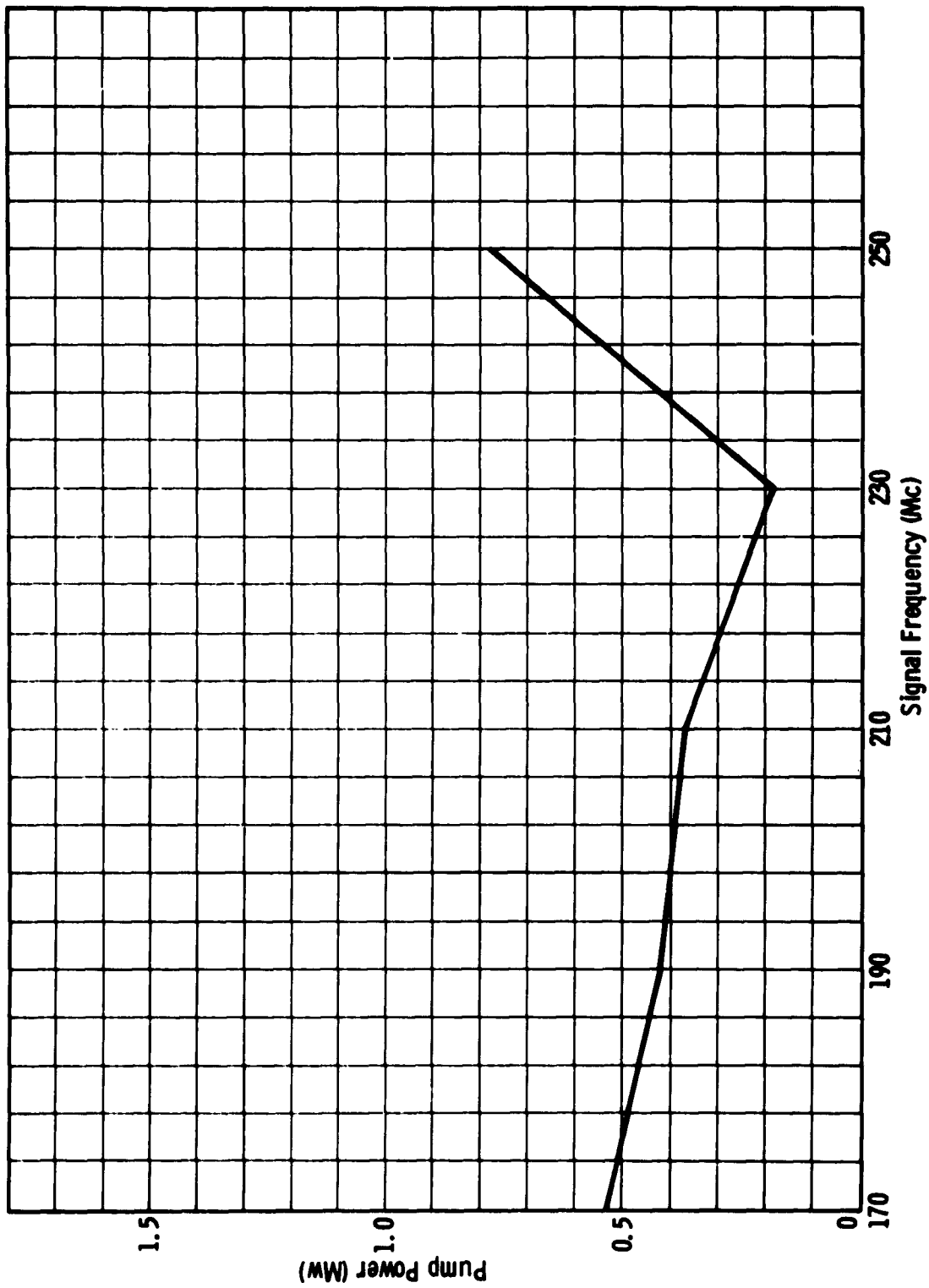


Figure 2-18. Pump Power vs Signal Frequency for Parametric Amplifier (Model LPA01) with Gain Constant at 16 DB

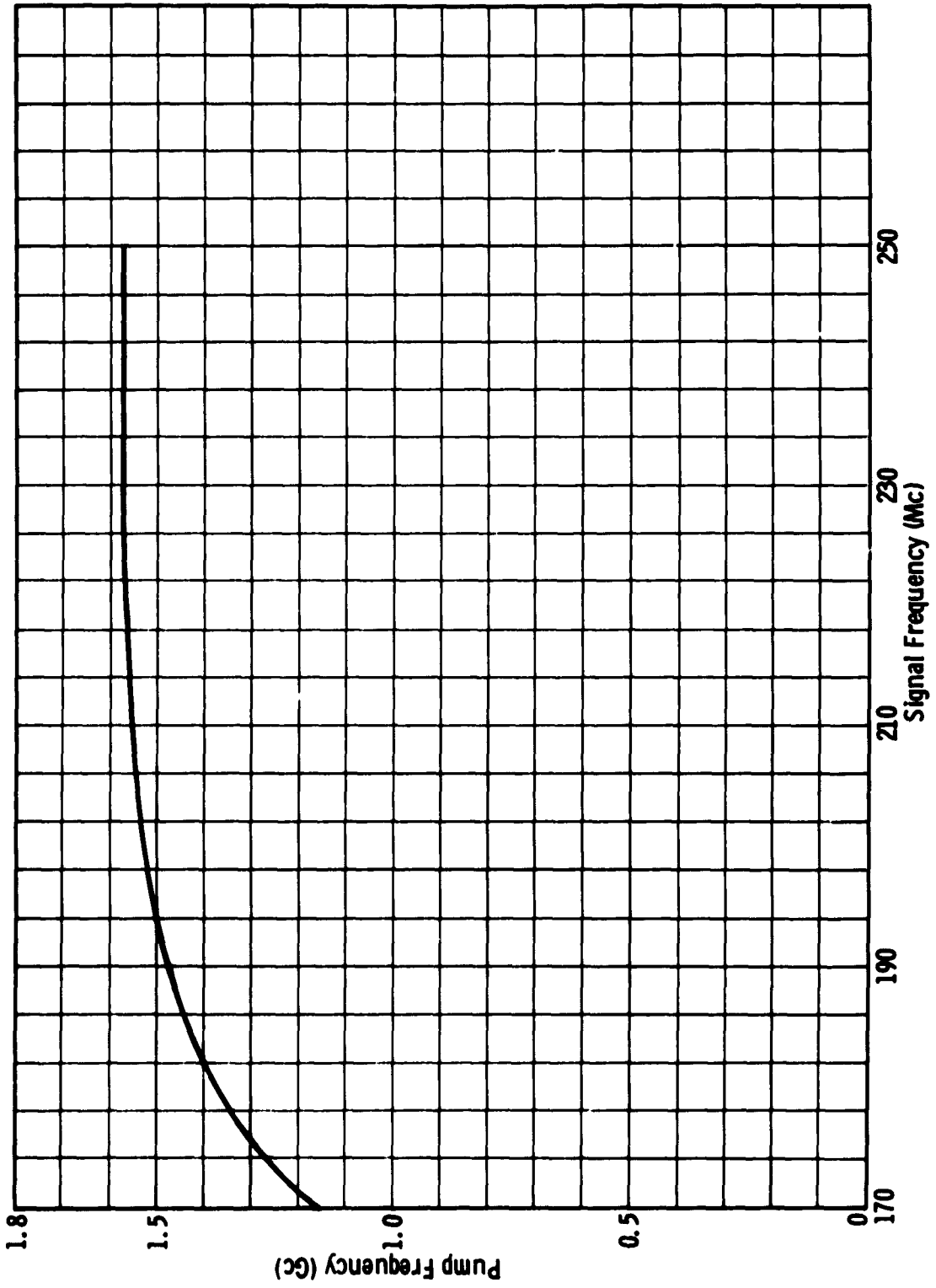


Figure 2-19. Pump Frequency vs Signal Frequency for Parametric Amplifier (Model LPA01)

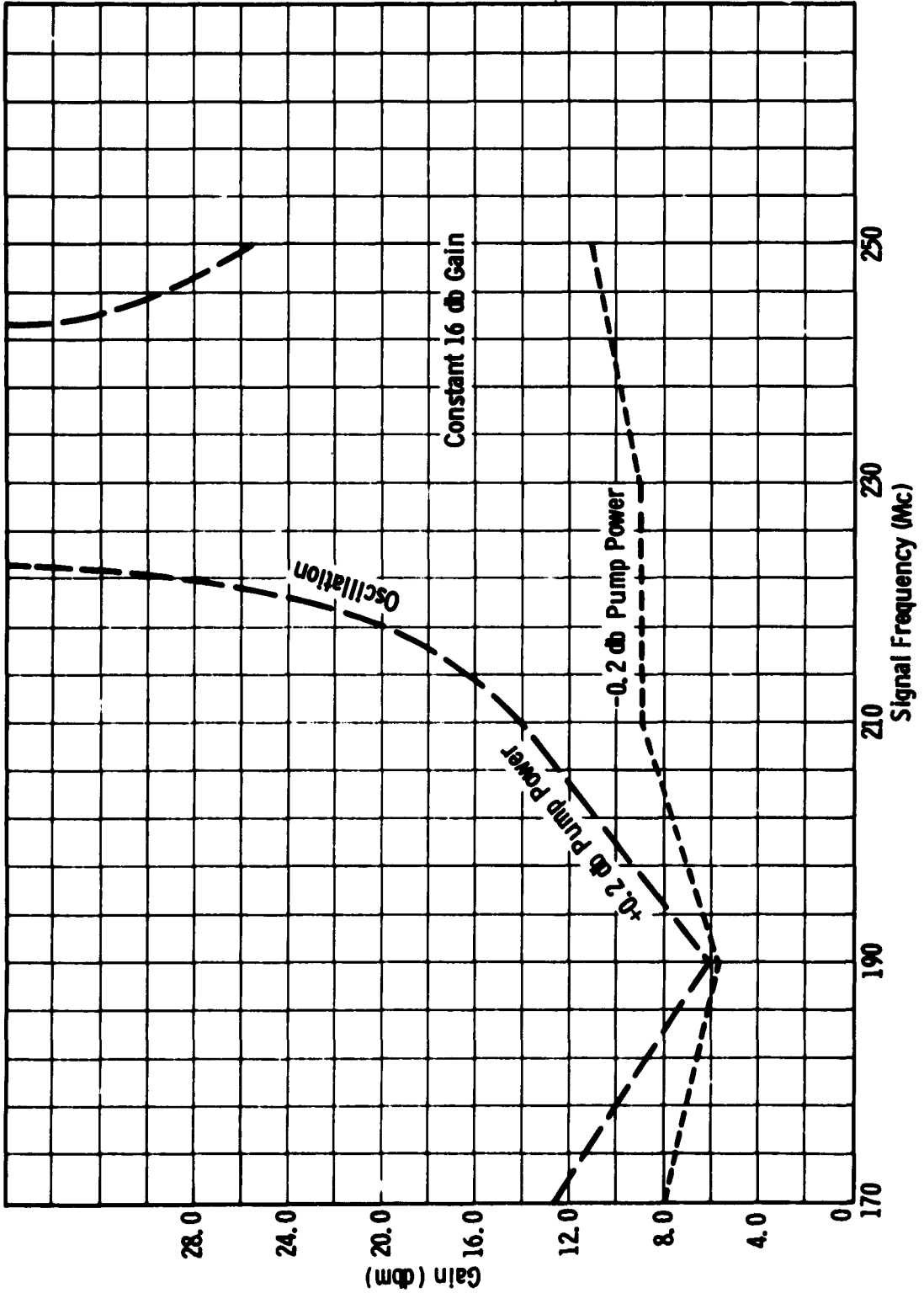


Figure 2-20. Stability to Pump Power for Parametric Amplifier (Model LPA01) with Gain Constant at 16 db

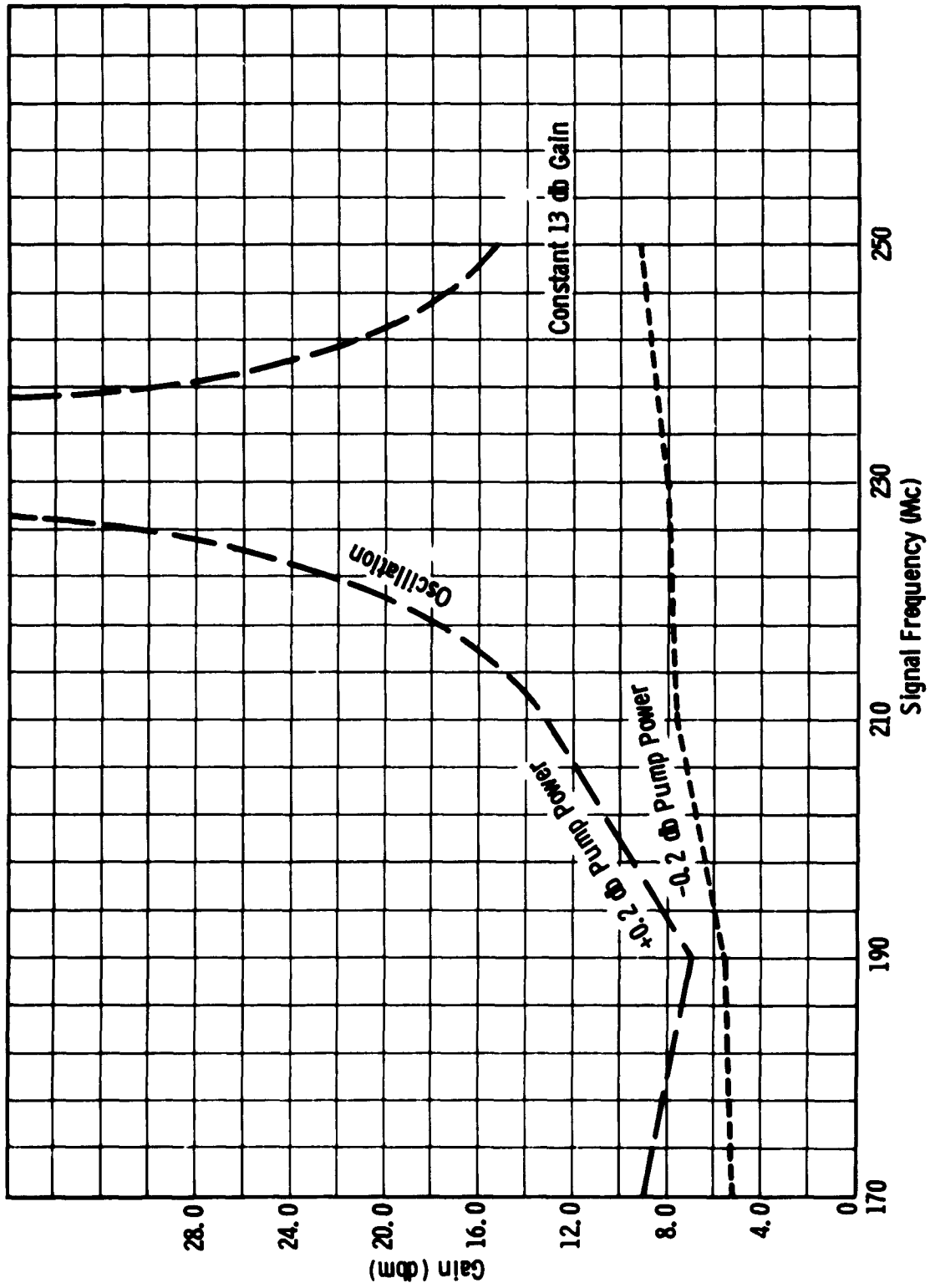


Figure 2-21. Stability to Pump Power for Parametric Amplifier (Model LPA01) with Gain Constant at 13 db

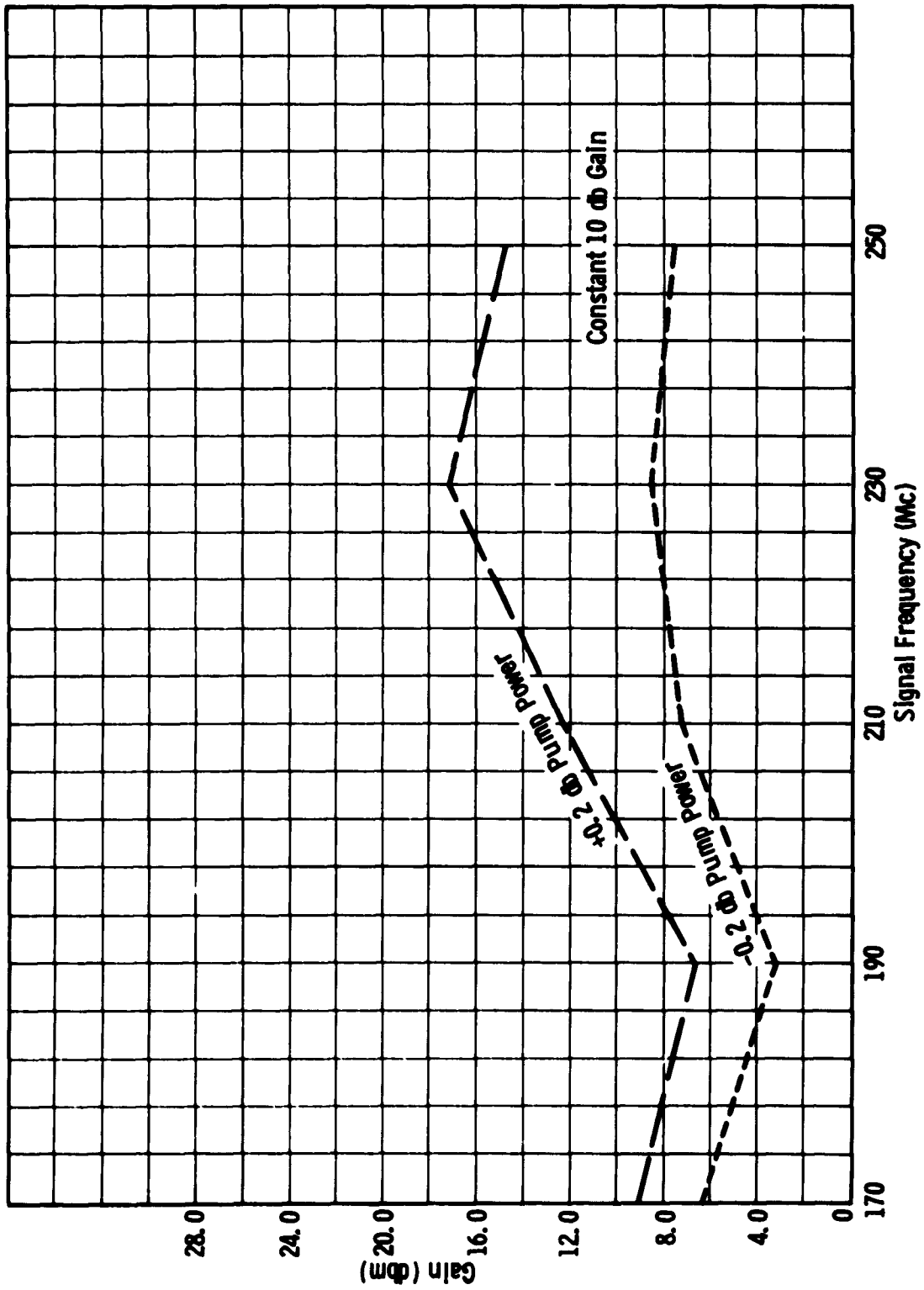


Figure 2-22. Stability to Pump Power for Parametric Amplifier (Model LPA01) with Gain Constant at 10 db

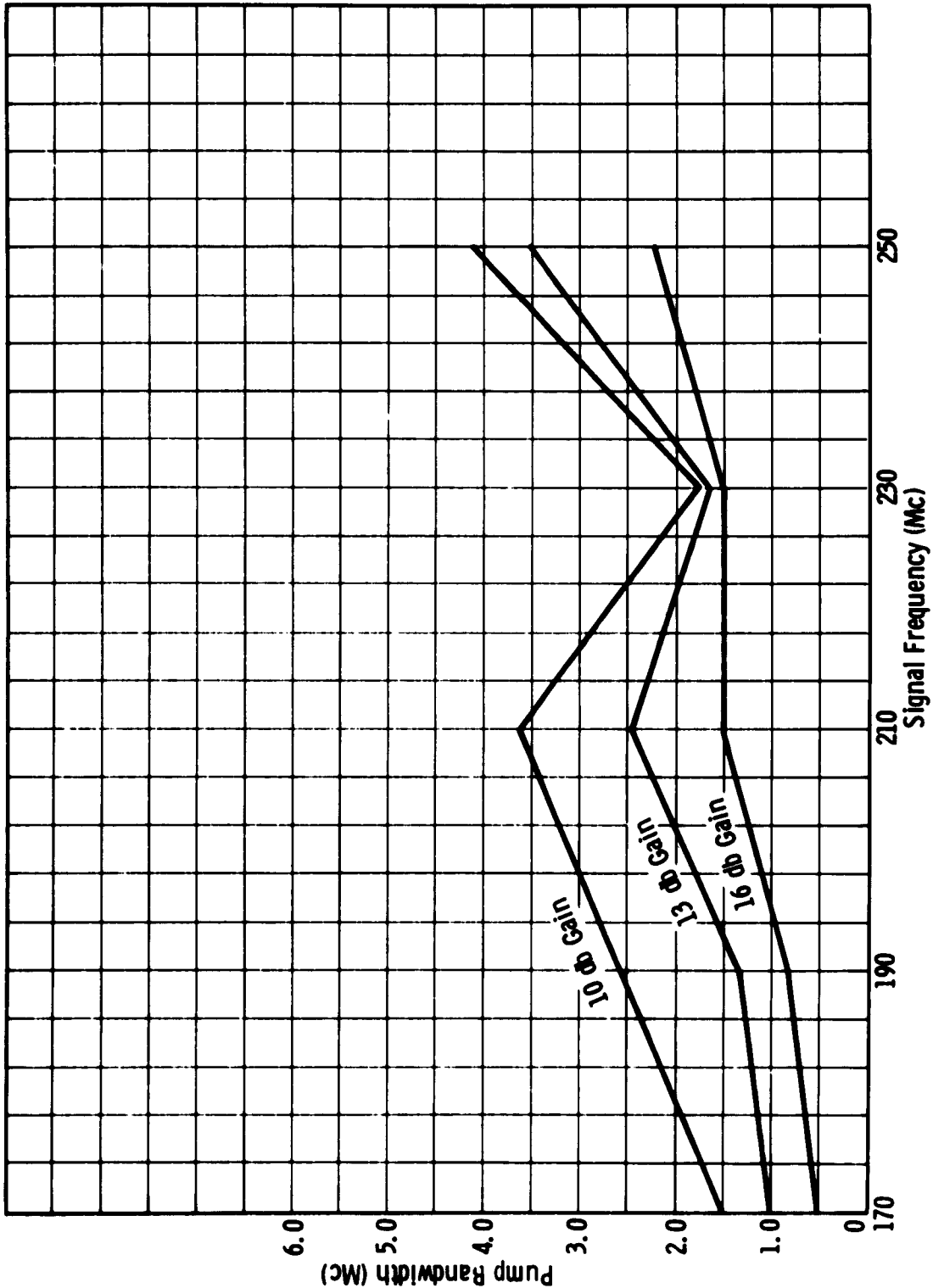


Figure 2-23. Pump Bandwidth vs Signal Frequency for Parametric Amplifier (Model LPA01)

delivered as part of this program. At the time of its development, that amplifier had the highest gain bandwidth product of any S-band nondegenerate amplifier reported in the literature.

The amplifier developed during this program is a single diode S-band parametric amplifier, operating in the nondegenerate mode with a large gain bandwidth product.

Specifically, bandwidths up to 80 mc have been measured at a center frequency of 2.5 gc, with voltage gain-bandwidth products of 500 mc and noise figures of 2.0 db.

The amplifier utilizes bandpass filters in the input and idler circuits in a manner similar to that suggested by Seidel and Herrmann<sup>6</sup> for degenerate-mode configurations. Applying broadband filters to the signal and idler circuits increased the bandwidth from 20 mc for the single-tuned case to 80 mc. Also utilized, for convenience in tuning and obtaining a wide bandwidth, is a separate tuning adjustment for the pump and an external idler load. A unique feature of this amplifier is that it can be operated in the following modes: (1) wideband with the idler termination at room temperature, (2) wideband with a cooled idler termination for lower noise figures, (3) narrowband without the external idler termination for minimum noise figure, and (4) regenerative up-converter with an X-band output, thereby yielding a low-noise two-port device with increased gain over the equivalent one-port device having the same regeneration.

The amplifier, shown in Figure 2-24, has low-loss, low-noise tuners constructed for minimum back lash and susceptibility to vibration. Diode bias is applied via the fourth port of a four-port circulator, thereby decreasing the radiation problems normally encountered in conventional diode biasing circuits. Figure 2-25 is a block diagram representation of the parametric amplifier. The input filter consists of two quarter-wavelength stub tuners (non-contacting) in strip transmission line, and the idler filter consists of three direct coupled cavities in RG52/U waveguide. The position of the idler cavities is important, and in the first models this position was adjustable. However, an optimum position for the first idler cavity was found which has proven satisfactory on subsequent models. The high-pass filter located on the pump side of the varactor is a short section of waveguide beyond cutoff which slides inside the RG52/U waveguide. The cutoff frequency of this filter is 10.5 gc; therefore, the filter acts as an adjustable short for the 9.0 gc idler circuit, while passing unaffected the 11.5 gc pump.

Typical results for this amplifier are as follows:

$f_o =$	2500 mc
$BW_{3 \text{ db}} =$	70 mc
$BW_{0.5 \text{ db}} =$	65 mc
Bandpass ripple =	< 0.75 db,
Gain =	17.0 db
Noise figure (less circulator) =	2.0 db,
$G^1 2 BW_{3 \text{ db}} =$	495 mc .



Figure 2-24. S-Band Parametric Amplifier

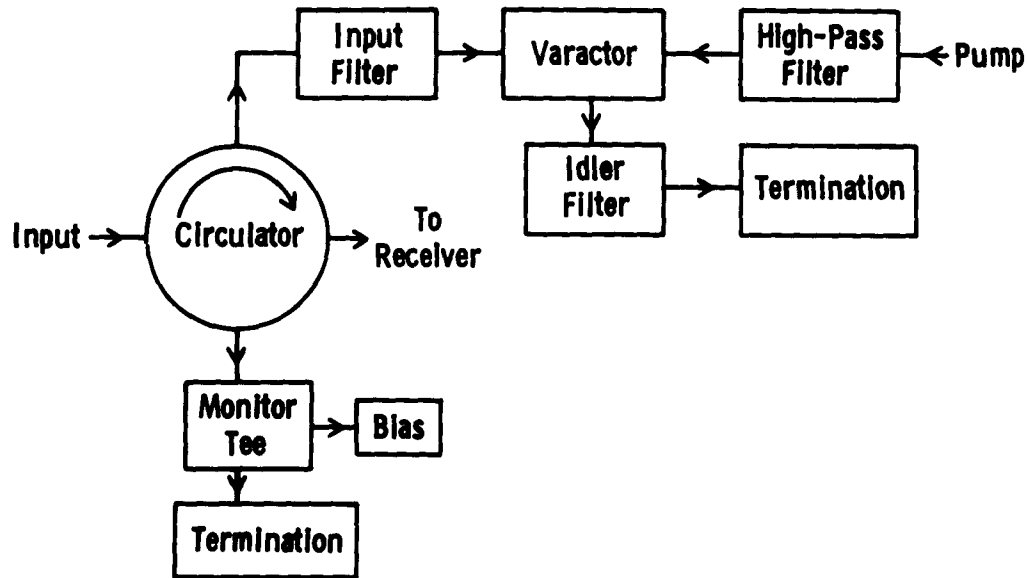


Figure 2-25. Block Diagram of S-Band Parametric Amplifier (Model SPA01)

## 2.5 THE X-BAND AMPLIFIER

The major effort on this program was directed towards the development of X-band parametric amplifiers. The objectives of this work are given in paragraphs 1.1.4, 1.1.5, and 1.1.8. The objectives encompass both degenerate- and nondegenerate-mode amplifiers. As a result of this program, a breadboard of a degenerate-mode amplifier was built and a nondegenerate-mode amplifier was developed and delivered.

### 2.5.1 Degenerate-Mode Amplifier

A breadboard version of a degenerate-mode amplifier was developed during this program. The amplifier consisted of two crossed waveguides, with the varactor coupling these guides. The signal is applied via a standard RG52/U waveguide from a circulator to the amplifier signal circuit. The signal circuit consists of a low-pass filter, a quarter-wave transformer from standard guide height to one-half standard guide height, the diode mount, and a non-contacting tuner. The pump circuit consists of a noncontacting tuner, the diode mount, a pump level attenuator, a directional coupler, an E-H tuner and a Raytheon 6253 klystron, all for RG53 U waveguide. A photograph of the amplifier assembly itself is shown in Figure 2-26.

A block diagram of the test setup for the X-band amplifier is shown in Figure 2-27.

The X-band signal (usually either a pulsed carrier or noise) passes through the circulator into the parametric amplifier. With the pump power attenuated to a low value, the X-

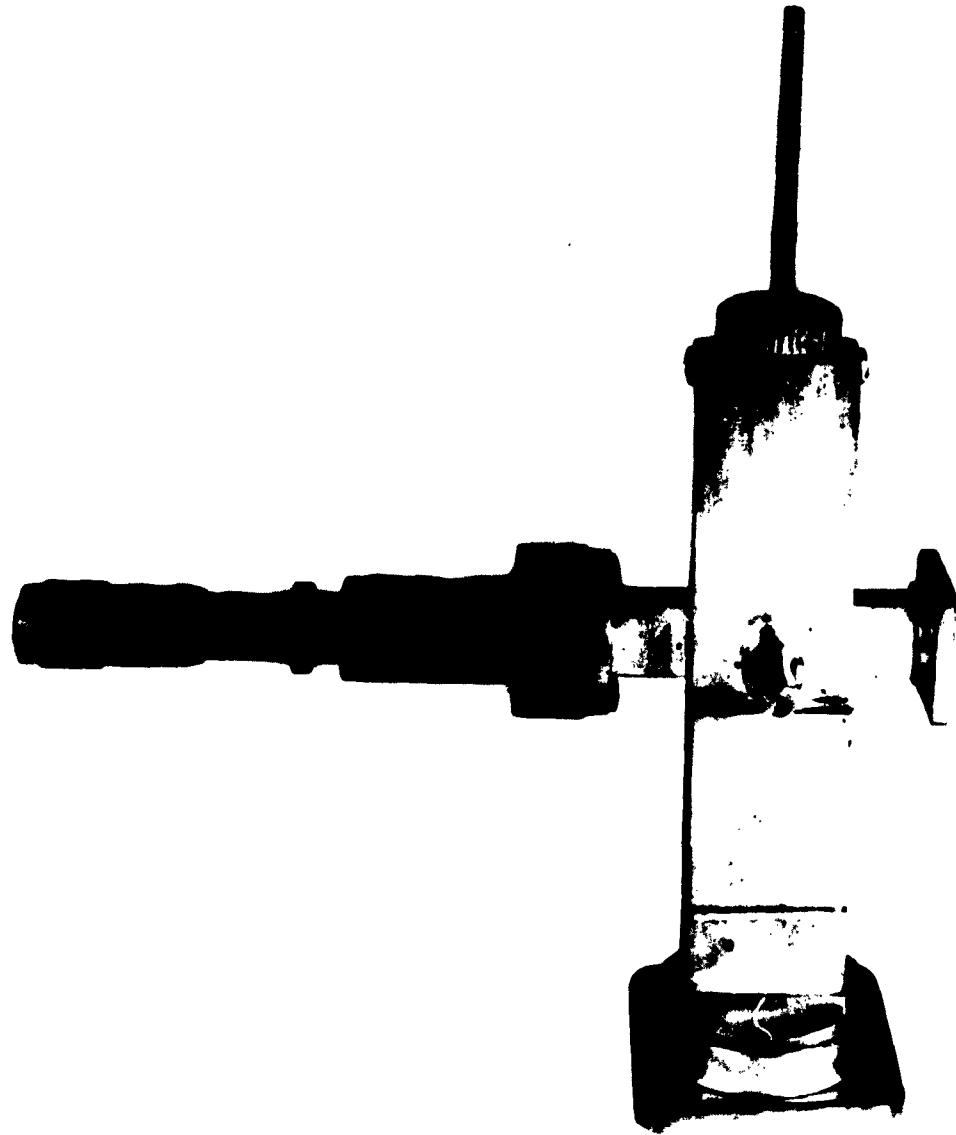


Figure 2-26. Experimental X-Band Degenerate Mode Amplifier

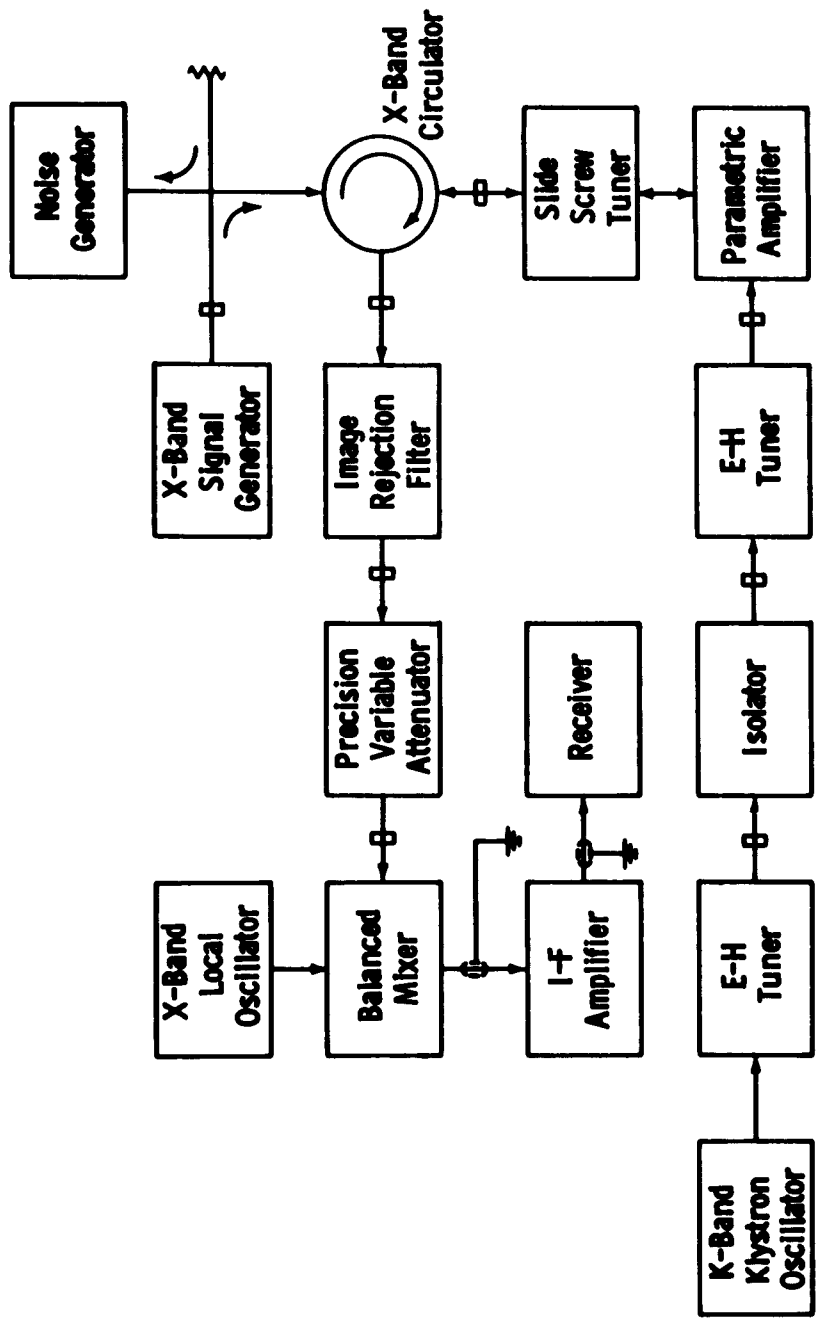


Figure 2-27. Arrangement for Bench Testing of X-Band Parametric Amplifier, Block Diagram

band signal is partially absorbed in the varactor and partially reflected back through the circulator into the balanced mixer. The pump signal is supplied by a Raytheon 6253 klystron, tunable from 18 to 22 gc. An E-H tuner is utilized to obtain maximum power out of the klystron (about 50 mw), with full pump power applied to the amplifier signal and pump mix to produce the idler frequency which is nearly the same as the signal frequency. The signal circuit is also used for the idler because of the proximity of the signal and idler frequencies. The idler reacts with the pump in the varactor to reproduce the signal, thereby completing the positive feedback path. The amplified signal goes back through the circulator into the balanced mixer and the i-f amplifier.

The successful operation of this amplifier depends primarily on the quality of the varactor. Several MA460C and MA460E diodes were tried without success. The first diode to operate this amplifier was a point-contact gallium arsenide made at the Bell Telephone Laboratories. The performance of the degenerate-mode amplifier at 9.31 gc with the BTL diode is given in Table 2-4.

TABLE 2-4. PERFORMANCE DATA FOR DEGENERATE-MODE X-BAND PARAMETRIC AMPLIFIER

Gain (db)	Frequency (gc) Pump	Signal	Bandwidth (mc)	Noise Figure (db)	Pump Power (mw)
20	18.610	9.310	10	---	15
16	18.610	9.310	16	6.9	15
13	18.610	9.310	21	---	15
10	18.610	9.310	40	7.1	15

One gallium arsenide diode built by Motorola's Semiconductor Division also operated the X-band amplifier. This diode gave a 6.5 db single-channel noise figure at a 9.2 gc signal with 10 db gain.

There were two disadvantages with the gallium arsenide diodes. One disadvantage is that the quality of the diodes gradually deteriorated with age. After about 6 months of shelf environment, neither gallium arsenide diode discussed above would operate the amplifier. The other disadvantage is that the diodes are quite fragile, both electrically and mechanically. These diodes burn out easily and because of the quartz sleeve, break with application of a relatively low shear-type force.

In an attempt to overcome the limitations of the gallium arsenide diode, extensive testing of silicon diodes was continued. Finally, a Hughes experimental silicon diode was obtained which gave 16 db gain and a 5.2 db single-channel noise figure. Since then this type of performance has been repeated with several MA4298 diodes.

When improved diodes such as the MA4298 became available, it was felt the optimum X-band amplifier was no longer a degenerate type. Accordingly, the effort on the degenerate-mode configuration terminated and work began on the development of a nondegenerate-mode configuration.

### 2.5.2 Nondegenerate-Mode Amplifier

In accordance with the objectives outlined in paragraphs 1.1.4 and 1.1.5, an investigation of a nondegenerate-mode amplifier was initiated. The basic goal of this investigation was to construct and deliver a rugged parametric amplifier operating at 8.3 gc with a noise figure as low as the state of the art permits.

During the development, two major problems had to be solved. Both problems involved attainment of suitable components--mainly a rugged varactor with high enough Q and a pump klystron with high enough power output.

To determine the quality of diode required, the theoretical noise temperature corresponding to specific cutoff frequencies were calculated.

The performance of the X-band amplifier can be theoretically predicted using equation (30) for amplifier noise temperature.

$$T_e = \frac{G_1}{G_g} T_1 + \frac{f_{10}}{f_{20}} \left(1 + \frac{G_1}{G_g}\right) T_2 \quad (30)$$

where

- $T_e$  is the amplifier noise temperature
- $G_1$  is input circuit conductance
- $G_g$  is source conductance
- $T_1$  is input circuit temperature
- $f_{10}$  is signal frequency
- $f_{20}$  is idler frequency, and
- $T_2$  is idler circuit temperature.

Assuming the only signal and idler circuit loading is the diode, and the temperature of the diode is 290 K, equation (30) can be modified to equation (31),

$$T_e = T_d \frac{1 + \left(\frac{f_c}{f_{20}}\right)^2 \left(\frac{C_1}{C_0}\right)^2}{\left(\frac{f_c}{f_{10}}\right) \left(\frac{f_c}{f_{20}}\right) \left(\frac{C_1}{C_0}\right)^2} - 1 \quad (31)$$

where

- $T_d$  is the diode temperature.

For the diodes on hand, the cutoff frequencies are about 100 gc at -1 volt bias, and the  $C_1 : C_0$  ratio is about 0.16. With a pump frequency of 23 gc, the noise figure is calculated to be 4.7 db. For 100-gc diodes, the optimum pump frequency is 21 gc, the use of which would yield a 4.3 db noise figure.

If a diode with a 150-gc cutoff at -1 volt bias could be obtained, the noise figure would be 3 db. Diodes of such quality have been made in the laboratory, and were ordered for this

program; however, the diodes could not, at the time, be produced with any measurable yield. The high-Q diodes, which were ordered but not received, included silicon junction and gallium-arsenide junction diodes. Some high-cutoff gallium-arsenide point-contact diodes were obtained as government-furnished equipment; however, these proved too fragile for use in the X-band amplifier.

From a study of the available diodes, the desire to test a large number of diodes of a single type to insure a satisfactory yield, and the available program funds, the MA4298 was chosen as the best diode for this program. Since these MA4298 diodes have cut-off frequencies slightly in excess of 100 gc at -1 volt, the expected noise figure is 4 db with a 23-gc pump.

Initially, one and only one 4298 diode was found which operated the X-band nondegenerate amplifier. This diode achieved a 3.5 db noise figure using 60 milliwatts of pump power at 25.5 gc. The pump used was an EMI R9547 klystron operating at full capacity. Unfortunately, this diode burned out, probably because of a static-electric potential while its resistance was being measured, leaving the program without an operational amplifier.

Rather than searching for a specially selected diode to operate the amplifier, a survey of klystrons was initiated to obtain higher pump power. Several United States and foreign klystron manufacturers were contacted to determine availability and price for klystrons having greater than 150-mw output from 21 to 25 gc. Considering price and delivery, the OKI model 24V10 klystron from Japan appeared optimum. Accordingly, the 24V10 klystron proved to be excellent as shown by the performance curve in Figure 2-28.

With the 24V10 klystron, operation was obtained for almost all MA4298 diodes. This permitted an optimization of the amplifier and a continuation of the program.

Although 24V10 is not a ruggedized klystron, it is more than adequate for laboratory parametric amplifiers. Since this klystron was ordered, a more rugged klystron has become available. This new klystron, the Elliott Brothers' 12RK4, is now being manufactured by Litton Brothers as an American made component. The 12RK4 has a 500-milliwatt output capability and a narrow 400-megacycle tuning range in the band from 21 to 25 gc. Because of the relatively fixed-frequency nature of the 12RK4, an optimum design procedure for an X-band parametric amplifier would be to do the initial experimentation with the 24V10 to find the optimum pump frequency and then order a 12RK4 for the final model. Unfortunately, for this program, the 10-week delivery of the 12RK4 precluded its use since the klystron became available only a short time before the conclusion of this program.

Using the OKI 24V10 klystron as a pump, a finalized 8.3-gc parametric amplifier was assembled and tested. A photograph of this amplifier is shown in Figure 2-29 and a block diagram of the test setup shown in Figure 2-30.

The amplifier consists of crossed RG52 U (signal) and RG91/U (idler and pump) waveguides with the MA4298 coupling the two guides. The MA4298 is inserted from below the RG91 U guide, and a contact placed on the diode probes into the X-band (RG52/U) guide. A choke section is placed between the two waveguides to minimize pump leakage into the signal guide. Tunable shorts are placed behind the diode on both waveguides. A three-port

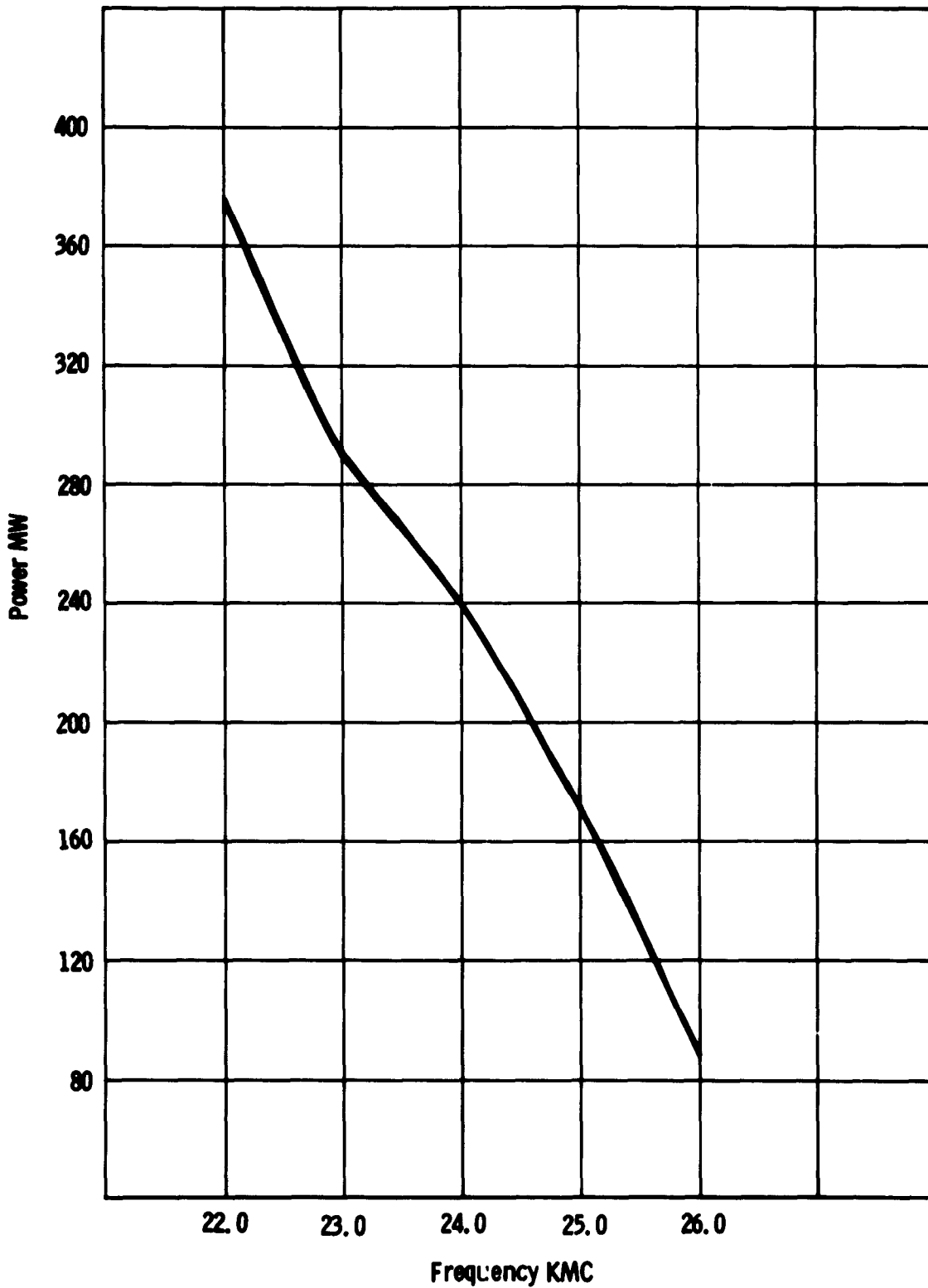


Figure 2-28. OKI 24V10 Klystron S/N 131 Output Power versus Frequency



Figure 2-29. Photograph of the 8.3 gc Parametric Amplifier

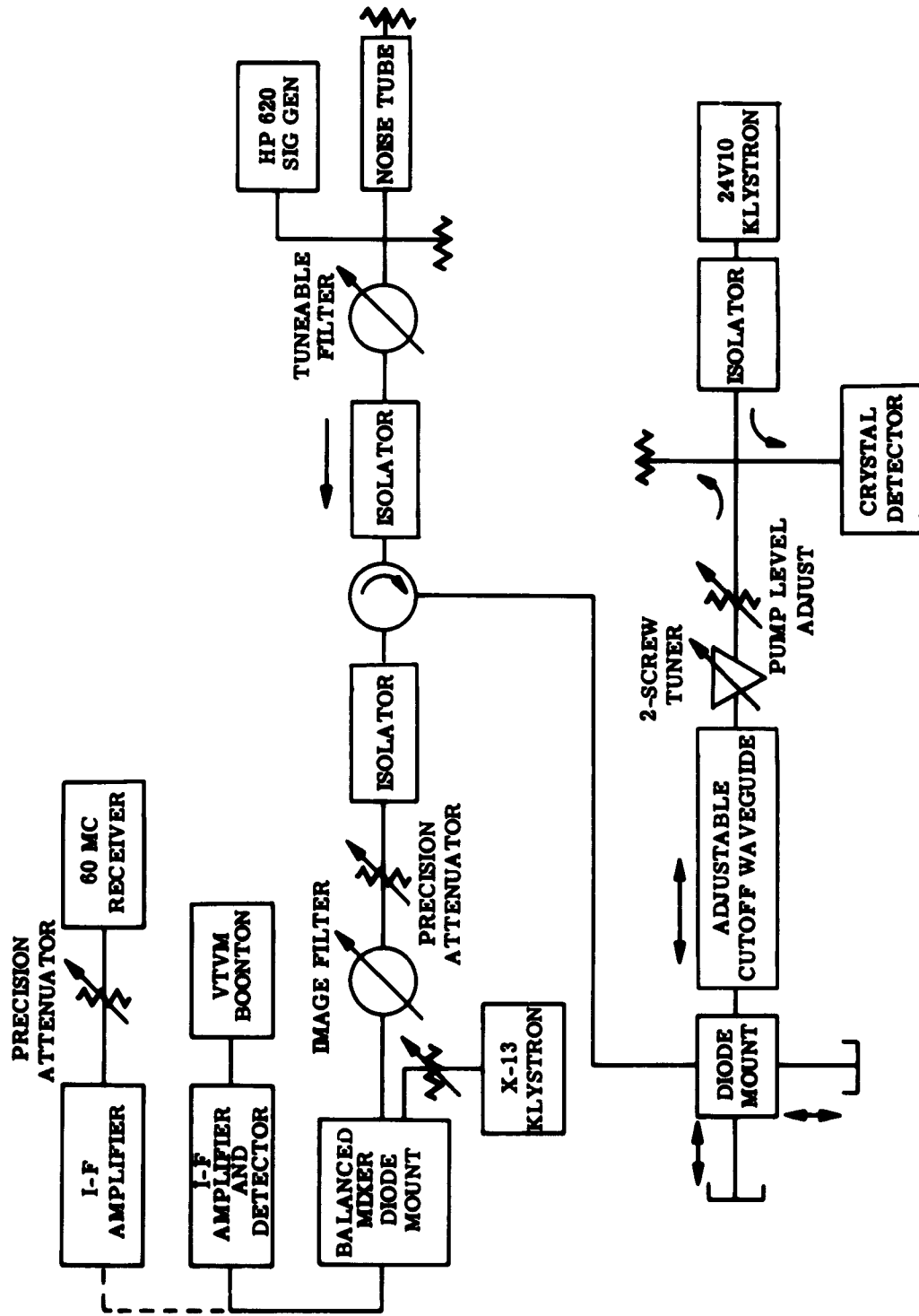


Figure 2-30. Block Diagram of X-Band Test Setup

wye circulator feeds one end of the signal guide. One end of the idler and pump guide is connected to a waveguide beyond the cut-off filter whose input is an RG63/U waveguide for the 18-to 26-gc band. Next in line in the RG63/U waveguide is a two-screw tuner to optimize pump power, followed by a pump leveler attenuator, a directional coupler, and finally the klystron. It is recommended that an isolator be placed between the klystron and the directional coupler to minimize the pulling of the klystron while the parametric amplifier is being tuned.

The test circuit consists of (in addition to the parametric amplifier) two isolators, two tunable filters, a balanced mixer and receiver, a noise tube plus termination, and a signal generator. The isolator and filter on the input of the amplifier are only used in the measurement of noise figure and are not needed in operation.

An accurate measurement of noise figure is not necessarily a straightforward procedure. A list of possible errors that can occur, as well as the corrective action needed to avoid these errors follows:

1. Gain of the parametric amplifier changes between the fired and unfired conditions of the noise tube because of insufficient circulator isolation. Use of an isolator before the circulator eliminated this problem.
2. Pump leakage from the parametric amplifier interfered with the mixer performance. Placing a tuned filter in front of the mixer to reject the pump (and also the image) alleviated this problem.
3. Noise at the idler frequency generated in the noise tube was amplified and converted to signal in such a manner to make the noise figure appear lower than actual. The use of a tunable filter after the noise tube eliminated this problem.
4. Effect of insertion loss from noise tube to circulator increased the apparent noise figure. This was eliminated by careful measurement of this insertion loss and subsequent subtracting from the measured noise figure.
5. Incomplete coupling of the noise tube to the waveguide and the effect of the termination being at 300 K rather than 290 K increased the apparent noise figure. By measurement of fired insertion loss and analyses of effect of the 300 K termination, a proper correction can be evolved which eliminates these errors. For this particular test setup, a 0.2 db correction on noise figure was used.

Using the test circuit of Figure 2-30, performance of the X-band amplifier has been evaluated for eight diodes, the data being presented in Table 2-5. With four diodes, two modes of operation were found; these were called the inner and outer modes respectively. These modes correspond to positions of the idler short with respect to the varactor diode.

With the idler short close to the diode, a position of the waveguide beyond cut-off filter can be found to give gain for most diodes; this is called the inner mode. The other mode of operation occurs with the idler short out from the diode about 1.3 inches. Again, a position of the waveguide beyond cut-off filter can be found to minimize pump power. With each case, pump frequency should be adjusted slightly for minimum pump power and maximum gain capability.

TABLE 2-5. PERFORMANCE OF THE X-BAND AMPLIFIER WITH SEVERAL MA4298 DIODES

Diode No.	Mode	Gain db	Pump Frequency gc	Pump Power mw	Noise Figure db	Bandwidth mc	Diode Capacitance pf	Cutoff Frequency gc
1	outer	15	22.98	170	3.5	18	---	---
2	outer	15	23.00	265	3.7	20	---	---
3	outer	15	23.08	235	4.0	25	---	---
5	outer	15	23.11	370	3.75	14.5	0.69	152
6	outer	15	23.08	280	3.4	18	0.74	158
7	outer	15	23.26	230	4.7	6	0.88	150
8	outer	15	22.99	190	3.5	12	0.76	153
5	inner	15	22.86	205	3.75	20	0.69	152
6	inner	15	22.82	195	3.5	17	0.74	158
7	inner	15	23.03	170	4.9	12	0.88	150
8	inner	15	23.31	350	4.8	20	0.76	153

Table 2-5 shows that noise figures between 3 and 5 db are consistently obtained. In the inner mode, bandwidths above 12 megacycles are consistently obtained whereas in the outer mode, a greater variation of bandwidths occur.

Capacitance for the various diodes are given for diodes 5 through 8 but not for diodes 1 through 3. The higher number diodes were received with the capacity information.

Variation of gain with pump frequency is shown in Figure 2-31 for both the inner and outer modes. With the inner modes, pump frequency can change 16.5 megacycles between the three db points, whereas for the outer mode the pump frequency can only change 11.4 megacycles. In this respect, the inner mode is better.

Gain versus pump power is shown in Figure 2-32. For higher gain, the change of gain with respect to pump power is 7 db per db change of pump power, which is typical for parametric amplifier performance.

The tuning range was measured and is plotted on Figure 2-33. The tuning range is over 400 megacycles with noise figures below 5 db. Actually, the upper end of the tuning range was limited by a tuning of the bandpass filters used in the test setup.

Figure 2-34 shows the temperature characteristics of the X-band amplifier. Two separate temperature tests were run; one from room temperature to approximately 200 F and the other from room temperature down to -60 F. The amplifier gain was relatively stable with increasing temperature; however, there was a fairly significant discontinuity in the gain with decreasing temperatures. Although an oscillation was not detected as the temperature was reduced, it is suspected that one did occur at about 40 F. For temperatures below 40 F, amplifier gain is relatively constant.

### 2.5.3 Broadband X-Band Amplifier

In accordance with paragraph 1.1.8 of the program's objectives, a study of broadband X-band amplifiers was undertaken. The analysis contained herein is derived from newly developed broadbanding theories<sup>8</sup> using multiple filter networks which supplement the previously discussed theory<sup>6</sup>.

#### 2.5.3.1 Analysis of a Broadband Single-Diode Amplifier

In this section, bandwidth that can be achieved using realistic diodes will be calculated. Prior to this, the derivation of equations used in the calculations will be summarized.

The diode model to be used in the analysis is shown in Figure 2-35. The cartridge capability  $C_d$  can be included in the accompanying filter if a series-resonant mode is employed. Resistance,  $R_s$ , and inductance,  $L$ , can be included in a series arm of the filter. Using  $C_0$  and  $C_1$  the following impedance matrix can be derived by inversion of the admittance matrix given by Rowe<sup>9</sup>.

$$\begin{bmatrix} V_1 \\ V_2^* \end{bmatrix} = \begin{bmatrix} j(-X_{11}) & j(-X_{12}) \\ j X_{12} & j X_{22} \end{bmatrix} \begin{bmatrix} I_1 \\ I_2^* \end{bmatrix} \quad (32)$$

where

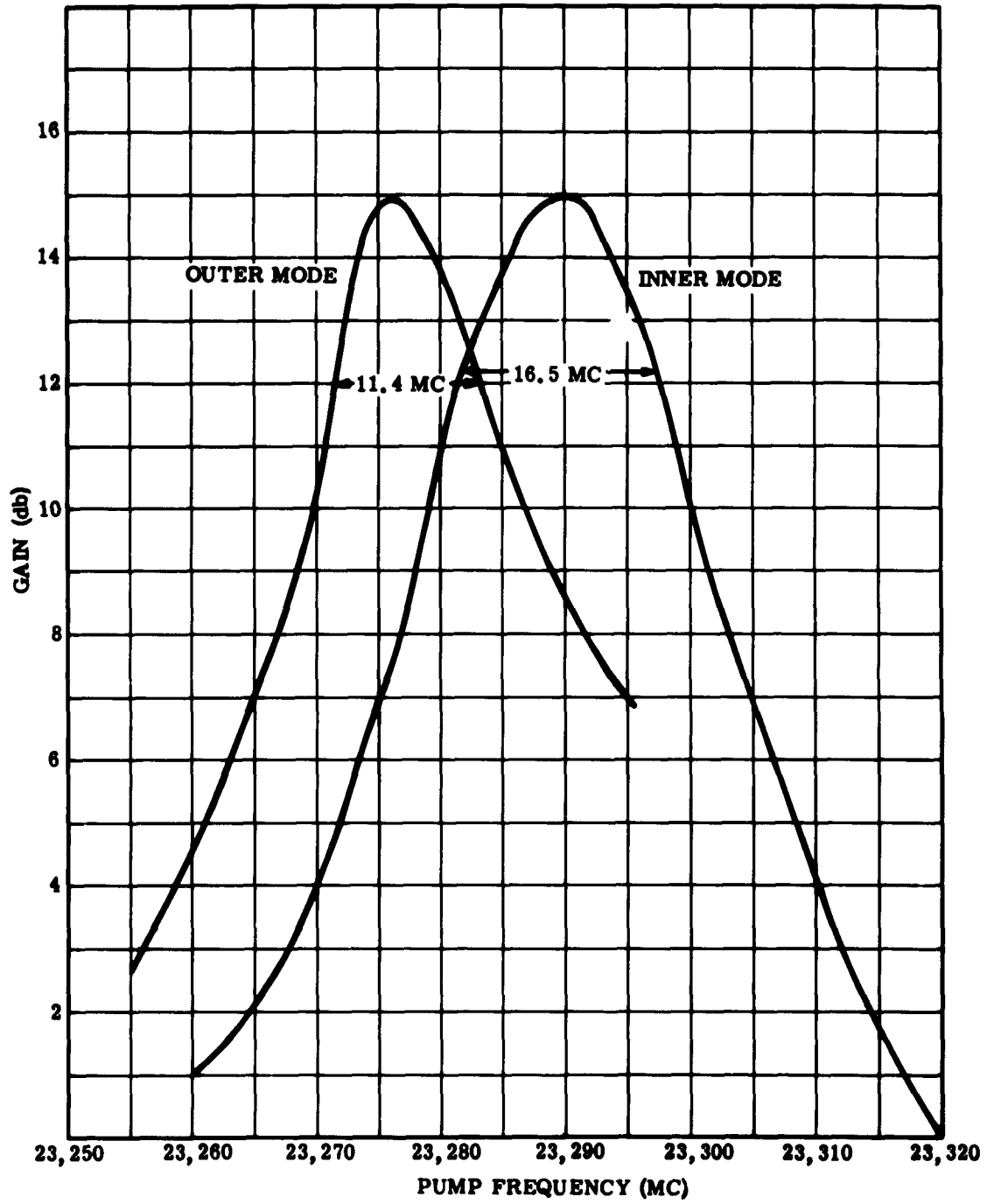


Figure 2-31. Gain versus Pump Frequency for Two Modes of Operation

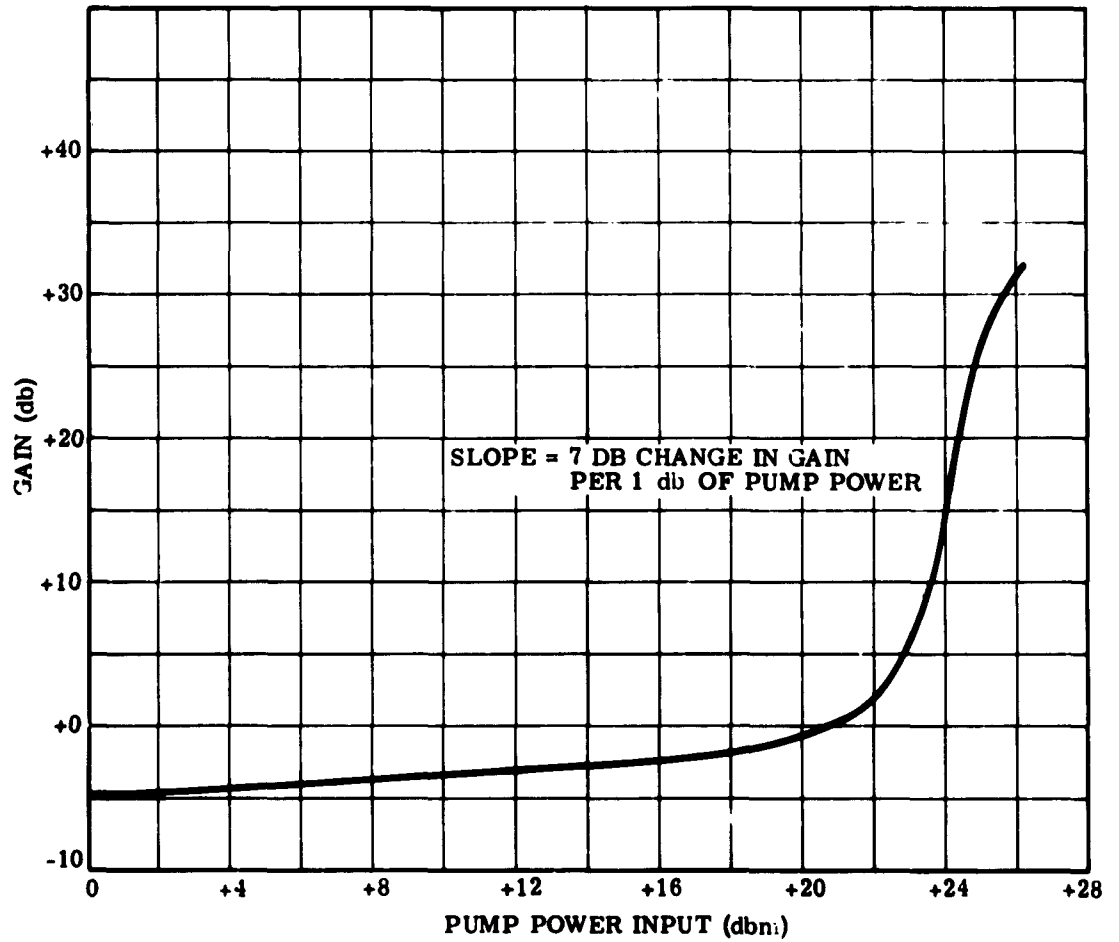
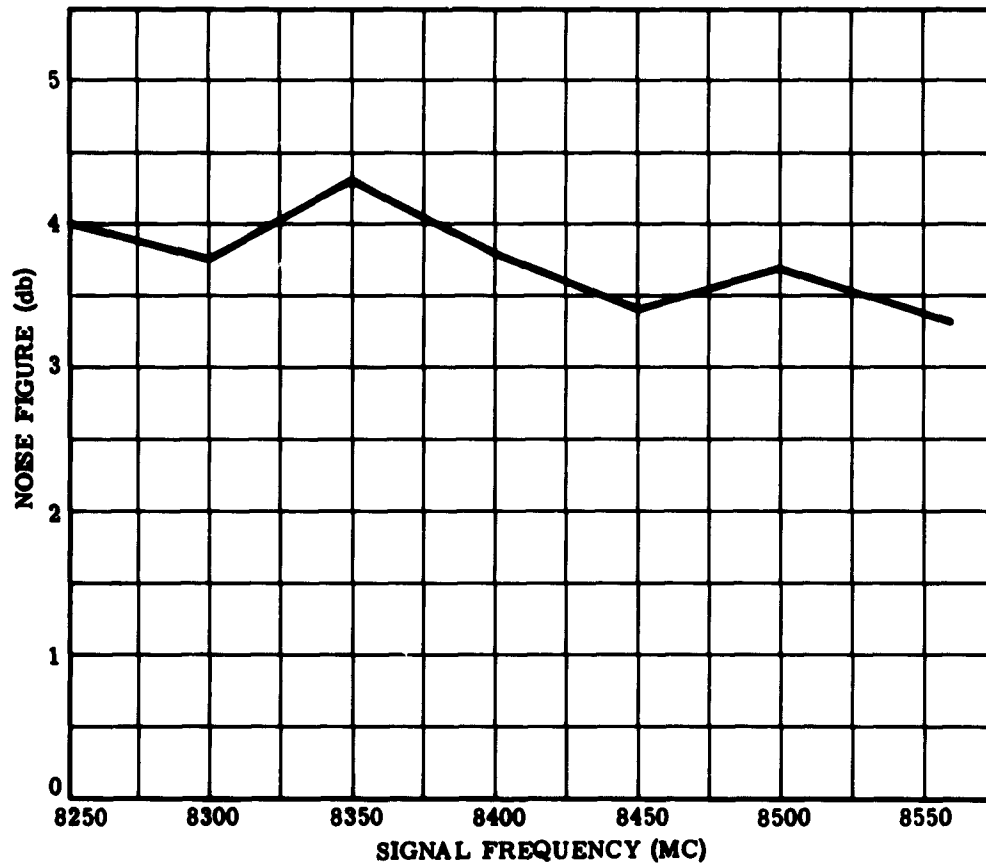


Figure 2-32. Typical Gain vs Pump Power for the X-Band Parametric Amplifier



**Figure 2-33. Noise Figure vs Signal Frequency for X-Band Parametric Amplifier**

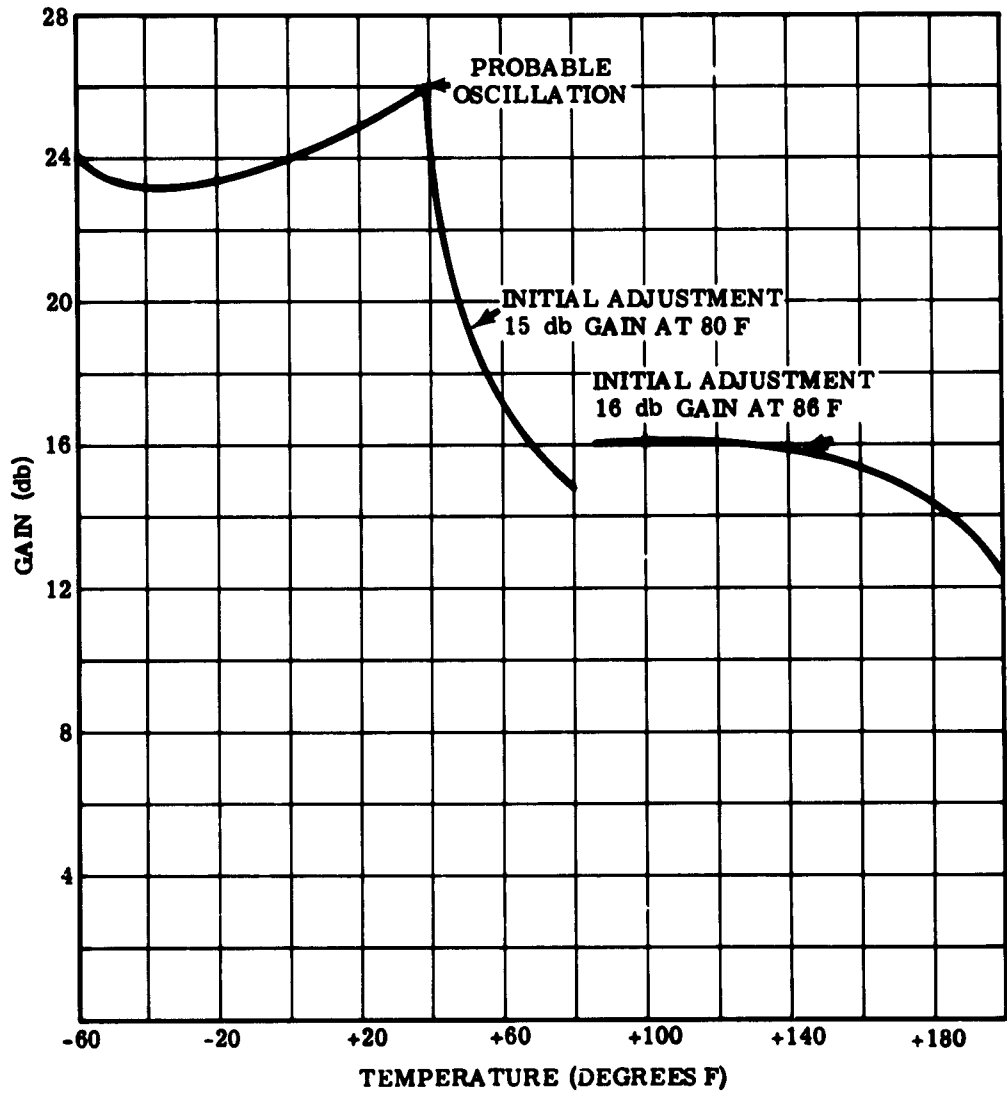


Figure 2-34. Temperature Characteristics of the X-Band Parametric Amplifier

$$X_{11} = \frac{1}{2\pi f C_0 (1-a^2)} = \frac{1}{2\pi f C_0^s} ; \quad X_{12} = \frac{a}{2\pi f' C_0 (1-a^2)} = \frac{1}{2\pi f' C_1^s} ;$$

$$X_{21} = \frac{a}{2\pi f C_0 (1-a^2)} = \frac{1}{2\pi f C_1^s} ; \quad X_{22} = \frac{1}{2\pi f' C_0 (1-a^2)} = \frac{1}{2\pi f' C_0^s} ;$$

$$a = C_1 / C_0$$

$f$  = signal frequency, and

$f'$  = idler frequency.

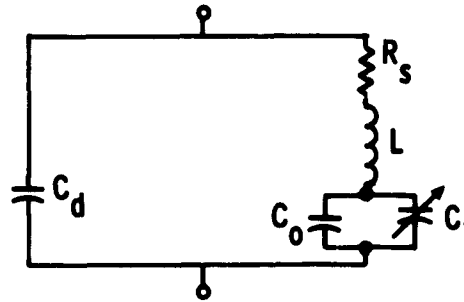


Figure 2-35. Model of Varactor Diodes Used in the Analysis

The self reactance terms  $X_{11}$  and  $X_{22}$  can be included in the general filter network. Coupling terms  $X_{21}$  and  $X_{12}$  link idler and signal energies.

A parametric amplifier representation which is convenient for purposes of analysis is shown in Figure 2-36. Unprimed terms refer to the signal frequency circuit, and primed terms to the idler frequency circuit. The impedance presented to the signal by the idler circuit is given by

$$Z_2 = \frac{-X_{12} X_{21}}{Z_a'^*} \quad (33)$$

where  $Z_a'^*$  is the complex conjugate of the impedance  $Z_a'$  defined in Figure 2-36. Both  $X_{12}$  and  $X_{21}$  are positive quantities, and if  $Z_a'$  is real and positive,  $Z_2$  will be real and negative. This is the basis of the parametric amplifier.

The actual power gain of the parametric amplifier using a circulator is given by the square of the reflection coefficient.

$$\frac{P_o}{P_{in}} = |\Gamma|^2 = \left| \frac{Z_m - Z_o}{Z_m + Z_o} \right|^2 \quad (34)$$

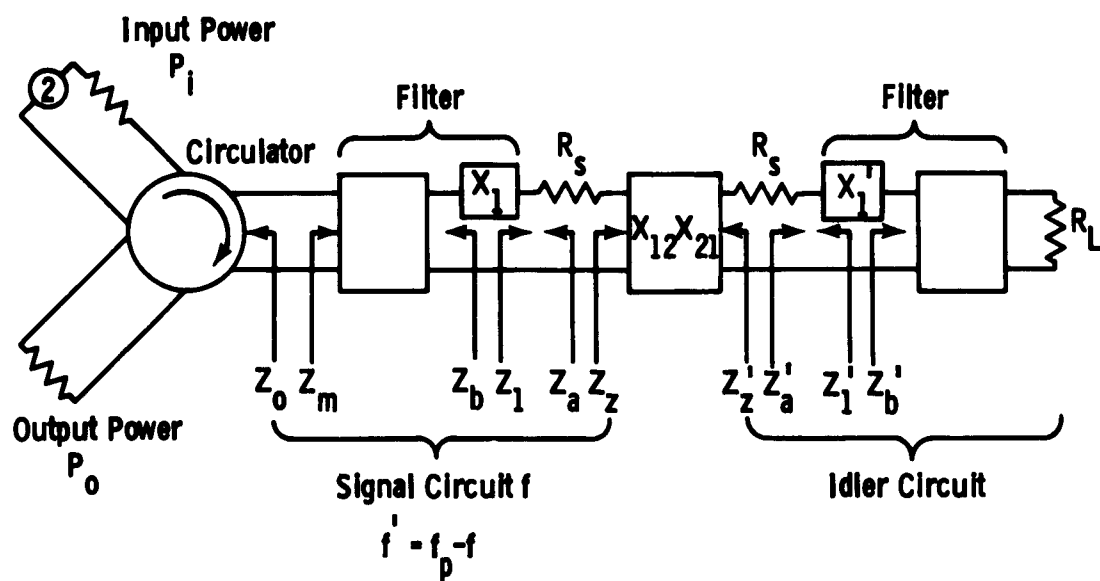


Figure 2-36. Nondegenerate Parametric Amplifier Representation

Since the network between the circulator and the series resistance  $R_s$  is nondissipative, the input reflection coefficient can be given by<sup>10</sup>

$$|\Gamma|^2 = \left| \frac{Z_b - Z_o^*}{Z_b + Z_1} \right|^2 \quad (35)$$

Substituting for  $Z_1$  leads to

$$\frac{P_o}{P_{in}} = \left| \frac{(Z_b - R_s) + \left( \frac{X_{12}X_{21}}{Z_a'^*} \right)^*}{(Z_b + R_s) - \left( \frac{X_{12}X_{21}}{Z_a'^*} \right)} \right|^2 \quad (36)$$

At the center of signal band  $f_o$  and idler band  $f_o'$ , it is assumed that  $Z_b = R_{bo}$  and  $Z_a'^* = R_{bo}' + R_s$ .

Therefore

$$\Gamma_o^2 = \frac{(R_{bo} - R_s) + \frac{(X_{12})_o (X_{21})_o}{R_{bo}' + R_s}}{(R_{bo} + R_s) - \frac{(X_{12})_o (X_{21})_o}{R_{bo}' + R_s}} \quad (37)$$

From the definitions given under equation (32), the following substitutions can be made.

$$(X_{12})_o = a(X_{22})_o = a (X_{11})_o \left( \frac{f_o}{f_o'} \right) \text{ and} \quad (38)$$

$$(X_{21})_o = a (X_{11})_o \quad . \quad (39)$$

The Q of the diode is defined as

$$Q_d = \frac{(X_{11})_o}{R_s} \quad (40)$$

$$Q_d' = Q_d \left( \frac{f_o}{f_o'} \right) \quad (41)$$

then

$$\Gamma_o = \frac{\left( \frac{R_{bo}}{(X_{11})_o} - \frac{1}{Q_d} \right) \left( \frac{R_{bo}'}{(X_{11})_o} + \frac{1}{Q_d} \right) + a^2 \left( \frac{f_o}{f_o'} \right)}{\left( \frac{R_{bo}}{(X_{11})_o} + \frac{1}{Q_d} \right) \left( \frac{R_{bo}'}{(X_{11})_o} + \frac{1}{Q_d} \right) - a^2 \left( \frac{f_o}{f_o'} \right)} \quad (42)$$

For maximum amplifier bandwidth, the signal and idler filters should have the same bandwidth. If  $\delta$  is the signal fractional bandwidth and  $\delta'$  is the idler fractional bandwidth, then

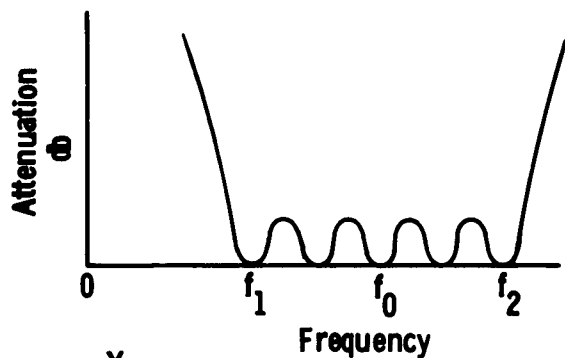
$$\frac{\delta}{\delta'} = \frac{f_o}{f_o'} \quad . \quad (43)$$

At this point, one must digress to discuss filter theory. The philosophy of design is to incorporate the varactor into two bandpass filters; one filter for the signal and the other filter for the idler. From general network theory, the limit on bandwidth of the filter is determined by the capacitance of the varactor. To obtain the widest possible bandwidths for a given  $C_o$ , filters with very sharp skirts must be employed. This, of course, means having a Tchebyscheff response.

Bandpass filters having Tchebyscheff responses are generally designed, as are other modern network filters, as low-pass prototypes and then transformed in frequency and impedance. To aid the filter designer, extensive tables are given of normalized low-pass filter elements.<sup>11</sup> A lumped-element bandpass filter derived from a low-pass prototype is shown in Figure 2-37.

The particular low-pass prototype parameters selected depend on the number of filter elements desired and the ripple that can be tolerated.

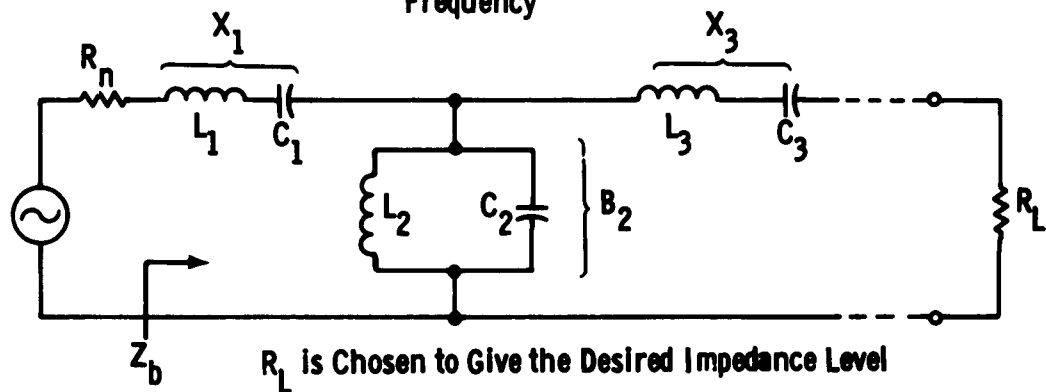
Generally, microwave filters are constructed with distributed elements rather than lumped elements. Therefore, to utilize the filter design given here, distributed approximations must be made for the lumped elements that are calculated. The basis of these



$$f_0 = \sqrt{f_1 f_2}$$

$$\delta = \frac{f_2 - f_1}{f_0}$$

$$\omega_0 = 2\pi f_0$$



For Series Branches

$$L_f = \left( \frac{R_L}{\delta \omega_0} \right) \left( \frac{\omega_1 L_j}{r_L} \right) ; \quad C_f = \left( \frac{\delta}{\omega_0 R_L} \right) \left( \frac{r_L}{\omega_1 L_j} \right)$$

For Shunt Branches

$$C_k = \left( \frac{1}{\delta \omega_0 R_L} \right) \left( \omega_1 C_k r_L \right) ; \quad L_k = \left( \frac{\delta R_L}{\omega_0} \right) \left( \frac{1}{\omega_1 C_k r_L} \right)$$

where  $C_k$ ,  $L_j$ , &  $r_L$  are elements of the low pass prototype, and  $\omega_1$  is the cutoff frequency of the low pass prototype - usually taken as 1.

Figure 2-37. Relations for Design of Lumped Element Bandpass Filters  
Low-Pass Prototypes (after Matthaei, G. L.)

approximations is that for a given filter arm the reactance at  $f_0$  for the lumped filter must be equal to that of the distributed filter. Further, the  $dx/d\omega$  of the lumped-element filter must be the same as that of the distributed-element filter. To facilitate this transformation between lumped and distributed filters, slope parameters are calculated as designated by the following equations.

For series branches,  $f$  near  $f_0$

$$x_j = (\text{slope parameter}) = \frac{\omega_0}{2} \frac{dx_j}{d\omega} \Big|_{\omega = \omega_0} = \frac{R_{bo}}{\delta} \left( \frac{\omega_1 l_1}{r_L} \right) \quad (44)$$

where

$$R_{bo} = Z_b \Big|_{\omega = \omega_0}.$$

For shunt branches,  $f$  near  $f_0$

$$b_k = (\text{slope parameter}) = \frac{\omega_0}{2} \frac{dB_k}{d\omega} \Big|_{\omega = \omega_0} = \frac{1}{\delta R_{bo}} (r_L \omega_1 C_k). \quad (45)$$

Of particular importance are the slope parameters for the first series arms of the signal and idler filters ( $x_1$  and  $x'_1$ ). These slope parameters are dependent on the  $C$  and  $L$  of the varactor, which ultimately determine the bandwidth limitation. Actually,  $x_1$  and  $x'_1$  are not independent. The conditions for simultaneous series resonance at  $f_0$  and the fact that  $C_0^s$  is a common element add a complicating factor. Generally, an additional element, usually in the form of a shorted transmission line, has to be added in series to insure proper conditions.

Returning to parametric amplifier design, it is helpful if the following substitutions are made in equation (42).

$$R'_{bo} = R_{bo} \left( \frac{f_0}{f'_0} \right) \left( \frac{x'_1}{x_1} \right) \quad (46)$$

$$\gamma = \frac{f'_0}{f_0} \frac{x_1}{x'_1} \quad (47)$$

$$q = a Q_d \sqrt{\frac{x_1}{x'_1}} \quad (48)$$

$$u = \frac{R_{bo}}{a x_1} \frac{\sqrt{x_1 x'_1}}{(X_{11})_0} = \frac{\delta}{a} \left( \frac{r_L}{\omega_1 l_1} \right) \left( \frac{\sqrt{x_1 x'_1}}{(X_{11})_0} \right) \quad (49)$$

then

$$\Gamma_0 = \frac{\left( u - \frac{1}{q} \right) \left( \frac{u}{\delta} + \frac{1}{q} \right) + \frac{1}{\delta}}{\left( u + \frac{1}{q} \right) \left( \frac{u}{\delta} + \frac{1}{q} \right) - \frac{1}{\delta}} \quad (50)$$

Rearranging

$$u = -\frac{1}{2q} \left( \frac{\Gamma_o + 1}{\Gamma_o - 1} + \gamma \right) + \sqrt{\left[ \frac{1}{2q} \left( \frac{\Gamma_o + 1}{\Gamma_o - 1} + \gamma \right) \right]^2 + \left( \frac{\Gamma_o + 1}{\Gamma_o - 1} \right) \left( 1 - \frac{\gamma}{q^2} \right)}. \quad (51)$$

Parameter  $u$  is plotted versus  $\delta$  with  $q$  as a parameter in Figure 2-38 for 10 db gain, 15 db gain and 20 db gain. From  $u$  the fractional bandwidth can be calculated using equation (49).

### 2.5.3.2 Wideband Amplifier Design

To determine the feasibility of a wideband X-band amplifier, a sample theoretical design was undertaken assuming the use of the best commercially available diode - the MA4362 pill varactor.

The assumed parameters for the MA4362 are listed as follows:

- (a) Operating junction capacitance = 0.2 pf
- (b) Case capacitance = 0.2 pf
- (c) Cartridge inductance = 0.8 nhy
- (d)  $f_c$  = 200 gc
- (e) fsr (self-resonant) = 12.5 gc
- (f)  $a = \frac{C_1}{C_o} = 0.25$

Assume  $f_o = 8.3$  gc,  $f_p = 25.3$  gc and  $f'_o = 17$  gc (idler frequency).

To insure resonance at both signal and idler frequencies, a short section of transmission line must be added in series as determined by the following relations:

$$\omega_o L - \frac{1}{\omega_o C} + Z_o \tan \frac{\omega_o l}{c} = 0 \quad (52)$$

$$\omega'_o L - \frac{1}{\omega'_o C} + Z_o \tan \frac{\omega'_o l}{c} = 0 \quad (53)$$

$$\left. \frac{dx}{d\omega} \right|_{\omega_o} = L - \frac{1}{\omega_o^2 C} + \frac{Z_o l}{c} \sec^2 \frac{\omega_o l}{c} \quad (54)$$

$$\left. \frac{dx}{d\omega} \right|_{\omega'_o} = L - \frac{1}{\omega'_o{}^2 C} + \frac{Z_o l}{c} \sec^2 \frac{\omega'_o l}{c} \quad (55)$$

where

$Z_o$  is the characteristic impedance of a shorted transmission line

$l$  is the length of the shorted transmission line, and

$c$  is the velocity of light =  $3 \times 10^{10}$  centimeters per second.

Equations (50) and (51) express the series resonance at  $f_o$  and  $f'_o$  and equations (52) and (53) the reactance slope, which are necessary in calculating  $x_1$  and  $x'_1$ . For the diode parameters assumed, a transmission line with an impedance of 29 ohms and a length of 0.61 centimeters is required. The corresponding slope parameters  $x_1$  and  $x'_1$  are 135 and 157, respectively.

The sample design utilizes two resonators with a 0.1 db ripple. The low-pass filter prototype parameters are:

$$\begin{aligned} l_1 &= 0.592 \\ C_2 &= 0.376 \\ r_L &= 1.1008 \\ Q_1 &= 1. \end{aligned}$$

Then,  $\gamma = 1.76$ ,  $q = 5.3$ , and  $u = 0.9$ , from Figure 2-38 for 15 db gain. The fractional bandwidth is given by

$$\delta = \frac{u a}{\left(\frac{r_L}{Q_1 l_1}\right) \left(\frac{\sqrt{x_1 x'_1}}{(X_{11})_o}\right)} = 0.0735 \text{ or } 7.35 \text{ per cent.}$$

The calculated bandwidth is 610 mc.

To calculate the idler and signal waveguide dimensions, the following relations can be used:

$$R_{bo} = \delta x_1 \left( \frac{r_L}{Q_1 l_1} \right) = 18.5 \text{ ohms} \quad (56)$$

$$R'_{bo} = R_{bo} \left( \frac{f_o}{f'_o} \right) \left( \frac{x'_1}{x_1} \right) = 10.5 \text{ ohms}$$

For the idler waveguide using reduced height RG91/U guide, a height of 0.011 inch is needed, as shown below:

$$R'_{bo} = Z_{V1} = \frac{\pi}{2} \frac{b}{a} \frac{E_y}{H_x}, \quad (57)$$

where

$$\frac{E_y}{H_x} = \frac{\mu_1}{\epsilon_1} \frac{1}{\sqrt{1 - \left(\frac{\lambda_1}{2a}\right)^2}}$$

where

$b$  = height of the waveguide

$a$  = width of the waveguide

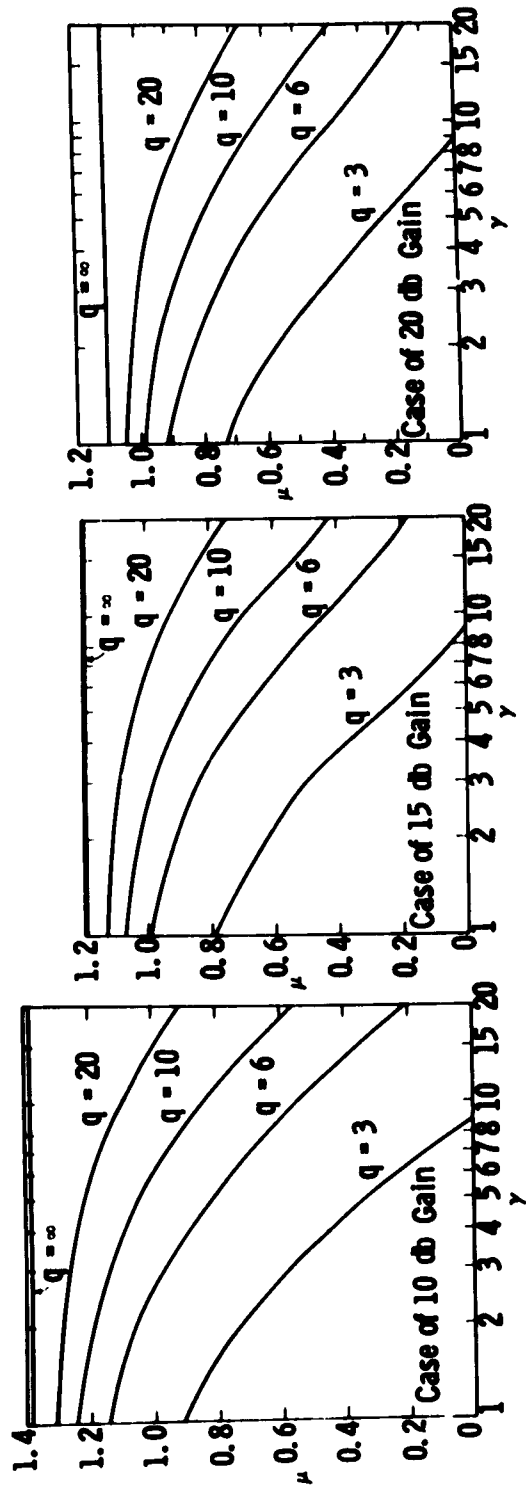


Figure 2-38. Charts for Determining the Bandwidth of Nondegenerate Parametric Amplifiers (after Matthaei, G. L.)

$E_y$  = transverse electric field  
 $H_x$  = transverse magnetic field  
 $\mu_1$  = permeability of waveguide  
 $\epsilon_1$  = permittivity of waveguide, and  
 $\lambda_1$  = wavelength.

To obtain  $R_{bo}' = 10.5$  ohms with  $a = 0.702$  inch,  $b$  should be 0.011 inch, which is probably too small for practical consideration.

The above analysis shows that even with state-of-the-art diodes, achievement of wide-band operation would be difficult. However, more recently than when the analysis was made, new diodes having low values of parasitic reactances were made available. For future programs, the above analysis could be utilized for these new diodes to achieve wide-band operation when such is desired.

## 2.6 STUDY OF THE K- AND V-BAND AMPLIFIERS

In accordance with paragraph 1.1.9 of the program's objectives, the feasibility of K- and V-band amplifiers were investigated.

Using the graph derived by Greene and Sard<sup>7</sup> in Figure 2-39, it can be shown that a 4 db noise figure is obtainable. For a 15-gc amplifier, assuming  $\frac{C_0}{C_1} = 6.4$ , room temperature operation and a diode cutoff of 225 gc, the optimum pump frequency calculates to be 41.5 gc. If the diode were cooled to 100 K, a cutoff of only 113 gc would be required for a 4 db noise figure with a pump frequency of 25 gc.

For a 25-gc amplifier with a 50-gc pump, a diode cutoff frequency of 250 gc is required to achieve a 5 db single-channel noise figure. For a 35-gc amplifier with a 70-gc pump, a diode cutoff frequency of 280 gc is required to achieve a 6 db single-channel noise figure. The only type diode that now has such a high cutoff frequency is the Western Electric gallium-arsenide diode; however, it is anticipated that other sources will soon be available.

During the last phase of this program, some diffused junction varactor diodes were fabricated with the following characteristics:

Breakdown voltage @ 10 $\mu$ a	9.0 - 14.0 volts
Leakage current @ 5 V	1.2 - 30 $\mu$ a
$C_{\text{package}}$	0.241 - 0.248 pf

Early units had a capacitance of 2.4 - 3.6 pf at zero bias and showed a capacitance change of 2:1 over the bias range permitted. Processing changes resulted in a zero bias capacitance of 0.7 - 1.5 pf and a capacitance change of  $\sim 2:1$  from zero to + 4 volts. However, these diodes were still not of sufficient quality to consider for K- or V-band parametric amplifiers; consequently, no further diode studies were attempted.

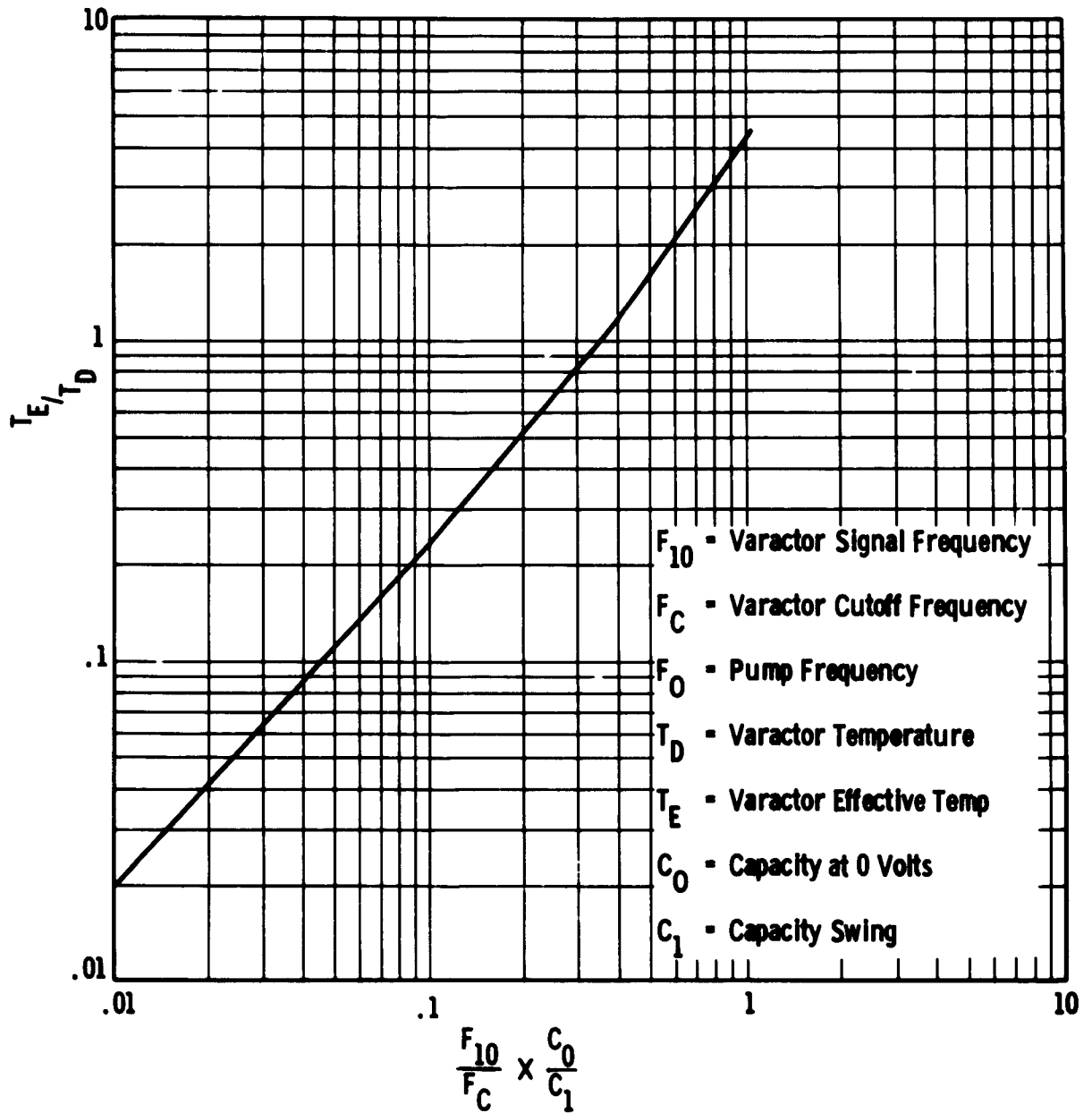


Figure 2-39. Noise Figure vs Varactor Characteristics

## 2.7 THE THIN-FILM AMPLIFIER AND OSCILLATOR

In accordance with paragraph 1.1.2 of the program's objectives, an investigation of a thin-film amplifier and oscillator was conducted. The results of this investigation were negative; however, it was felt that the thin films were not single-crystal, as needed. Upon the advice of the Advisory Group on Electron Devices, this phase of the program was terminated. A summary of the work is presented here.

A program was carried out to analyze the possible modes of behavior of the device. The analysis was based fundamentally on a comparison of input and output power from the device. The theory considers the cavity system shown in Figure 2-40. The device is considered to operate by conductivity modulation; that is, the conductivity of the thin film of germanium which couples the two cavities is modulated at an r-f rate by an electromagnetic disturbance in cavity 2. The modulated conductance causes an r-f component of current to exist. Under proper matching conditions, this r-f energy can be coupled out of cavity 1. If the power necessary to modulate the conductance of the thin film is less than the power extractable from the second cavity, the device amplifies signals.

The analysis proceeds as follows. (See Appendix 1 of quarterly report No. 3, April 1959, for details.) The expression for conductivity of the germanium film is compared with the expression for change of conductivity produced by changes induced by an electric field. The ratio of these two expressions is the fractional change in conductivity. This expression is now solved for the electric field, and the input power necessary to maintain this field is determined from the Q of the first cavity.

The fractional change in conductivity also is the modulation factor for a current flowing in the film. This expression then is used to obtain the r-f component of power dissipated in the film. Under optimum loading conditions, half of this power is extractable.

The extractable power is then compared with the input power to determine the gain of the device. An expression for the gain has been obtained and is presented below.

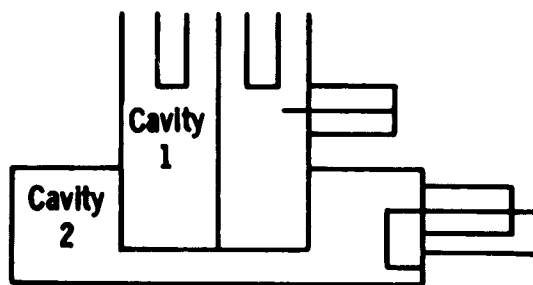


Figure 2-40. Theoretical X-Band Cavity System for Thin-Film Amplifier-Oscillator

$$P.G. = \frac{V^2 \epsilon Q \times 10^7}{16 \pi^2 R_o t^2 n^2 e^2 f V_{eff}}$$

where

V is applied d-c voltage  
 $\epsilon$  is dielectric constant of film support  
 Q is Q of cavity 2  
 $R_o$  is resistance of film in ohms  
 t is film thickness in cm  
 n is carrier concentration in film in a cubic centimeter  
 e is electronic charge,  $4.8 \times 10^{-10}$  esu  
 f is frequency in 1/sec, and  
 $V_{eff}$  is effective volume of cavity 2 in  $cm^3$ .

If we assume the following values of the above parameters,

V = 600 volts  
 $\epsilon$  = 11 (sapphire)  
 Q = 300  
 $R_o$  =  $1/2 \times 10^5 \Omega$   
 t =  $1/2 \times 10^{-4}$  cm  
 n =  $1/2 \times 10^{14}$   
 f =  $10^{10}$   
 $V_{eff}$  = 0.05

The power gain is greater than unity. The above choice of parameters gives the threshold for activity. A slight change in the value of any of the parameters, particularly the squared terms, could change the prediction from active to inactive.

Feedback considerations indicate that with a proper adjustment of the feedback ratio, the power gain on oscillation level of a device having gain greater than unity will be limited only by the internal losses in the d-c supply.

No mention has been made here of considerations that may limit the frequency response of this device. It has been suggested that the time involved in charging the germanium film will be such as to cause relaxation effects at frequencies above 100 mc. The analysis of this effect involves the solution of a radial transmission line and has not been carried out exactly.

A cavity system to operate at 10 gc was designed and constructed adhering as closely as possible to the original designs of Dr. Robillard. The only significant difference was in the tuning mechanism of the coaxial cavity, which in Motorola's design was a slideable shorting stub.

Initial tests were made with the inactive cavity (no film attached) to ascertain Q's. Loaded Q of the input cavity was about 300. The apparatus used for these measurements is shown schematically in Figure 2-41.

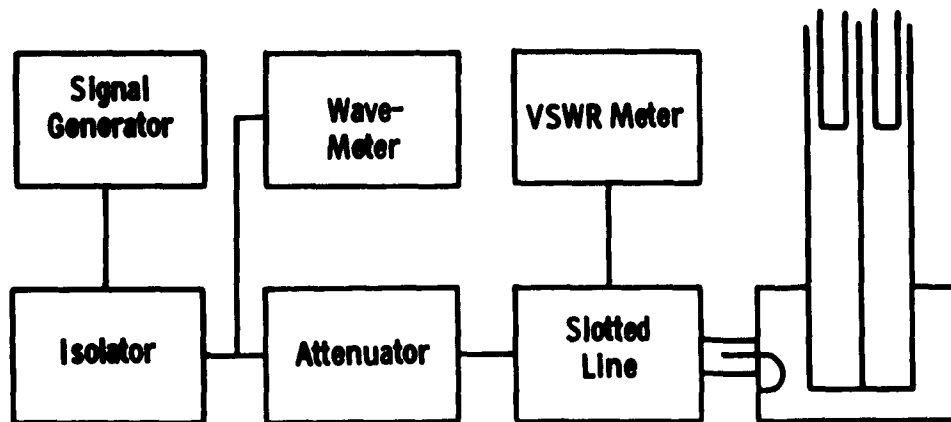


Figure 2-41. Test Arrangement for Measuring Q's of Inactive Cavity

The original tests on the completed assembly were carried out using the equipment of Figure 2-42 with the detection system on the output cavity. A d-c potential was applied to the film as indicated in Figure 2-42. The d-c voltage was varied from 0 to 400 volts manually after maximizing the output with the device operating as a transmission system. The adjustable parameters included:

- signal frequency and power level
- resonant frequency of input (rhumbatron) cavity (tuning screw)
- resonant frequency of output (coaxial) cavity (tuning plunger)
- output probe location
- d-c voltage on film.

When the d-c film voltage exceeded 400 volts, arcing occurred in the interior of the system and measurements were terminated. Subsequent examination of the dismantled assembly indicated that a short circuit had occurred between the tuning plunger and the inner conductor of the coaxial cavity.

A second trial was conducted with a new film mounted as before. The inner coaxial conductor was wrapped with low-loss insulating tape. The circuitry of Figure 2-43 was used for these measurements. It consists essentially of the previous test circuitry, except that instead of applying a manually-variable dc to the film, a 1000-cycle voltage of 0-700 volts amplitude is applied. This sweeping of the film voltage made it possible to eliminate this parameter as a variable.

The assembly was exhaustively tested for both amplification and oscillation using the circuitry described above. No activity was observed when the assembly was operated as a transmission or reflection device, or as an amplifier or oscillator.

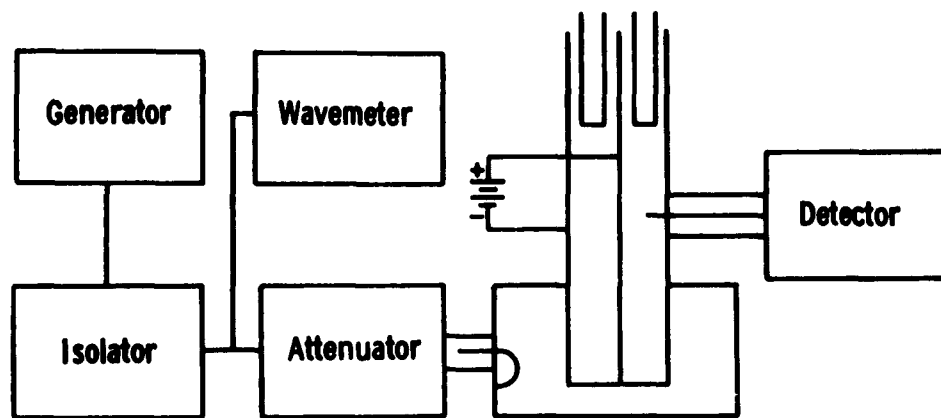


Figure 2-42. Schematic of Test Arrangement for Thin-Film Amplifier-Oscillator

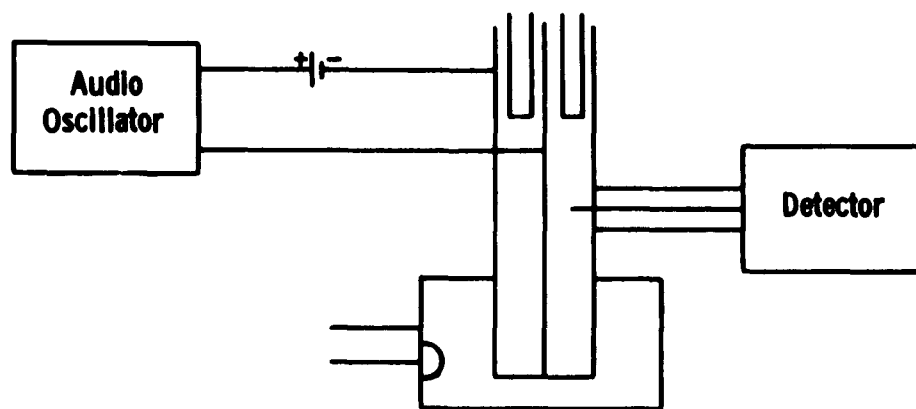


Figure 2-43. Schematic of Test Arrangement for Second Series of Amplifier-Oscillator Tests

The results of all experimental tests on this device were negative. However, they are not considered to be conclusive since the films used may not have been single crystals. The quality of the crystal films was doubtful. Equipment to measure degree of monocrys- tallinity, resistivity, and Hall Effect had not been completed when these films were pre- pared, so it was therefore not known what values of the gain parameters should have been used. In addition, difficulty was encountered in making good contact between the cavity and film. This was primarily due to the fragile nature of the film. Because of the nega- tive results, and upon the advice of the Advisory Group on Electron Devices, this phase of the program was terminated.

## 2.8 STABILITY OF PARAMETRIC AMPLIFIERS

In accordance with paragraph 1.1.4 of the program's objectives, a study of parametric amplifier stabilizing techniques was initiated. As a result of this study, it is shown that the use of feedback to control amplifier gain can be very beneficial in improving stability.

An investigation was made to determine the feasibility of using the noise level out of the i-f amplifier to control the pump level. A block diagram of this type of control system is shown in Figure 2-44. In Figure 2-44, a lower sideband up-converter is utilized to demonstrate that stability can be achieved without an input circulator.

The theory for this stability system is as follows. Define:  $G = \text{loop gain} = f_1(P_p, Z_{in})$ , (59)  
 where gain is the function  $f_1$  of the pump  $P_p$  power applied to the varactor and amplifier input impedance. Control voltage  $E_o$  (applied to the diode attenuator) =  $E_{dc} + f_2(G)$  where (60)

$E_{dc}$  is the voltage applied to the diode attenuator with the gain of the parametric amplifier = 0

$f_2(G)$  is a function of gain, and

$P_p = a P_o$  where  $P_p$  is pump power applied to the varactor,  $P_o$  is power applied to the diode attenuator,  $a$  is attenuation of diode attenuator.

In the closed loop connection,  $a = a_o - f_3(E_o)$

where

$a_o$  is the attenuation with 0 volts applied to the diode, and

$f_3(E_o)$  is the attenuation that is the function of applied bias.

The sign on  $f_3$  is negative because the attenuation goes down with applied voltage for the particular diode attenuator used, as shown in Figure 2-45.

To calculate the effect of pump power changes on gain, some approximations will be made. It is assumed the input impedance ( $Z_{in}$ ) is constant and that the above functions are linear. This would be approximately correct for small deviations around an operating point. Then:

$$G = G_o + K_1 P ; \quad (61)$$

where

$G_o$  is parametric amplifier gain with zero pump power.

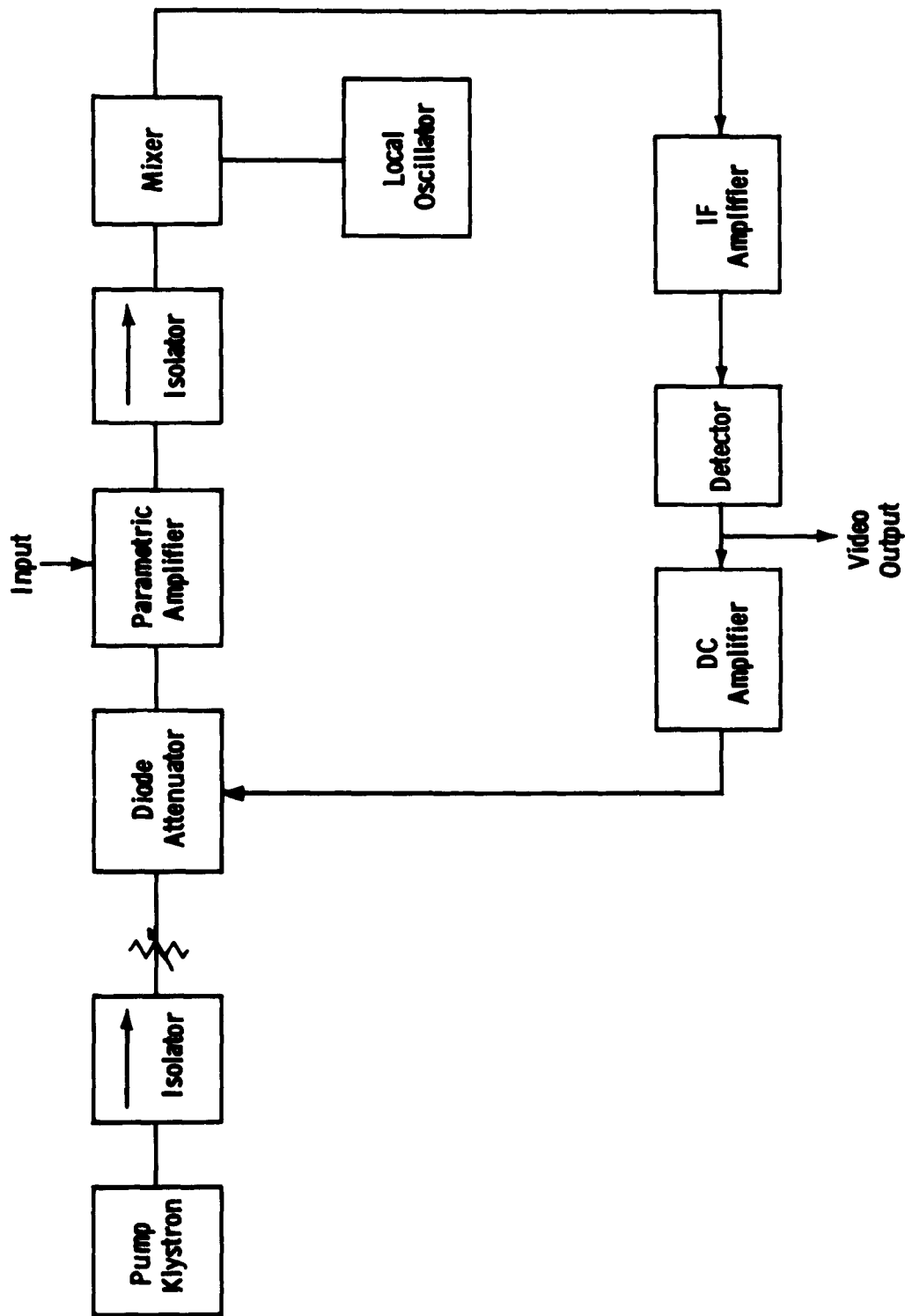


Figure 2-44. Block Diagram of Gain Control System Using Noise Level to Control Paramp Gain

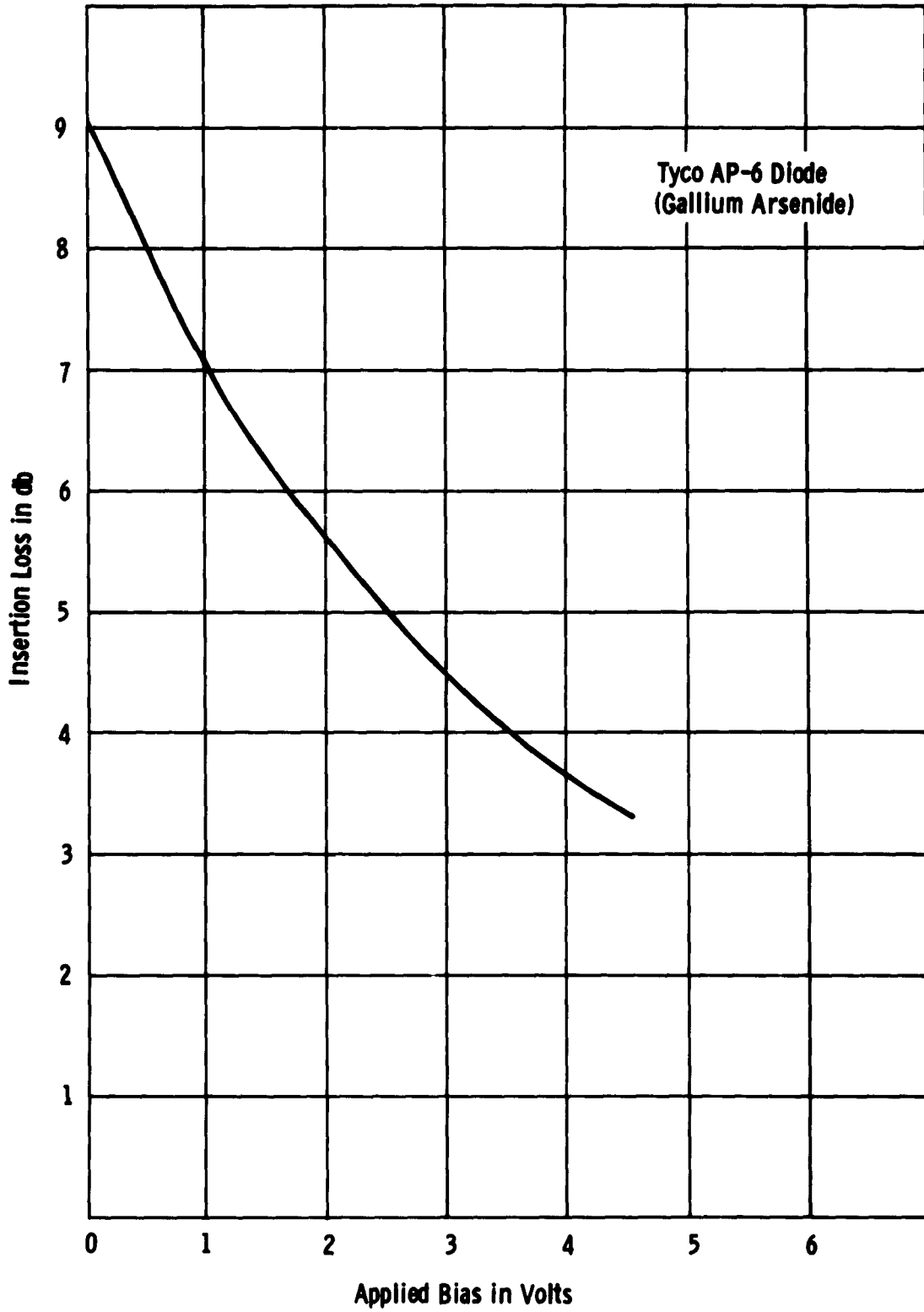


Figure 2-45. Insertion Loss Versus Bias for X-Band Diode Attenuator

Actually,  $G_o$  is an intercept of the tangent to the gain versus  $P_p$  curve at the operating point.

$K_1$  is the slope or proportionality constant.

$$E_o = E_{dc} + K_2 G \quad (62)$$

where

$K_2$  is the constant.

$$a = a_o - K_3 E_o \quad (63)$$

where

$K_3$  is the constant.

The open loop conditions are given by

$$G = G_o + a_o K_1 P_o \quad (64)$$

If

$$P_o = P_o + \Delta P \text{ and } G = G + \Delta G$$

then

$$\Delta G = a_o K_1 \Delta P \quad (65)$$

The closed loop gain change is given by:

$$\begin{aligned} G &= G_o + a K_1 P_o = G_o + a_o K_1 P_o - K_1 K_3 P_o E_o \\ &= G_o + a_o K_1 P_o - K_1 K_3 P_o E_{dc} - K_1 K_2 K_3 P_o G \end{aligned} \quad (66)$$

Again let

$$P_o = P_o + \Delta P \text{ and } G = G + \Delta G$$

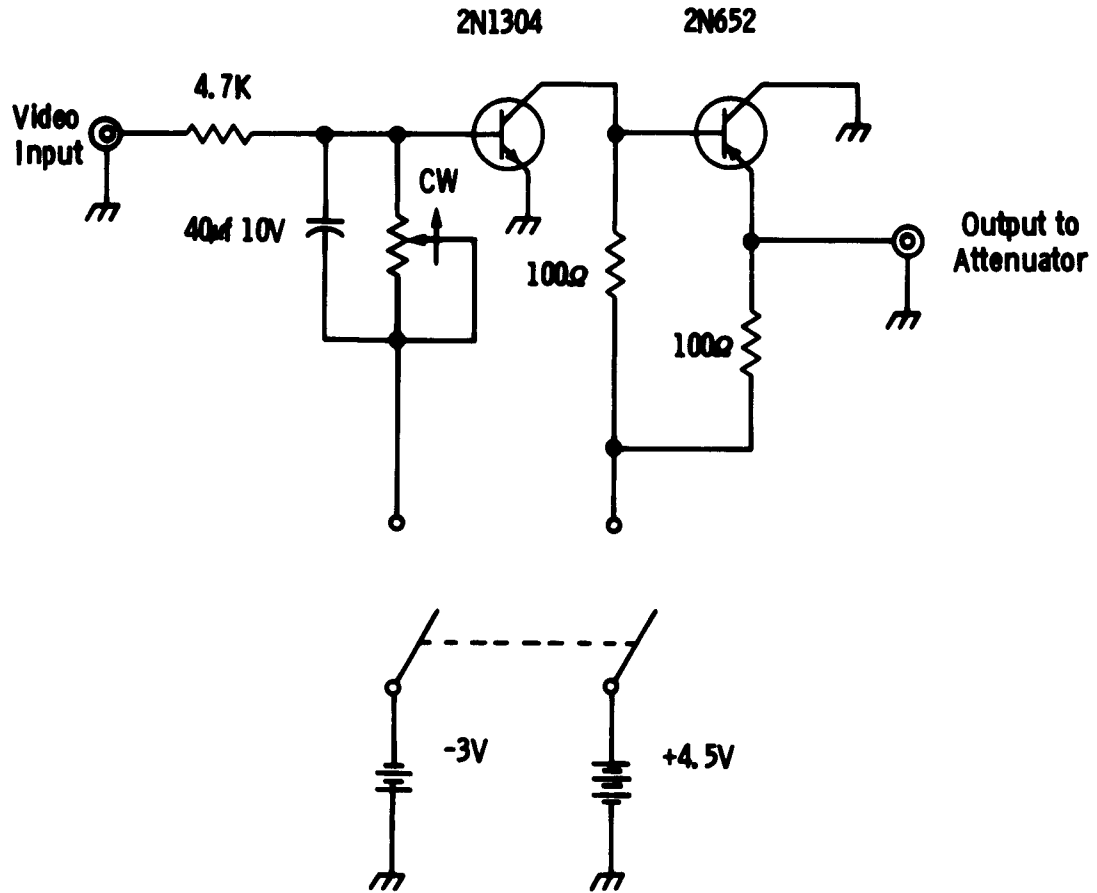
then

$$\Delta G = \frac{(a_o K_1 - K_1 K_3 E_{dc} - G K_1 K_2 K_3)}{1 + K_1 K_2 K_3 P_o} \Delta P \quad (67)$$

Comparison of equations (67) and (65) shows that if  $K_1$ ,  $K_2$  and  $K_3$  are large, smaller changes of gain would occur for the same change of  $P_o$  with the feedback loop closed. Therefore, the parametric amplifier ought to be more stable with respect to pump power changes if the loop is closed.

As an experimental verification of the above theory, a feedback loop was built around the S-band amplifier described in Quarterly Status Report No. 11. A schematic of the feedback amplifier built on the output of the 60 mc i-f amplifier to control pump power is shown in Figure 2-46. This amplifier controls the diode attenuator, whose characteristics are shown in Figure 2-45.

To verify the benefit of closing the loop, gain versus pump levels for both open and closed loop conditions were measured. The results for this are shown in Figure 2-47. It can be seen from Figure 2-47 that a 1 db change of pump power results in a 10 db change of paramp gain if the loop is open. On the other hand, when the loop is closed, a 1 db



**Test Date:**  
**Bias Threshold Set for +3.0 V Input**

Input	Output
+3.0 V	+4.58 V
+4.0 V	+0.85 V
+4.2 V	+0.55 V

Figure 2-46. Pump Power Feedback Amplifier

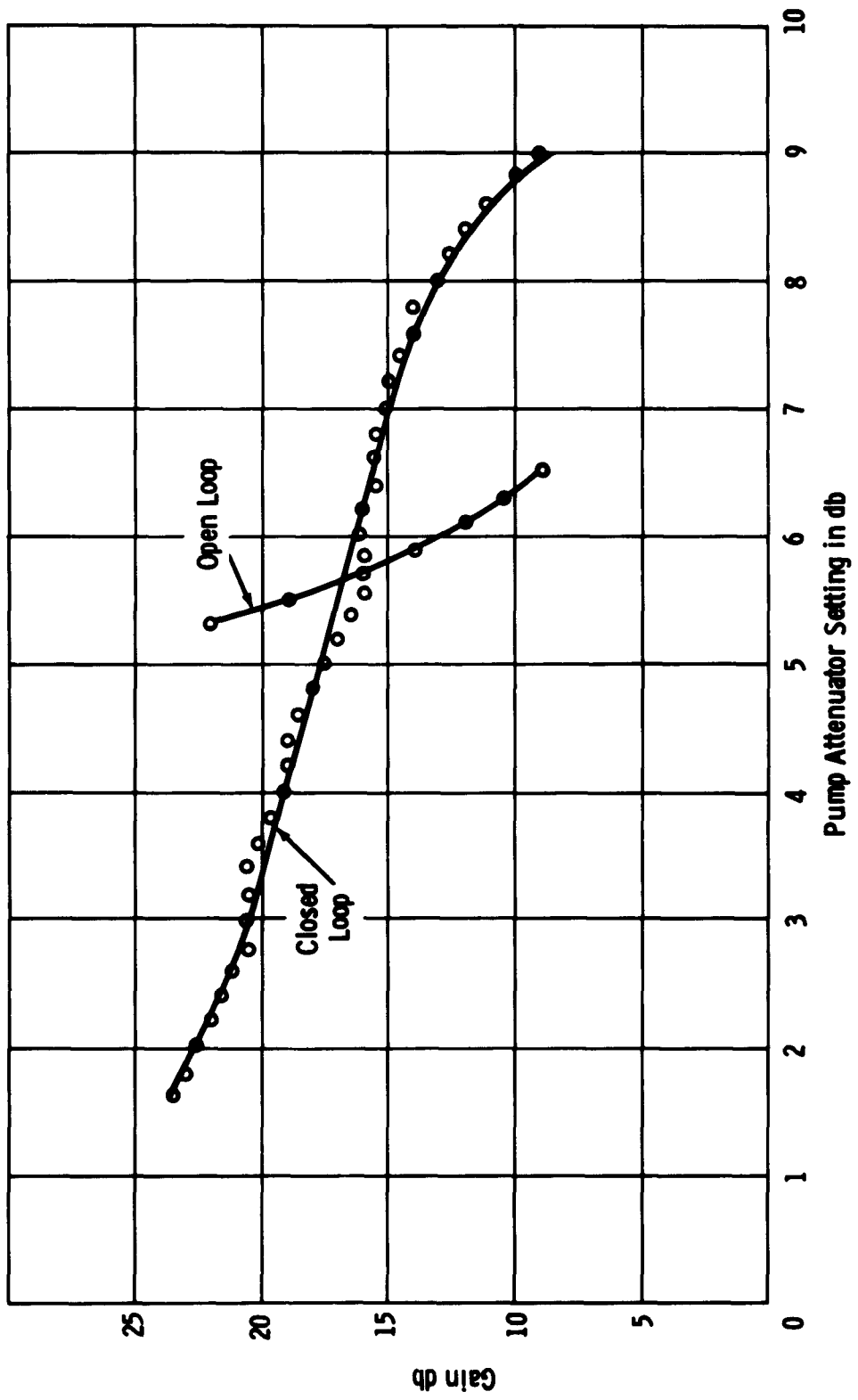


Figure 2-47. Effect of I-F Noise Control of Parametric Pump Level to Stabilize Parametric Amplifier to Pump Changes

change of pump power results only in a 1.5 db change in gain. The improvement of stability with respect to pump power is over 6 to 1. Further improvement of stability could be achieved by increasing gain of the feedback circuit. Figure 2-48 shows how the effects of antenna VSWR are drastically reduced (up to 8 to 1 for low VSWR's) with the feedback loop closed.

## 2.9 EFFECT OF COOLING A PARAMETRIC AMPLIFIER

In accordance with item (3) of paragraph 1.1.4 of the program's objectives, an investigation of the effects of cooling was conducted. It was shown that achievement of a 100 K noise temperature with a diode cutoff of 150 gc is possible. To achieve this noise figure, however, requires a cooling of the diode to 100K. Since the silicon diodes available at the time of this investigation could not be beneficially cooled, it was decided to utilize a gallium-arsenide diode. The only commercially available gallium-arsenide diode was the Texas Instruments' XD503. Accordingly, an XD503 was ordered; unfortunately because of fabrication problems, the XD503 was not delivered, and the cooling phase of this program was terminated before the XD503 was again available.

The use of cooled external idler terminations was briefly considered. However, analysis showed that use of such terminations is no better than terminating the idler with the diode. Accordingly, no further consideration was given to cooling the idler termination.

## 2.10 STUDY OF OTHER VARIABLE-REACTANCE AND NEGATIVE-RESISTANCE DEVICES

In accordance with paragraph 1.1.6 of the program's objectives, a study of other devices besides parametric amplifiers was undertaken. This study primarily consisted of monitoring a corporate research program on tunnel diode amplifiers.

Because of the growing importance of the solid state devices field, Motorola authorized a company-sponsored research program to investigate the characteristics and applications of the tunnel diode. Basic objectives were to produce a low-noise amplifier and to study the limitations of such a device.

The tunnel, or Esaki, diode utilizes the negative resistance that appears over a small portion of its current-voltage characteristic. This property results from a reduction in the number of charges tunneling through a heavily doped P-N junction with the application of a small forward bias, and provides the regeneration which yields power gain. Noise figures of such devices are low because of low current and, therefore, low shot-noise. Figure 2-49 shows the I-V characteristic of a typical tunnel diode.

Figure 2-50 shows the completed structure. Designed to operate at 450 mc, it is a strip transmission line cavity with the diode at the high impedance point. In addition to providing capacitive input tuning, special care was taken to minimize series lead inductance, and to prevent leakage into the bias circuit. Figure 2-51 is a schematic drawing of the final two-port amplifier.

A special mixer was developed for this program, and isolation from VSWR changes was provided by a specially developed Motorola uhf isolator. The results are as follows:

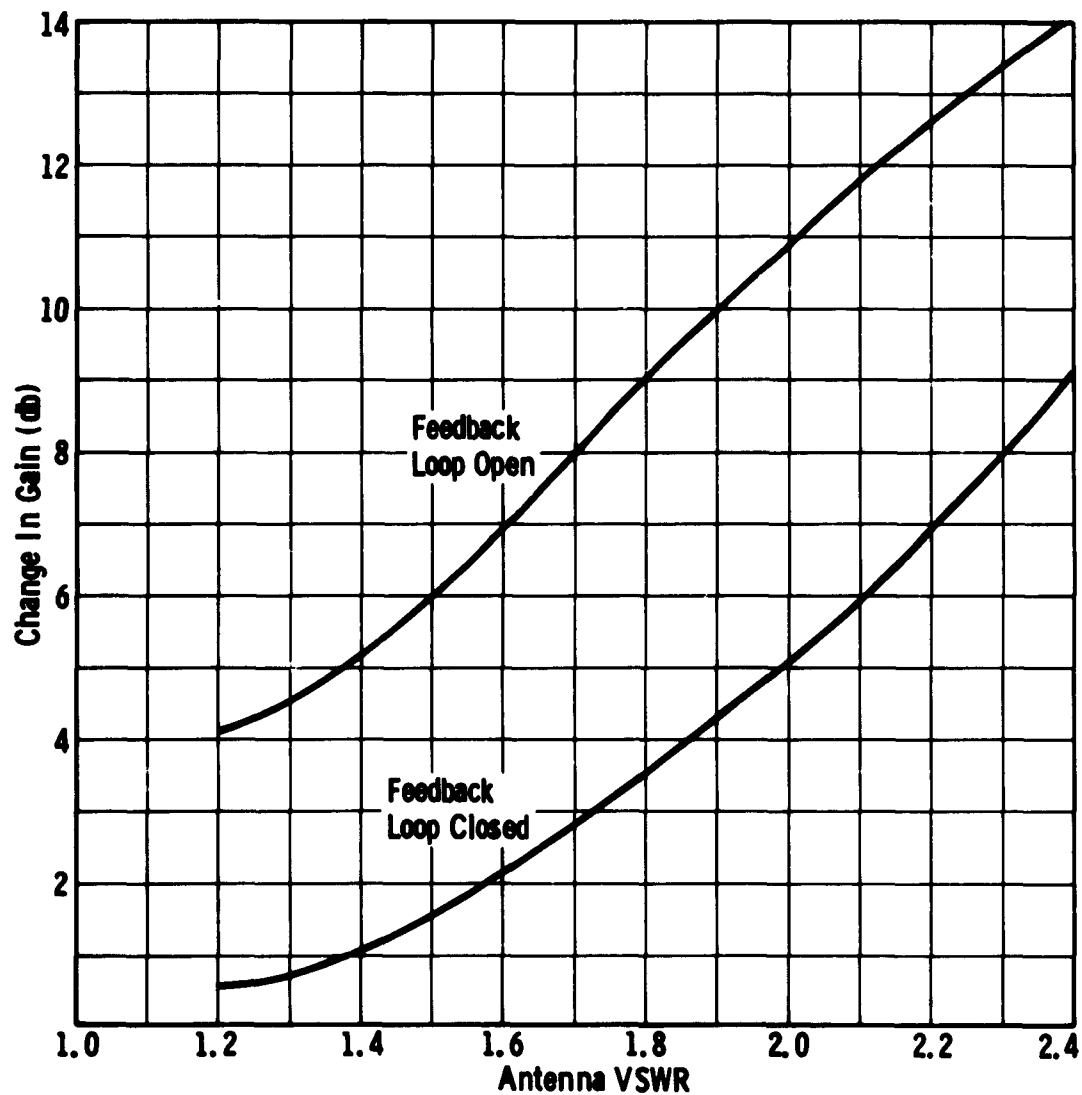


Figure 2-48. Effect of Antenna Mismatch with and without Feedback, Nominal Gain 15 db

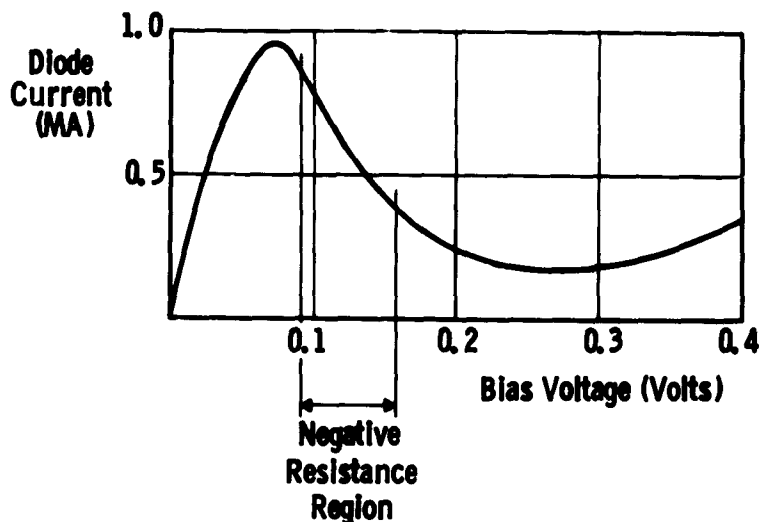


Figure 2-49. Typical I-V Characteristic of a Tunnel Diode

Tuning range	405-460 mc
Gain	15 db
Bandwidth	10-18 mc
Noise figure with isolator	4.2 db
Noise figure without isolator	6.0 db
(Gain) <sup>1/2</sup> bandwidth product	100 mc

As soon as a uhf circulator became available, it was used in conjunction with a one-port version of the amplifier. As expected, results were (1) reduction of initial insertion loss, (2) reduction of noise figure to 5 db, and (3) greater stability with respect to antenna impedance changes.

During the period covered by this report, tunnel diode investigations were extended to the following areas:

- (a) Recovery time of tunnel diode amplifiers.
- (b) Plotting of characteristic curves
- (c) Development of wideband amplifier
- (d) Development of narrowband amplifier.

Recovery time measurements included both CW and pulse-modulated interference at and near the signal frequency. The following data were obtained:

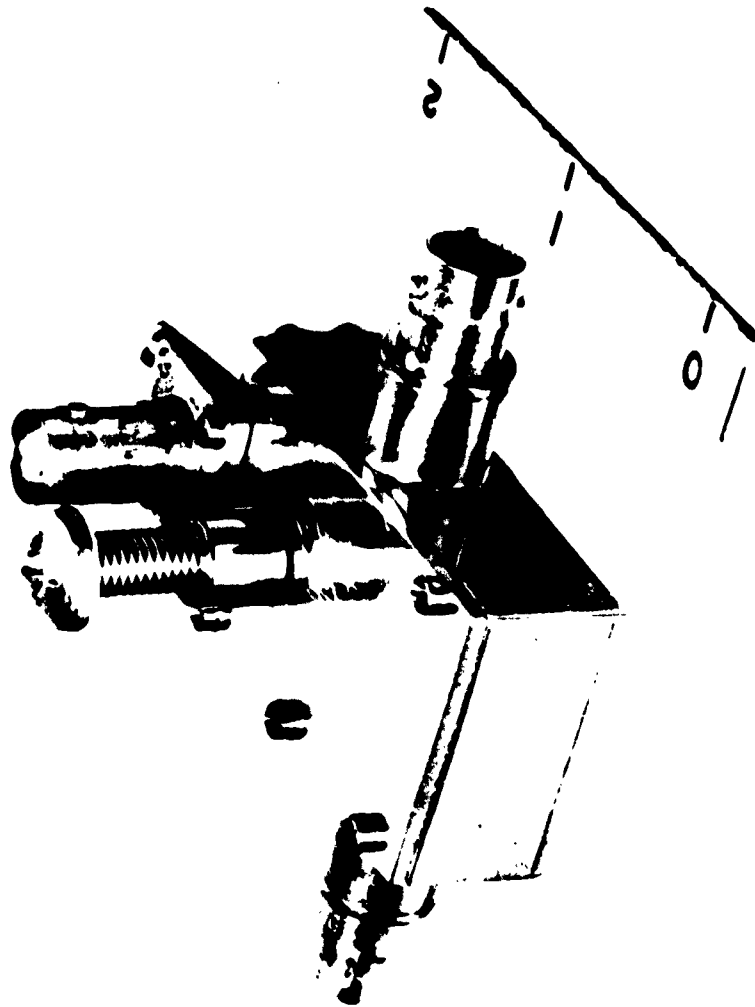


Figure 2-50. 450-MC Tunnel Diode Amplifier

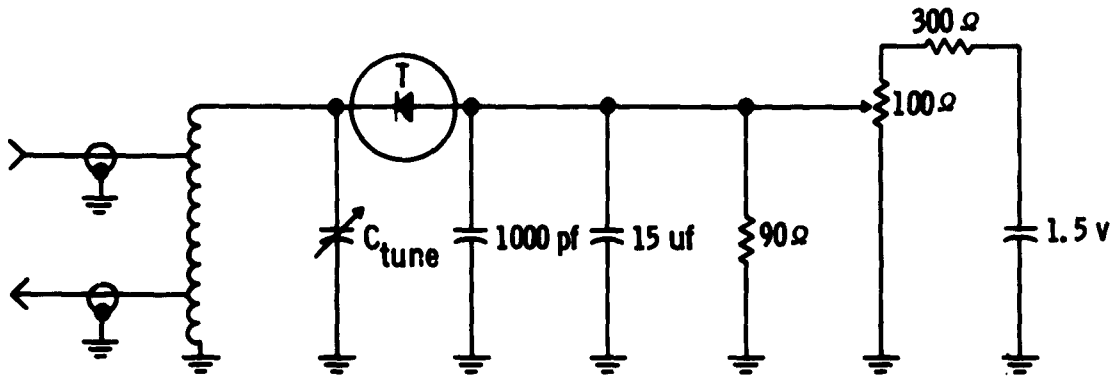


Figure 2-51. Schematic of 450-MC Tunnel Diode Amplifier

<u>Signal</u>	<u>Interference</u>	<u>Time Between Pulses</u>	<u>Degradation of Tangential Sensitivity</u>
Pulse modulated -44 dbm @ 450 mc	Pulse modulated 0.2 mw @ 450 mc	8 $\mu$ sec 20 $\mu$ sec	3 db None
Pulse modulated -62 dbm @ 450 mc	Pulse modulated 0.2 mw @ 460 mc	1 $\mu$ sec	1 db
Pulse modulated -100 dbm @ 450 mc	Pulse modulated 0.2 mw @ 460 mc	1 $\mu$ sec	2 db
450 mc, CW	CW 35 db below 0.2 mw		3 db

The circuit shown in Figure 2-52(a) was used to display characteristic curves of the tunnel diodes. These curves were plotted graphically and used to determine the characteristics most suitable for amplification and best noise figure. Negative conductance is shown as the slope of the curve in the negative region. The schematic of Figure 2-52(b) represents a circuit used with an  $R_x$  meter to determine diode capacitance, whereas Figure 2-52(c) shows a circuit used to measure the ohmic resistance.

A series circuit tunnel diode amplifier was designed and constructed as shown in Figure 2-53 with a bandwidth that proved much greater than in previous parallel connected amplifiers. Gain varied from 9.5 db at 280 mc to 13.0 db at 560 mc. A directional coupler was used to remove the amplified signal in lieu of the relatively narrowband circulator.

A narrowband amplifier was designed for use with the circulator. The response curve is shown in Figure 2-54, along with a schematic drawing of the device.

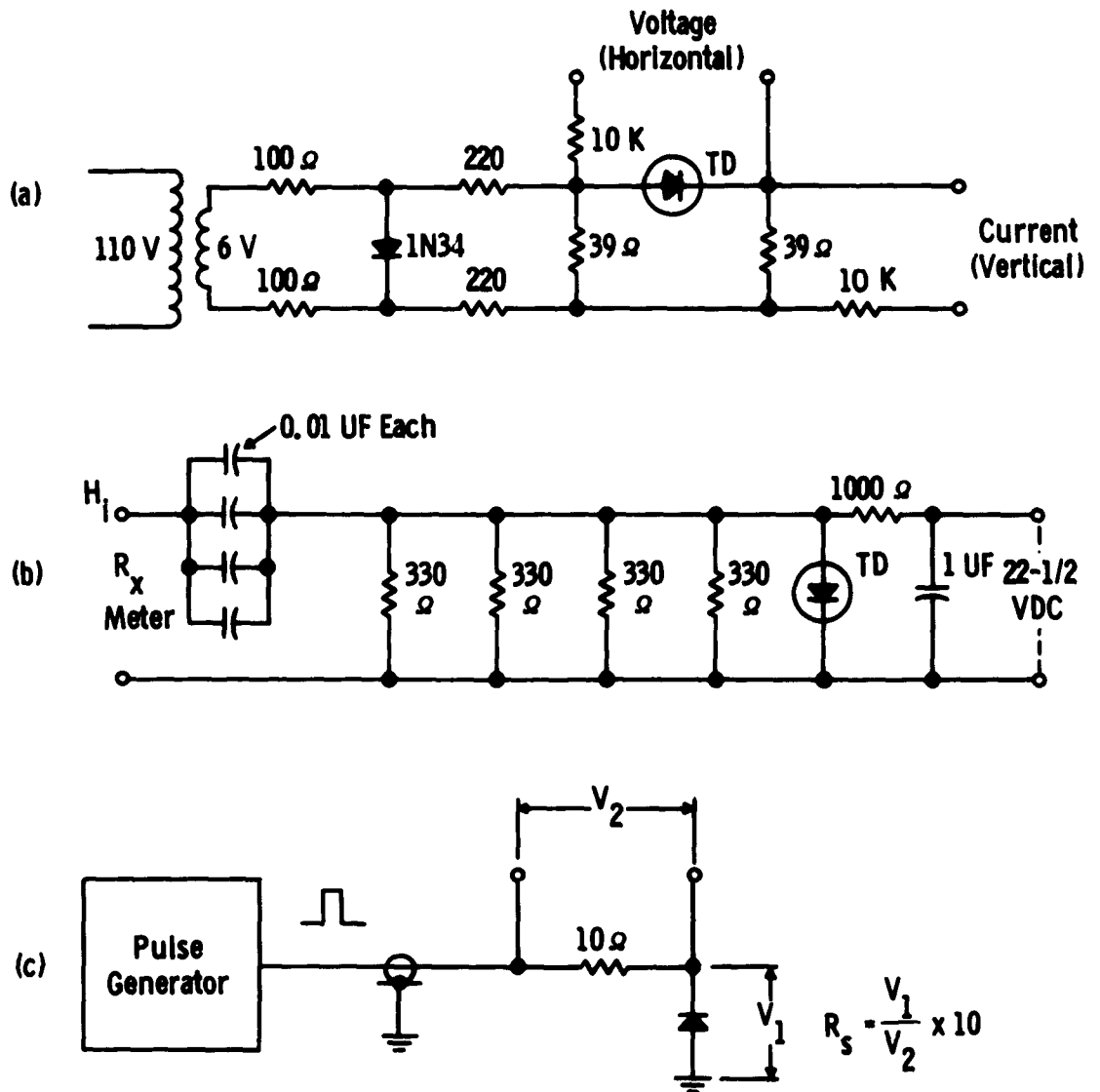


Figure 2-52. Circuits Used to Determine Tunnel Diode Characteristics

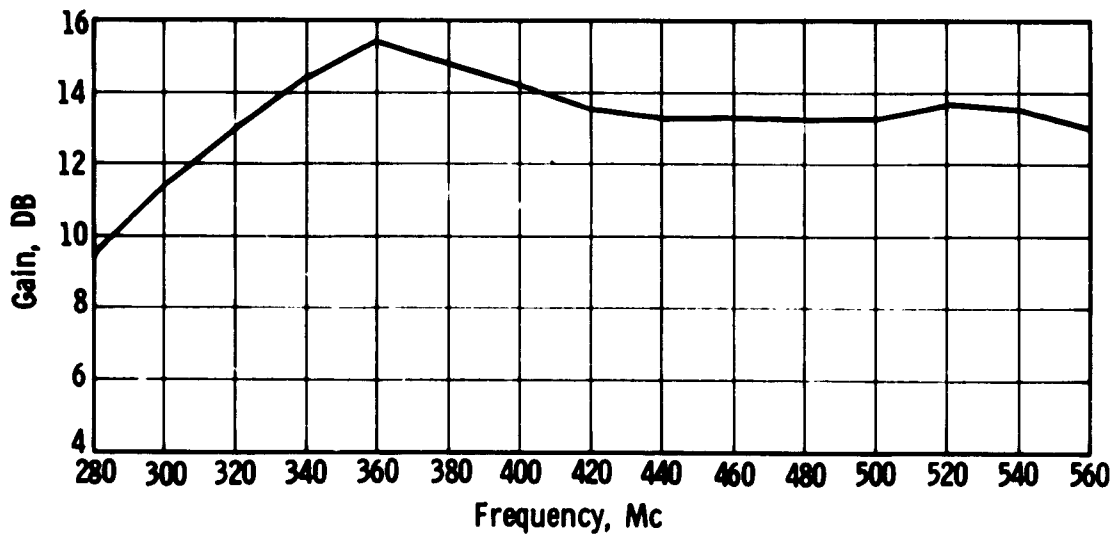
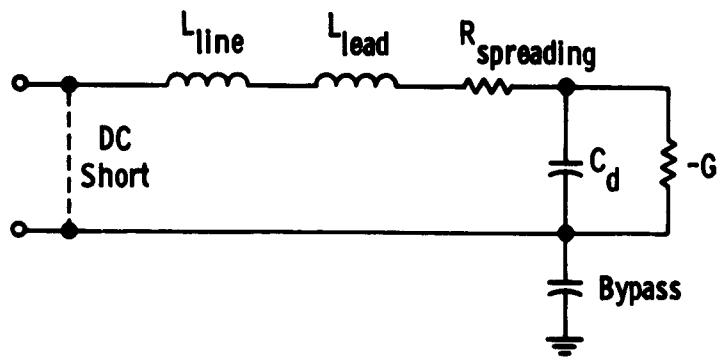


Figure 2-53. Gain versus Frequency of Wideband Tunnel Diode Amplifier. GE IN 2939 Diode

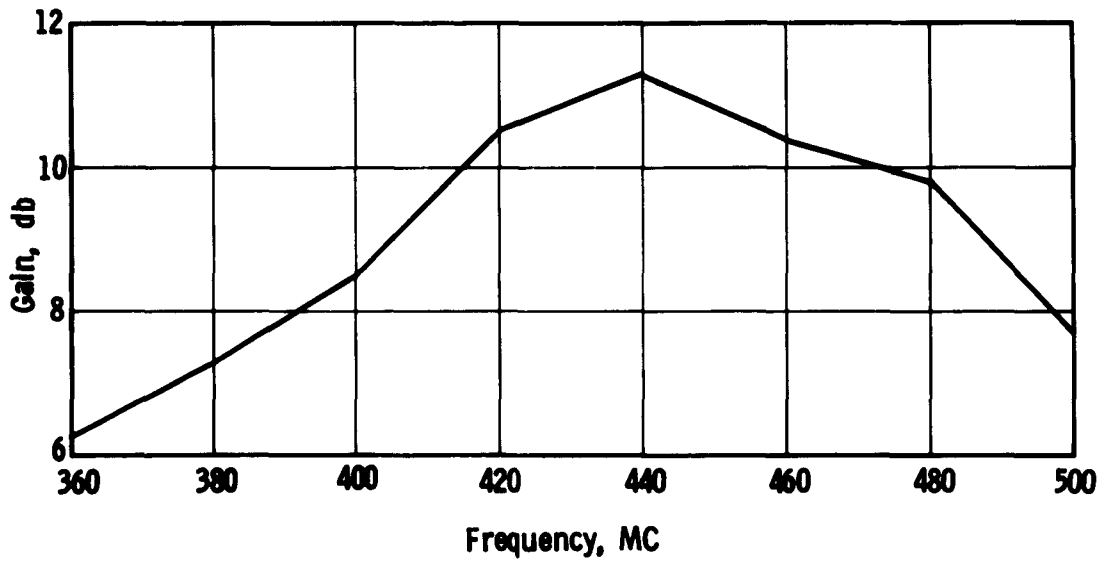
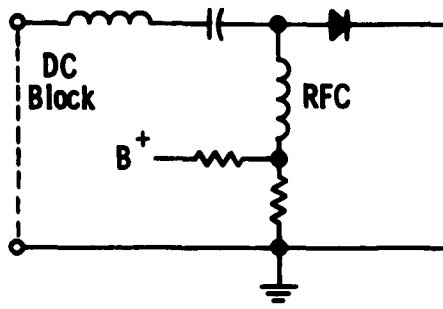


Figure 2-54. Gain versus Frequency of Narrowband Tunnel Diode Amplifier, GE IN 2939 Diode

## SECTION 3

### 3. SUMMARY AND CONCLUSIONS

The previous sections have been concerned with the theoretical and experimental results obtained during the study of low-noise parametric amplifiers and related devices. These related devices included tunnel diode and thin-film amplifiers.

The purpose of this section is to conveniently gather and describe briefly the highlights of the program's results.

#### 3.1 THE VHF PARAMETRIC AMPLIFIER

A low-noise parametric amplifier was developed for 220 mc which required less than 1 mw of pump power at 1500 mc. This amplifier is tunable from 180 to 250 mc. It has 16 db gain with 1 mc bandwidth and the noise figure is less than 1.5 db over the tuning band. At the time of development, the amplifier stability suffered from lack of a circulator. Now, however, circulators for such low frequencies are becoming available; accordingly, stable systems can be achieved using such an amplifier.

#### 3.2 THE S-BAND PARAMETRIC AMPLIFIER

An S-band parametric amplifier operating in the nondegenerate mode was developed having a gain of 17 db with a bandwidth of 70 mc. Filter techniques and an idler termination were employed to achieve the wide bandwidth. Even with the idler termination, noise figures as low as 2 db were measured.

#### 3.3 THE X-BAND PARAMETRIC AMPLIFIER

Both degenerate-mode and nondegenerate-mode amplifiers for X-band were developed. The degenerate-mode amplifier achieved a 5.2 db single-channel noise figure with 16 db gain using a silicon mesa diode.

The nondegenerate structure achieved a 3.5 db noise figure with 15 db gain and greater than 12 mc bandwidth. The nondegenerate amplifier was pumped at 23 gc with an OKI 24 V10 klystron. Pump power requirements were about 200 mw.

Two modes of operation were found with the nondegenerate X-band amplifier corresponding to two different idler tuning positions. With the idler short as close as possible to the varactor, a change of  $\pm 8.2$  mc of pump frequency could be tolerated before gain dropped 3 db; whereas with the idler short removed from the diode, the tolerable change of pump frequency is only  $\pm 5.7$  mc.

Sensitivity to pump power changes was found to be 7 db gain change to 1 db pump power change, which is typical for parametric amplifiers.

Tuning range was found to exceed 400 mc with noise figure below 5 db. Temperature range between  $\pm 3$  db change of gain is from +55 F to +192 F. In general, the amplifier is more stable with a hot environment than a cold environment.

### **3.4 BROADBAND X-BAND AMPLIFIER**

A theoretical design for an X-band amplifier with a 600-mc bandwidth amplifier operating in the nondegenerate mode has been presented. It is apparent however, that before practical realizations of such designs can be achieved, diodes with extremely high self-resonant frequencies will have to be obtained.

### **3.5 STUDY OF K- AND V-BAND AMPLIFIERS**

Noise figures lower than 4 db at 15 gc and 5 db at 25 gc are possible if diodes having cutoffs in excess of 250 gc are used. The most promising diode for these applications is the Western Electric gallium-arsenide diode.

### **3.6 MEASUREMENT OF VARACTOR QUALITY**

Three methods of measurement of varactor quality were investigated. These methods included Harrison's, Houlding's, and the modified Houlding's methods. Of the three, the Houlding's method appeared best in that it is relatively easy to perform, appears to give accurate and consistent results, and permits calculation of series resistance.

### **3.7 STABILIZING PARAMETRIC AMPLIFIERS**

A particularly effective method of stabilizing parametric amplifiers was evolved during this program. This technique consists of feeding a d-c signal back to a pump power controller. This d-c signal is derived from rectified i-f amplifier noise. The stabilizing system is particularly applicable when pulsed signals are used with low duty cycles, or when the receiver is periodically terminated as radio astronomy receivers are, for example. The initial results using this feedback technique are a 6 to 1 improvement of gain stability with pump power changes, and an 8 to 1 improvement of gain stability with antenna impedance changes.

### **3.8 THIN-FILM AMPLIFIER**

It is apparent that the thin-film amplifier is not a feasible device, although it is felt that the films utilized were not single-crystal as they should have been. The possible advantages of the thin-film amplifier have been largely negated by the advent of the tunnel diode.

### **3.9 THE TUNNEL-DIODE AMPLIFIER**

From the study of tunnel-diode amplifiers which consisted only of monitoring a corporate research program, it is clear that the tunnel diode amplifier has some distinct advantages. At 450 mc, a 5 db noise figure was achieved with 15 mc bandwidth and 15 db gain. As contrasted to the parametric amplifier, no r-f pumping was required.

## BIBLIOGRAPHY

1. Manley, J. M., and Rowe, H. E., "Some General Properties of Nonlinear Elements, Part 1, General Energy Relations," Proc. IRE, July 1956.
2. Heffner, H., and Wade, G., "Gain, Bandwidth, and Noise Characteristics of the Variable-Parameter Amplifier," Journal of Applied Physics, Sept. 1958.
3. Eng, S. T., "Characterization of Microwave Variable Capacitance Diodes," PGMTT Symposium, May 9-11, 1960.
4. Harrison, R. J., "Parametric Diode Q-Measurements," Microwave Journal, Vol 3, No. 5, p. 43-46, May 1960.
5. Houlding and Norman, "Measurement of Varactor Quality," Microwave Journal, Vol 3, No. 1, p. 40-45, Jan. 1960.
6. Seidel, H., and Herrmann, G. F., "Circuit Aspects of Parametric Amplifiers," 1959 IRE WESCON Convention Record, Part 2, p. 83-90.
7. Greene, J. C., and Sard, E. W., "Optimum Noise and Gain-Bandwidth Performance for a Practical One-Port Parametric Amplifier," Proc. IRE, Vol 48, No. 9, Sept. 1960.
8. Matthaei, G. L., "A Study of the Optimum Design of Wideband Parametric Amplifiers and Up-Converters," 1960 PGMTT Symposium.
9. Rowe, H. E., "Some General Properties of Nonlinear Elements, Part 2, Small Signal Theory," Proc. IRE, Vol 46, p. 850-860, May 1958.
10. Bode, H. W., "Network Analysis and Feedback Amplifier Design," D. Van Nostrand Co., New York, 1945.
11. Weinberg, L., "Modern Synthesis Network Design From Tables," Electronic Design, September 15, 1956.